



NTNU – Trondheim
Norwegian University of
Science and Technology

Effects of Fracture Capillary Pressure and non-straight Relative Permeability Lines

Vegard Aleksander Amundse Kjosnes

Petroleum Geoscience and Engineering

Submission date: May 2012

Supervisor: Jon Kleppe, IPT

Norwegian University of Science and Technology

Department of Petroleum Engineering and Applied Geophysics

Table of Contents

Table of Contents	1
List of figures	4
List of tables	6
Acknowledgment.....	7
Abstract	8
1. Introduction.....	9
2. Theory.....	10
2.1 Definition of naturally fractured reservoirs	10
2.2.1 Capillary pressure	11
2.2.2 Previous work on fracture capillary pressure.....	11
2.3 Wettability.....	12
2.4.1 Relative permeability	12
2.4.2 Previous work on fracture relative permeability	12
2.5 Gravity drainage	14
2.6 Imbibition	15
2.7 Idealized fractured reservoir representation	16
2.8 Fracture relative permeability.....	17
2.9 Fracture capillary pressure	20
3. Modeling approaches.....	22
3.1 Conventional modeling	22
3.2 Dual porosity models.....	23
3.3. Possible disadvantages of the dual porosity model.....	27
3.3.1 Capillary continuity.....	27
3.3.2 Block to block interaction.....	28
3.3.3 Sharp saturation gradients in upscaled grid cells.....	30
4. The test system	32
4.1 Test model geometry	32
4.2 Fluid and rock properties	33
4.3 Case studies	35
4.4 Non straight fracture relative permeability	36

4.6 Capillary pressure in fractures.....	40
4.7 Summary from test model	48
4.8 Conclusion from test system	48
5. The full sized reservoir	49
Water injection.....	50
Natural depletion	54
Gas injection	57
Conclusion from full scale reservoir	59
6. Conclusion	60
7. Further work.....	61
References.....	62
Nomenclature.....	64
Appendix1: Figures from simulations and equations.....	65
Appendix2: Reservoir and fluid description of the full-scaled reservoir.....	75
Appendix3: Upscaling	81
Appendix4: Eclipse files	84
Water injection -- original file	84
Water injection for the fine grid test system	84
Water injection for the dual porosity test system	86
Gas injection – original file	89
Gas injection for the fine grid test.....	89
UPSCALING	92
UPSCALING – SIMULATIONS WITH 50 GRID BLOCKS	92
UPSCALING – SIMULATIONS WITH 10 GRID BLOCKS	95
UPSCALING – SIMULATIONS WITH 5 GRID BLOCKS	98
FULL SCALE RESERVOIR -- THE SPE6 MODEL.....	101
WATER AND GAS INJECTION	101
INCLUDE FILES	107
P:\MASTER\INCLUDE\FINEGRID.DATA /	107
P:\MASTER\INCLUDE\FINEGRID.DATA / - DURING CAPILLARY CONTINUITY.....	109
P:\MASTER\INCLUDE\PROPS.DATA /	111
P:\MASTER\INCLUDE\REGIONS.DATA /	113

P:\MASTER\INCLUDE\REGIONS.DATA / - DURING CAPILLARY CONTINUITY 115
P:\MASTER\INCLUDE\SUMMARY.DATA / 117
P:\MASTER\INCLUDE\TSTEPWAT.DATA / 118
P:\MASTER\INCLUDE\SPE6\SUMMARY_SPE6.DATA / 119

List of figures

Figure 1: Block heights effect on recovery (Kjøsnes, 2011).	14
Figure 2: Gravity drainage, difference in density makes the oil leave the matrix block (Kjøsnes, 2011). ..	14
Figure 3: Capillary pressure curve of an intermediate wet rock (Kjøsnes, 2011).	15
Figure 4: An idealized Warren-Root representation of a fractured reservoir (Warren, J.E. and Root,P.J, 1963).....	16
Figure 5: Zero fracture capillary pressure vs. non-zero fracture capillary pressure.	20
Figure 6: Capillary curve for zero and nonzero fracture capillary pressure. High fracture capillary pressure increase recovery.	20
Figure 7: The orange color represent the increased recovery caused by fracture capillary pressure.....	21
Figure 8: Different simulators attempt to simulate an easy task but results show big differences between simulators (Firoozabadi, A and Thomaset L.K, 1989).....	22
Figure 9: Conventional modeling of a single matrix block, showing a low permeability matrix surrounded by high permeability fractures (Kjøsnes, 2011).....	23
Figure 10: Dual porosity representation of a fractured reservoir (Bourbiaux and Leonnier, 2010).....	23
Figure 11: A simple dual porosity, dual permeability system (Eclipse reference manual, 2010)	24
Figure 12: A typical block of matrix material containing oil and water (Eclipse reference manual, 2010)	25
Figure 13: Shows schematic view of matrix fracture connection in a DUALPORO simulation. (Eclipse reference manual, 2010)	26
Figure 14: The transmissibility's during a DUALPERM simulation. New is the connection between the two matrix blocks (Kjøsnes, 2011).....	26
Figure 15: Effect of capillary continuity (Kjøsnes, 2011).	27
Figure 16: Block to block interaction in gas oil system (Kjøsnes, 2011).....	28
Figure 17: Comparison between the single and dual porosity model to see how block-to-block interaction is measured (Kjøsnes, 2011).....	29
Figure 18: Sharp saturation gradients (Kjøsnes, 2011)	30
Figure 19: The problem of upscaling is shown when nine matrix blocks are converted to a grid cell (Kjøsnes, 2011).	30
Figure 20: Case1.1 Recovery with a change in the fracture relative permeability curve.	36
Figure 21: The recovery graph for $H_D=0.5$ and different injection rates for the single porosity system. ...	37
Figure 22: Case 1.1.1: Relative permeability is changed in a dual porosity system.....	38
Figure 23: The comparison in injection rate shows us that the dual porosity model does not model viscous forces in matrix blocks.	39
Figure 24: Case2.1 shows recovery with water injection and capillary pressure in the fractures. $P_c=-/+ 10$ kPa	40
Figure 25: Case1.1.2: Comparison between the dual porosity and single porosity model.	41
Figure 26: Case2.2 shows recovery with gas injection and fracture capillary pressure in the fractures (10kPa).....	42
Figure 27: Comparison between the dual porosity model and single porosity model for a gas injection case.....	43
Figure 28: Case 3.1 Recovery for six blocks with capillary continuity, fracture capillary pressure and water injection.....	44

Figure 29: Comparison between the dual porosity model, and single porosity model, when we have water injection and capillary continuity..... 45

Figure 30: Case 3.2 Recovery for six blocks with capillary continuity, fracture capillary pressure and gas injection..... 46

Figure 31: Comparison between the dual porosity model, and single porosity model, when we have gas injection and capillary continuity. 47

Figure 32: Recovery vs. time in a full-scale reservoir and different HD-values 50

Figure 33: When we look at the recovery in each block after 5 years of production we could see that the sweep for $H_D=1.0$ is improved. This means that the waterfront is moving more equally in all layers in the reservoir. 51

Figure 34: Gas production rate explode when low relative permeabilities applies..... 52

Figure 35: Recovery is shown for different natural depletion situations. All three situations get low recoveries. 54

Figure 36: Oil and gas production rate..... 55

Figure 37: A comparison of recovery in the reservoir with natural depletion under different production rates..... 56

Figure 38: This plot shows the recovery vs. time for the gas injection case. When fracture capillary pressure is assumed, we get a highly increased recovery. 57

Figure 39: The oil production rate when gas is injected. 58

Figure 40: This is the time difference with the single porosity model and dual porosity model for the test system. This is a very small system, and if the simulation model were bigger, the single porosity model would have been even slower..... 65

Figure 41: Recovery for dual porosity model when viscous displacement is included (VISCD)..... 66

Figure 42: Low H_D values decrease the recovery for the single porosity model as well, but only for very small injection rates. 67

Figure 43: Reservoir pressure for full field reservoir with water injection and different HD values. 68

Figure 44: Different layers drains at different times in the original file..... 69

Figure 45: When we have HD equal to 1 we get a more evenly drainage of the matrix fracture cells. If we compare this result with Figure 44 we could see that this model drains the matrix blocks more evenly, that again mean a better sweep for low HD values. 70

Figure 46: We reduced the horizontal fracture permeability and saw that this made a gas breakthrough when K_{fh} was reduced by 90%..... 71

Figure 47: Comparison of recovery for the original reservoir and the same reservoir with tall matrix blocks (50ft)..... 72

Figure 48: Comparison of oil production rate for the original reservoir and the same reservoir with tall matrix blocks (50ft). 73

Figure 49: Equations to calculated fracture relative permeability assuming gravity segregation (Chimá, A., Chávez, E. and Calderón, Z., 2010). 73

Figure 50: Fracture relative permeability calculated with viscosities at bubble point conditions compared to the straight permeability lines. 74

Figure 51: Above the full-scaled reservoir is shown during water injection. The perforations for the two wells vary, but they always have the same placement..... 75

Figure 52: Imbibition capillary curve in matrix for oil-water.....	76
Figure 53: Imbibition relative permeability curve in matrix rock.....	76
Figure 54: Full field reservoir density during production life.....	78
Figure 55: Surface/interfacial tension from eclipse file.	79
Figure 56: Explanation to how the STOG keyword works from the eclipse reference manual (Schlumberger, 2010).	79
Figure 57: Surface tension is not modeled in the reservoir.	80
Figure 58: For all grid block sizes the recovery is perfectly similar.	81
Figure 59: Oil production rate is similar for all grid block sizes.....	82
Figure 60: Time consumption (ELAPSED) is incredible much smaller when we have many matrix blocks in one grid cell.	83

List of tables

Table 1: Calculated H_D values for the water oil system at bubble point for the full-scaled reservoir.	17
Table 2: Calculated H_D values for the gas oil system at bubble point (5545 psi) for the full-scaled reservoir.	17
Table 3: Calculated H_D values for the gas oil system at 4000 psi for the full-scaled reservoir.	18
Table 4: Fracture relative permeabilities vs. water saturation for different H_D values	18
Table 5: Basic fluid and rock properties for oil-water imbibition.....	33
Table 6: Imbibition relative permeability and capillary pressure in matrix rock	33
Table 7: Imbibition relative permeability and capillary pressure in fracture.....	34
Table 8: The capillary pressure curves and relative permeability curves for the full-scale reservoir is from SPE6 own data.	75
Table 9: Fracture capillary pressure and gas fracture relative permeability (when fracture capillary pressure is applied).	77
Table 10: Layer data.	77
Table 11: Basic fluid and rock properties for oil-water imbibition.....	78

Acknowledgment

I would like to express my gratitude to Professor Jon Kleppe, for guidance and advice on my work. His wise suggestions helped me to choose a simulation problem and to put my thoughts in the right direction. I also would like to thank Jan Ivar Jensen for technical guidance on my simulations.

Trondheim, 25.05.2012

Vegard Kjøsnes

Abstract

The goal of this thesis is to study the effects of fracture capillary pressure and non-straight fracture relative permeability curves. In a fractured reservoir matrix-fracture fluid exchange is mainly controlled by gravity and capillary forces, but knowledge of how this altered fracture properties affect the total reservoir behavior is however low.

In this thesis two different reservoir models are used, the first is a small test system to see how the dual porosity model behaves compared to the single porosity model. The second model is a full-scale reservoir model to see impacts on a full reservoir.

From the small test system it was observed good matches between the single porosity model and the dual porosity model, so we accepted that the dual porosity simulator was able to simulate these properties in a fractured reservoir well.

In the full-scale reservoir it was observed that non-straight fracture permeability lines changed the sweep completely in the reservoir. Oil was drained from all layers more evenly than while following the straight-line permeability curve.

The importance of fracture capillary pressure is clearly seen in the test system and the full-scale reservoir. The study show that fracture capillary pressure influence both the gas/oil gravity drainage and the water/oil capillary imbibition process, but the effect is more pronounced in the gas-oil drainage case. For the gas oil drainage case the final recovery was more than doubled.

1. Introduction

The study of naturally fractured reservoirs is a subject that is described extensively in the literature for the last three decades. Most reservoirs are to some extent fractured, but in many cases the fractures just have insignificant impact on performance of the reservoir, and they may be ignored. Obviously a naturally fractured reservoir is defined as a reservoir where the fractures have a significant impact on performance and recovery. Such fractures are formed naturally during specific events in geological history. Fluid flow in fractures is of interest to engineers in many aspects, e.g. to environmental engineers in the flow of hazardous wastes into groundwater, or to geologist in groundwater movement, and to petroleum engineers. Traditionally fractured reservoirs have suffered from a low recovery, and therefore researchers around the world have tried to understand the physics behind them better. In oil rich regions like the Middle East and the Mexican gulf, oil production from fractured reservoirs accounts for the bulk petroleum production. And of the world's total output of oil today, 25-30% is estimated to be from fractured reservoirs (Lian, P.Q and Ma. C.Y., 2012). Since reservoirs with easy producible oil gets depleted first, we could expect this number to increase in the future and Chimá et al. (2012) states that 60% of the world's remaining proven hydrocarbon reserves are thought to be in naturally fractured (e.g. carbonates) and hydraulically fractured (e.g. shale gas) reservoirs. As the oil price increase, the more important an effective production of a reservoir has become, and the need to fully understand fractured reservoirs is increasingly important.

2. Theory

The theory in this thesis is mainly learned through the course Fractured Reservoirs which is held by Ole Torsæter and Hassan Karimaie and the lecture material from this course (Torsæter, Ole, 2010). As my own project in 2011 also investigated fractured reservoirs, much of the theory is also found there (Kjøsnes, 2011).

2.1 Definition of naturally fractured reservoirs

A reservoir is defined as fractured only if there is a continuous network of fractures throughout the reservoir. In a fractured reservoir we would then have two distinct porous media systems. One is the highly permeable fractures that conduct most of the flow and the other is the low permeable matrix, where most of the oil is contained. The identification of a continuous fracture network in carbonate reservoirs normally results from:

- 1) Significant mud losses that occur during drilling operations
- 2) Cores examination in the laboratory
- 3) Observations on outcrops during the exploration phase
- 4) Use of televiewer in the well during logging operations
- 5) Special behavior of transient pressure analysis during well testing operations (double slopes)
- 6) Low vertical temperature variation
- 7) Core permeability vs. observed well test permeability

The importance of fractures can be understood by:

$\frac{\text{observed well test permeability}}{\text{core permeability}}$, since this relationship in a fractured reservoir can alter significantly from the factor one.

A problem we encounter when the matrix permeability do not represent the reservoir permeability is that we now have two medias where we have to consider flow, the slow flowing matrix and the fast flowing fractures. Since the permeability of the fractures is much higher than the matrix permeability, the fluids will flow towards the well through the fractures, and the matrix will feed the fractures with oil and gas.

Because of the existence of two types of porosity, fractured reservoirs are often referred to as a dual porosity or dual permeability system. Since a dual porosity system contains two porosity types, a conventional modeling could be hard. That is why many simplified methods to model dual porosity models are made. The advantages of the dual porosity models are easily seen when we compare the time consumption of a conventional model run and a dual porosity model run (Figure 40 in Appendix1).

2.2.1 Capillary pressure

In a fractured reservoir the capillary pressure curve plays a much more important role than in a conventional reservoir. Capillary forces in fractured reservoirs are one of the driving mechanisms, while the role of capillary pressure for a conventional reservoir is more limited. Capillary pressures oppose drainage for a gas oil system, but might help for a water oil imbibition system. Capillary pressure is defined as the pressure difference between two immiscible fluids.

$$P_c = P_{nonwetting\ phase} - P_{wetting\ phase}$$

In oil-water systems, water is typically the wetting phase, and for a gas-oil system, oil is the wetting phase (always).

2.2.2 Previous work on fracture capillary pressure

E.S Romm (1966) experiments showed straight lines for relative permeability and zero capillary pressure in the fractures. Up until today, this has been used in reservoir simulation without a clear understanding of how these parameters affects reservoir performance. In fact, fracture capillary pressure could have a great influence in both gravity drainage and imbibition processes, even if the effect is more pronounced in a gas drainage case. Firoozabadi and Hauge (1990) presented a theoretical analysis that questioned the general zero assumption and made a phenomenological model for fracture capillary pressure. In their experiments, they imposed capillary pressures as high as 275 kPa in the fractures between a stack of matrix blocks, clearly showing that the assumption of zero capillary pressure not necessarily is correct.

Firoozabadi et al. (1990) made an experimental study where they examined the effect of capillary pressure in fractures. They studied three different alternatives, one with $P_{cf}=0$, one with $P_{cf}=\text{constant}$ and one where $P_{cf} = P_{cf}(S_w)$. In this study they showed that a constant fracture capillary pressure is not consistent with the experimental results, and simulation results indicates that fracture capillary pressure might have a similar form as the matrix.

Porte et al. (2005) studied the effect of relative permeability and fracture capillary pressure on oil recovery with numerical simulation of naturally fractured reservoirs. Their results where that fracture capillary pressure could change the final recovery of a reservoir a lot. For a gas-oil case, the recovery could be increased by a factor two if there is a fracture capillary pressure present. They also conclude that the recovery increment is bigger for small matrix blocks and of less importance for water imbibition. The fracture capillary pressure is only valid for narrow fractures, and Porte estimates that for a fracture wider than 100 microns, zero capillary pressure could be used.

Noroozi et al. (2010) made simulations on an Iranian field to check how big impact non-straight lines and fracture capillary pressure could have on this specific field. Their simulations reviled that straight fracture relative permeability lines could be used, and that capillary pressure could be turned to zero in the water case. If the depletion happens with gas injection or without injection fracture capillary pressure seems to give an extra final recovery of up to 60%.

2.3 Wettability

Wettability is defined as the tendency for one fluid to wet a rock surface in the presence of another fluid. It is a characteristic property of the rock fluid interaction.

In the petroleum section, wettability is associated either with water-wet rocks, or with oil wet rocks. If a rock is completely water wet, an oil-filled core that is submerged into water will be completely filled with water. And for a completely oil wet rock, no water will be imbibed when submerged into water. No rocks are gas wet, so in order to get gas into the pores of a porous rock we would need to apply a capillary pressure so that the gas is forced into the rock. This pressure is equal to the pressure that is needed to force a droplet of oil out of the biggest pore throat.

2.4.1 Relative permeability

Relative permeability is the ratio of the permeability of a fluid at a particular saturation, and the permeability of that fluid at 100% saturation. For oil the formula would take the following form: $k_{ro} = \frac{k_{oil}}{k_{absolut}}$. The relative permeability is one of the most significant parameters used in reservoir simulation, as it is critical in the prediction of the flow rate of a phase in the presence of another. In a fractured reservoir, evaluation of relative permeability is difficult since we have a discontinuity in the multiphase flow when going from matrix to fracture. As relative permeability is one of the key parameters to the recovery vs. time curve, this could in a dual porosity simulation be used as a history matching parameter to better match the recorded history or results from a single porosity run. Traditionally relative permeability in fractures is assumed to be a straight line, only dependent on the fluid saturation

It is important that capillary pressure, wettability and relative permeability not are viewed as isolated problems, as they are all linked closely together.

2.4.2 Previous work on fracture relative permeability

E.S. Romm (1966) performed the definitive work on fracture relative permeability in 1966, and he concluded that relative permeability is a linear function of saturation. Several authors have found this not to be accurate. Regardless of this, Romms conclusion about straight-line permeabilities is still widely used today.

Fourar et al. (1992) conducted an experimental study of horizontal artificial fractures. They measured the relative permeability with videotape observations. The relative permeability curve was found to be similar to classical curves in porous mediums, but not unique functions of saturations. They found the sum of gas and liquid relative permeabilities to be less than one for all saturations.

Rossen and Kumar (1994) showed that percolation theory forbids simultaneous multiphase flow under certain restricted conditions. They quantified the gravity segregation as a dimensionless parameter H_D , where the extent of this is given by: $H_D = \frac{\Delta\rho g H}{\gamma/b_0}$. For large values of H_D the percolation theory breaks down and relative permeability approach straight lines.

Pieters and Graves (1994) used an experimental method and computed relative permeability ratios using Welges (1952) interpretation of the Buckley Leverett theory, after fractional flow was obtained from the displacement. Their conclusion was the relative permeability is not a linear function of saturation, and that relative permeability in fractures appears similar to the behavior in a porous media.

Persoff and Pruess (1995) also conducted a laboratory experiment with carefully controlled flow rates and pressure conditions. Two-phase flow exhibited persistent instabilities with cyclic pressure and flow rate variations under conditions of constant boundary conditions. Measurement on relative permeabilities indicated strong phase interference, with relative permeabilities that is reduced to very small values at intermediate saturations, for both phases.

Porte et al. (2005) estimated how much the potential oil recovery could be increased/decreased when the relative permeability curve altered from the original straight-line approach. They found that straight-line permeability can lead to oil recovery errors as high as 70% in water oil systems and to underestimate the time to final recovery by a factor of three. The theoretical basis for the relative permeability study is the one performed by Rossen and Kumar (1994), and Porte showed that for a H_D less than five non-straight lines should be used.

Chimá, Chávez and Calderón (2010) demonstrate analytical that relative permeability is not a linear function of saturation. This study is based upon Darcy's law, Newton's law and the equation of change for isothermal systems and the concept of shell momentum balance (Bird R.B., Steward W.E. and Lightfoot E.N., 2002). When assuming gravitational segregation between the two phases, a newtonian and incompressible fluid with constant properties and that the flow is laminar and in steady state, they are able to make the analytical derivation of the equation. The equation they developed gives similar results as Pieters and Graves (1994), and the one of Romm, but contrary to Romms equation, which was a pure equation of saturation, this equation, relates the relative permeability to both saturation and viscosity. The equation they found is shown in Figure 49 and how this alters from the straight relative permeability lines is shown in Figure 50 (Appendix1).

Chimá and Geiger (2012) worked further on the work of Chimá, Chávez and Calderón and made an equation to predict fracture relative permeability in a gas-water system. After the equation was made, they compared results obtained experimentally by the authors Fourar and Bories (1995) and Diomampo (2001), since they had done experiments with water and gas. Other authors had made experiments with gas and oil, or water and oil and, and did not fit this new equation. It is apparent that the new relative permeability equation fits much better to the experimental results than the straight-line permeability estimated by Romm (1966).

2.5 Gravity drainage

Drainage displacement is the process where the nonwetting phase is displacing the wetting phase. This is contrary to the imbibition process where the wetting fluid is displaced by a nonwetting fluid. A common case is gas cap expansion, where gas (non-wetting phase) invades the fractures. For a fractured reservoir, gravity drainage is fully dependent on the block height (or capillary continuity). For small blocks, gravity could be excluded as a driving production mechanism.

2.5.1 Gas drainage

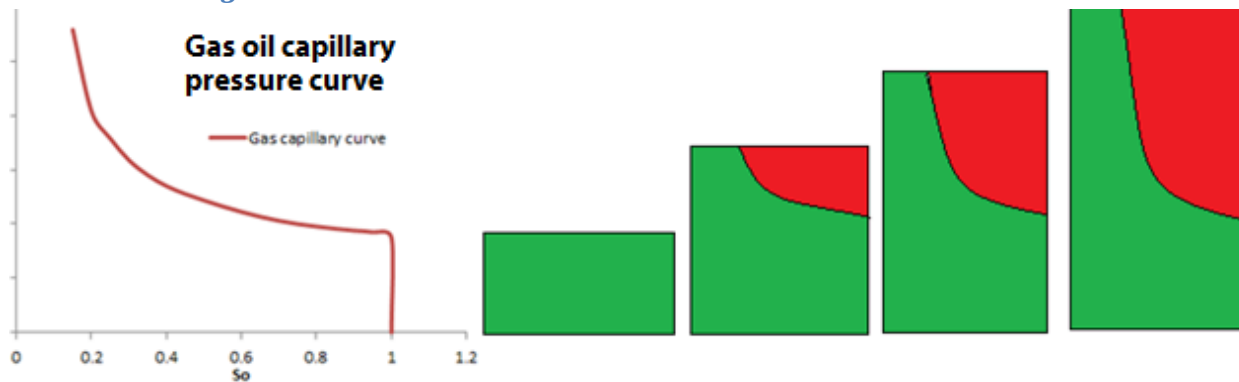


Figure 1: Block heights effect on recovery (Kjøsnes, 2011).

Gas is never the wetting phase in a rock, and to drain any oil the gas need to overcome the threshold pressure. The process of draining oil from a matrix block is called gravity drainage, pointing to the fact that gravity is the driving force. The density difference between gas and oil make the oil drain down, so it enters the fractures from where it could be produced. Here we see that higher blocks are able to give a higher recovery.

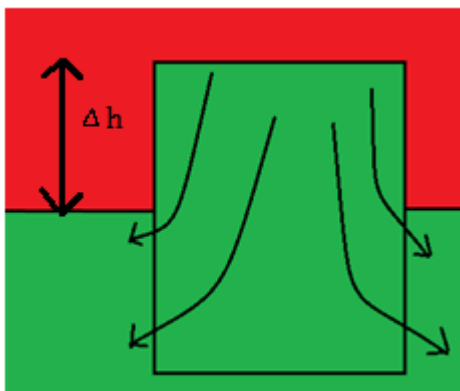


Figure 2: Gravity drainage, difference in density makes the oil leave the matrix block (Kjøsnes, 2011).

The pressure difference (capillary pressure) between the oil and gas phase at the top of the matrix block is given by: $\Delta P = g(\rho_o - \rho_g)\Delta h$

2.6 Imbibition

The displacement of nonwetting fluid in favor of the wetting fluid is defined as imbibition. In a fractured reservoir, if initially the matrix block is saturated with a nonwetting phase and the fractures are saturated with the wetting phase imbibition would take place. Imbibition has long been recognized as one of the main recovery mechanisms in water-wet rock. Especially in a fractured reservoir, spontaneous imbibition is recognized as a major recovery mechanism, since a limited capillary continuity cause problems for other displacement mechanisms. In the case of water injection or aquifer expansion, the water level in the fractures would raise and imbibition takes place. The rate of this imbibition depends on several things, where capillary pressure, matrix permeability, relative permeability, matrix shape and wettability are important.

Spontaneous imbibition is initially responsible of suction of the wetting phase into the rock, displacing the nonwetting phase. Further the imbibition is controlled by the capillary pressure. Capillary forces help the entrance of the wetting phase in the matrix during imbibition. The degree of importance from the capillary forces depends on the rocks wettability. For a strong water wet rock, spontaneous imbibition controls the oil recovery and the effect of capillary continuity is insignificant. But for an intermediate wet reservoir, the final recovery will depend also on capillary continuity.

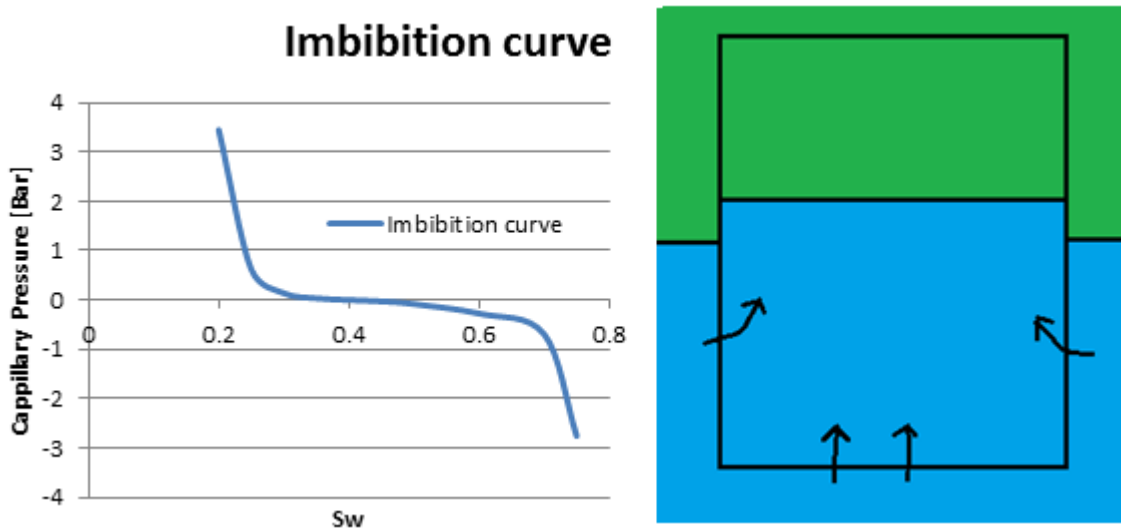


Figure 3: Capillary pressure curve of an intermediate wet rock (Kjøsnes, 2011).

For the example above, if the rock is initially fully oil saturated, some oil will be sucked into the rock and the water might even work against gravity in order to wet the rock.

2.7 Idealized fractured reservoir representation

There are several different ways of predicting recoveries. For making the calculations easier, Warren and Root (1963) developed an idealized model for studying the characteristic behavior for a system where a low permeable matrix contributed significantly to the pore volume, but not to the total flow capacity. In this system the flow towards the wellbore is considered to take place only in the fracture network, and the matrix only works to feed the fractures with fluids. In this idealized system, we would find a representative height for the matrix blocks. This height is of great importance for the recovery that is possible to get from the block, as the efficiency of the gravity forces is dependent on the block height. The block height is crucial to how much fluid that could be displaced due to gravity.

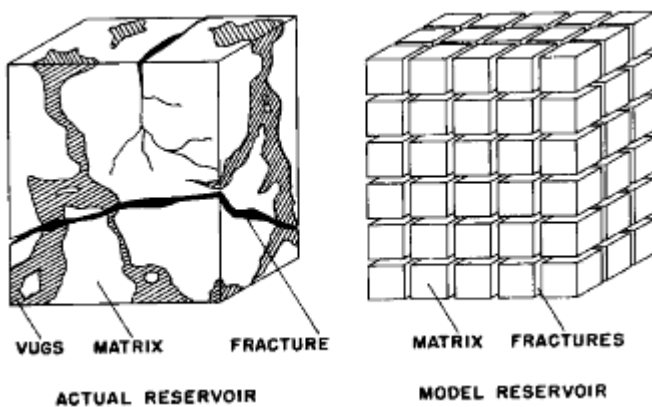


Figure 4: An idealized Warren-Root representation of a fractured reservoir (Warren, J.E. and Root, P.J., 1963)

2.8 Fracture relative permeability

In my simulations, the work of Rossen and Kumar (1994) is used to find better approaches for the straight-line assumption. They found that percolation theory forbids simultaneous multiphase flow under certain conditions. They used the dimensionless parameter $H_D = \frac{\Delta\rho g H}{\gamma/b_0}$, which essentially is the ratio between gravity and capillary forces, to evaluate the importance of changing the straight-line permeability. A high H_D value implies high gravity segregation. When H_D is higher than 10, this shows us high gravity segregation and straight-line fracture relative permeabilities are allowed. On the other hand, if H_D is close to zero capillary forces will dominate and percolation theory will prohibit simultaneously flow of two phases. In general, for H_D values less than five it is necessary to use non-straight lines. A gas oil system will have much higher H_D values than a water oil system, since we normally have bigger gravity differences between the phases and that gas-oil has less interfacial tension than water-oil. Therefore it is acceptable to make straight relative permeability lines for gas oil systems. Below we could see a calculation of different H_D values calculated for the oil and gas that I later will use in the full-scale reservoir simulation. ρ_w is the water density, ρ_o is oil density, $\Delta\rho$ is density difference, H is block height, γ is interfacial tension and b_0 is half-mean fracture opening.

Calculated H_D values for a water oil system (properties from full scale reservoir @ bubble point conditions)						
ρ_w	ρ_o	$\Delta\rho$	H	γ	b_0	H_D
Kg/rm ³	Kg/rm ³	Kg/rm ³	m	mN/m	cm	-
995	585	410	1	25	0.0001	0.16
995	585	410	1	25	0.001	1.61
995	585	410	1	25	0.01	16.1
995	585	410	1	25	0.1	161

Table 1: Calculated H_D values for the water oil system at bubble point for the full-scaled reservoir.

Calculated H_D values for a gas oil system (properties from full scale reservoir @ bubble point conditions)						
ρ_g	ρ_o	$\Delta\rho$	H	γ	b_0	H_D
Kg/rm ³	Kg/rm ³	Kg/rm ³	m	mN/m	cm	-
230	585	345	1	0.09	0.0001	37.6
230	585	345	1	0.09	0.001	376
230	585	345	1	0.09	0.01	3760
230	585	345	0.1	0.09	0.1	3760
230	585	345	0.01	0.09	0.1	376

Table 2: Calculated H_D values for the gas oil system at bubble point (5545 psi) for the full-scaled reservoir.

Calculated H_D values for a gas oil system (properties from full scale reservoir @ 4000 psi)						
ρ_g	ρ_o	$\Delta\rho$	H	γ	b_0	H_D
Kg/rm ³	Kg/rm ³	Kg/rm ³	m	mN/m	cm	-
189	621	432	1	0.8	0.0001	5.29
189	621	432	1	0.8	0.001	52.9
189	621	432	1	0.8	0.01	529

189	621	432	0.1	0.8	0.1	529
189	621	432	0.01	0.8	0.1	52.9

Table 3: Calculated H_D values for the gas oil system at 4000 psi for the full-scaled reservoir.

We could see that when we have small mean half apertures (b_o) of the fractures we get low H_D values, and then implying non-straight lines. If the aperture of the fractures is smaller than this, they will not give a very high permeability according to the formula $k_f = \frac{b^2}{12}$, which is the accepted formula for calculating the permeability between two parallel plates. For very narrow fractures, they might only have an insignificant effect on the rocks permeability, as the fracture permeability is low. Those reservoirs are not defined as fractured reservoirs. In Table 2 and Table 3 we could see that we have relatively high H_D numbers for all the tested cases in the gas oil simulation. This implies that we can use straight relative permeability lines. To use straight fracture relative permeability lines for gas oil systems is in agreement with other authors that have done similar studies like Porte et al. (2005) and Noroozi et al. (2010).

The used densities and surface tension for the calculations are found from the eclipse full-scale reservoir file and could be seen in Figure 54 and Figure 55 in Appendix2.

S_w	$H_D = \infty$		$H_D = 5$		$H_D = 1$		$H_D = 0.5$		$H_D = 0.0$	
	K_{rw}	K_{ro}	K_{rw}	K_{ro}	K_{rw}	K_{ro}	K_{rw}	K_{ro}	K_{rw}	K_{ro}
0.0	0.00	1	0.00	1	0.00	1	0.00	1	0.00	1
0.05	0.05	0.95	0.00	0.82	0.00	0.87	0.00	0.885	0.00	0.90
0.10	0.1	0.9	0.04	0.74	0.00	0.53	0.00	0.60	0.00	0.675
0.15	0.15	0.85	0.09	0.67	0.01	0.30	0.001	0.295	0.00	0.29
0.20	0.2	0.8	0.14	0.62	0.03	0.17	0.02	0.12	0.01	0.00
0.30	0.3	0.7	0.24	0.52	0.10	0.04	0.07	0.02	0.05	0.00
0.40	0.4	0.6	0.34	0.42	0.21	0.01	0.16	0.00	0.12	0.00
0.50	0.5	0.5	0.44	0.32	0.325	0.00	0.28	0.00	0.24	0.00
0.60	0.6	0.4	0.54	0.23	0.45	0.00	0.42	0.00	0.40	0.00
0.70	0.7	0.3	0.65	0.13	0.58	0.00	0.58	0.00	0.58	0.00
0.80	0.8	0.2	0.75	0.05	0.72	0.00	0.75	0.00	0.75	0.00
0.90	0.9	0.1	0.81	0.00	0.86	0.00	0.91	0.00	0.91	0.
1.00	1	0	1	0.00	1	0.00	1	0.00	1	0.

Table 4: Fracture relative permeabilities vs. water saturation for different H_D values

The corresponding relative permeability for different H_D values is seen in the table above. For low numbers where capillary pressures dominate, we could see that we have a very high irreducible oil and water saturation, and for $H_D=0$ we could not have simultaneous flow of two phases. The high irreducible oil saturations for these systems will do that a significant amount of the fracture oil will be unproducibile, and a higher amount of oil is therefore trapped in the fractures.

2.9 Fracture capillary pressure

In a gas oil drainage case fracture capillary pressure will help us to withdraw an extra amount of oil due to the increased capillary pressure that is obtained. The pressure in the fractures helps to overcome the threshold pressure, and therefore makes a higher recovery.

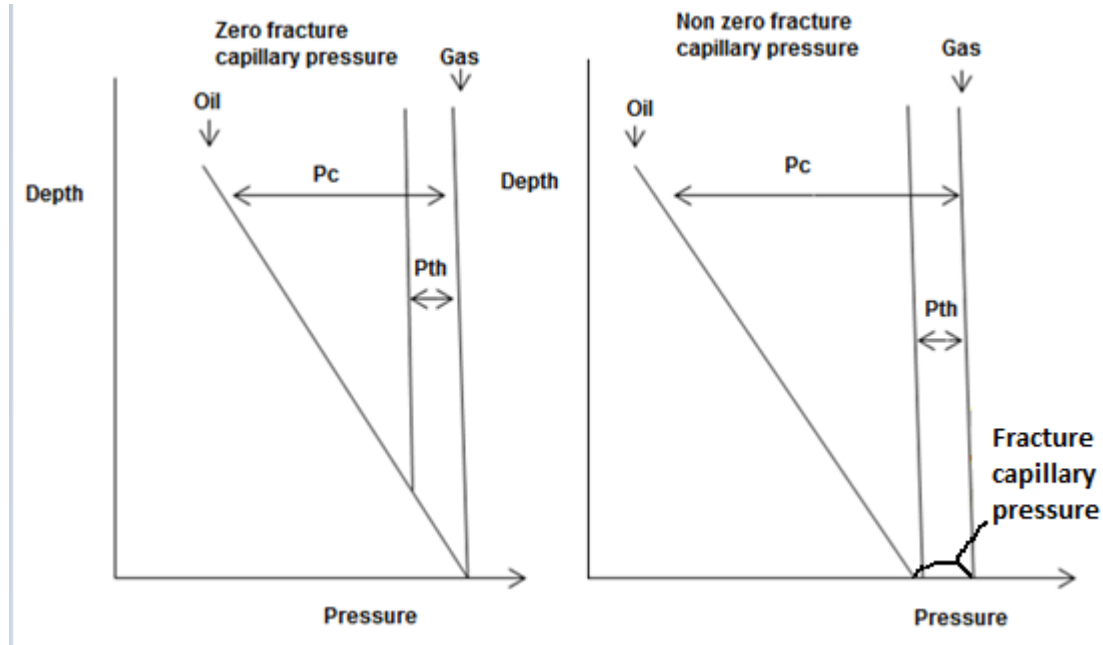


Figure 5: Zero fracture capillary pressure vs. non-zero fracture capillary pressure.

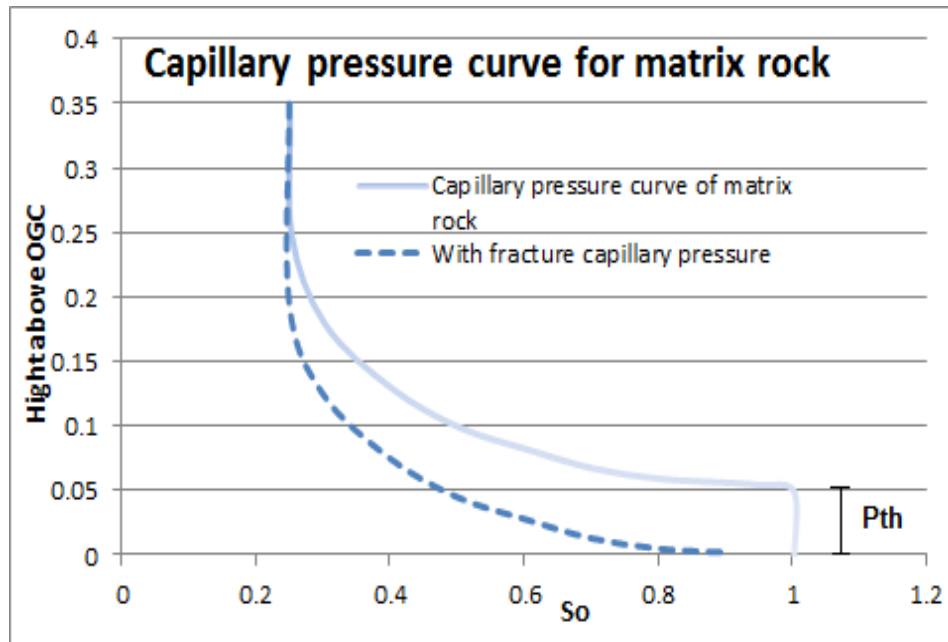


Figure 6: Capillary curve for zero and nonzero fracture capillary pressure. High fracture capillary pressure increase recovery.

The two figures above (Figure 5 and Figure 6) illustrate how fracture capillary pressure helps us to overcome the threshold pressure. As the oil and gas phase normally will be in a pressure equal position in the fractures, fracture capillary pressure makes us have a higher gas pressure, which in the end will give us a higher capillary pressure in the matrix blocks. For reservoirs with high blocks or capillary continuity between blocks, the effect of fracture capillary pressure may be limited, but for intermediate or small blocks, this might give a significant difference in recovery. Figure 7 shows us the additional recovery we could expect when we have fracture capillary pressure. The additional recovery is strongly linked to the capillary pressure curve of the matrix rock.

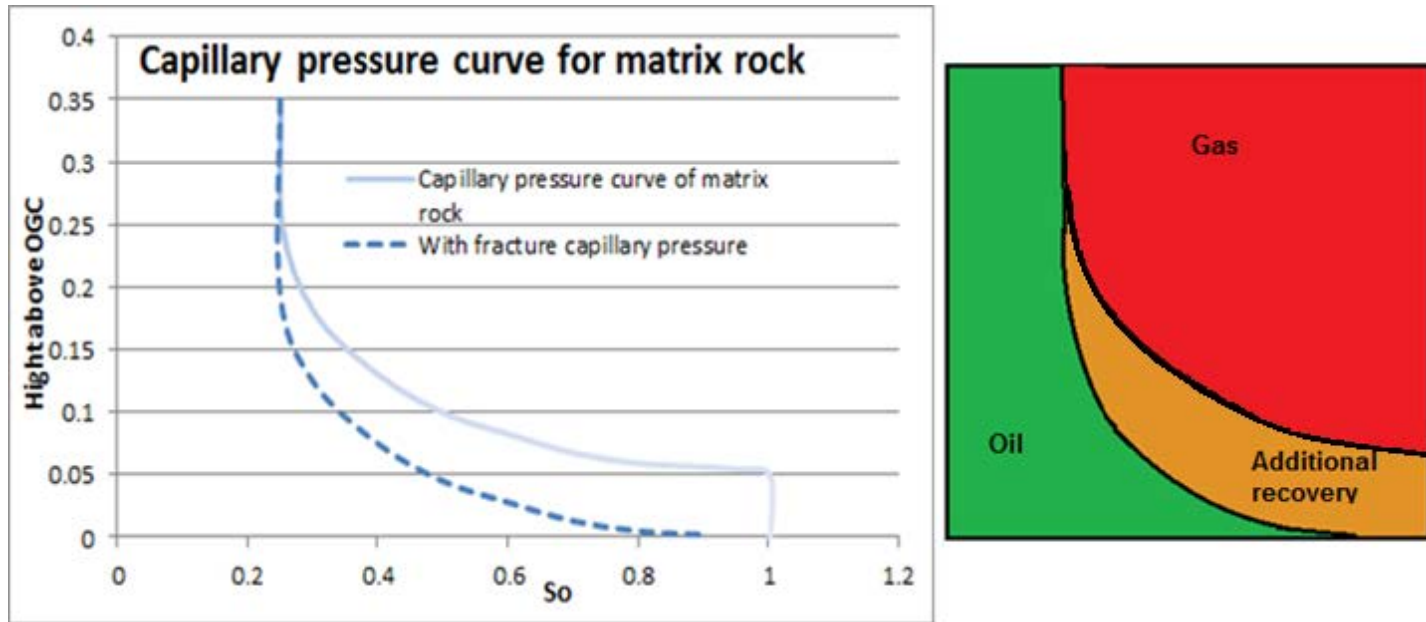


Figure 7: The orange color represent the increased recovery caused by fracture capillary pressure.

In the theoretical analysis performed by Firoozabadi and Hauge (1990) fracture capillary pressure curves (as function of wetting phase saturation) were developed for various fracture apertures ($t=2b_o$) of 10, 20 and 100 microns. The phenomenological model they used is derived from Young-Laplace equation of capillarity: $P_c = \gamma \left[\frac{1}{r_1} + \frac{1}{r_2} \right]$.

3. Modeling approaches

Petroleum field development has a big degree of uncertainty and is incredible expensive. Reservoir simulation could answer many critical issues to develop the field in the most effective way, both from an economical and technical way for a given reservoir. We could easily say that reservoir simulation has become a reservoir management tool for the reservoir in all stages of the reservoir lifetime.

Today's use of reservoir simulators are extensive. Reservoir simulations could be performed almost by "everyone". There are several different modeling approaches, which all try to solve the given problems in different ways. In this chapter we will look into two different modeling approaches; the conventional one, and the dual porosity model. The sixth SPE comparison study between dual porosity models (Firoozabadi, A and Thomas L.K, 1989) suggested that there was more difference between the simulators than we would like. Even if this study was conducted more than 20 years ago, big differences between simulators still remains. The simulator used in my simulations is ECLIPSE 100. This is a well used simulator and it will be discussed how ECLIPSE 100 is able to solve dual porosity problems.

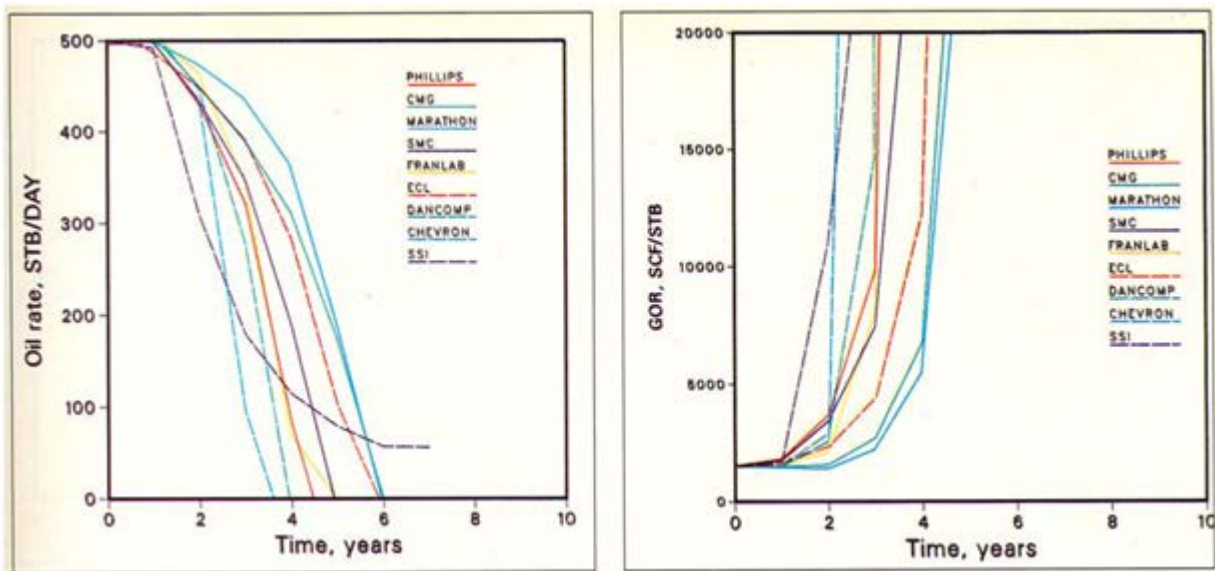


Figure 8: Different simulators attempt to simulate an easy task but results show big differences between simulators (Firoozabadi, A and Thomas L.K, 1989)

3.1 Conventional modeling

Conventional modeling, or single porosity modeling, is simply to use a standard reservoir simulator and model the fracture and matrix explicitly. You will then on a grid block to grid block basis, change the physical parameters so the model represents the actual reservoir. This kind of modeling is the most accurate, but also most computationally expensive. There are some methods to generate fracture networks for the whole field (Dershowitz, W, 1996), but this becomes impractical as the fracture network gets too excessive to model the flow in each individual fracture. Conventional modeling is however used on laboratory scaled simulations. In my experiments it is also used as a guide to see how

well the dual porosity model compares to this one, as single porosity modeling is understood as the correct solution to the problem.

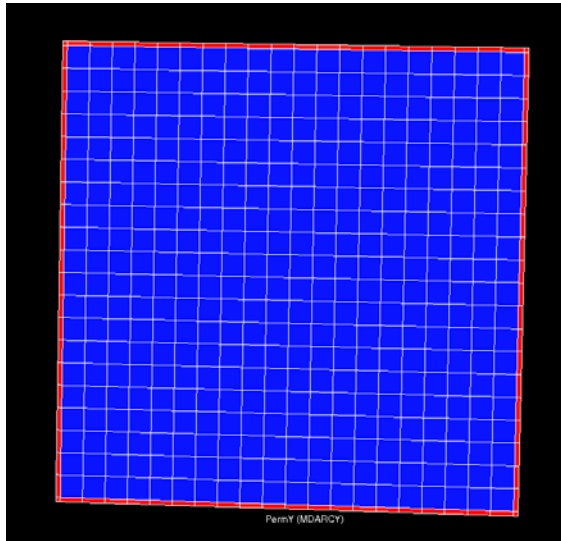


Figure 9: Conventional modeling of a single matrix block, showing a low permeability matrix surrounded by high permeability fractures (Kjøsnes, 2011).

3.2 Dual porosity models

Warren and Root (1963) proposed the simplified fracture model, and is the principle that most dual porosity models are based upon.

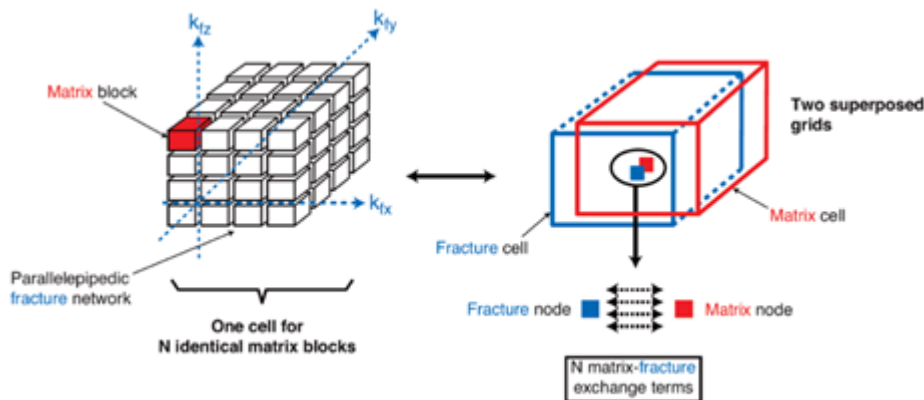


Figure 10: Dual porosity representation of a fractured reservoir (Bourbiaux and Leonnier, 2010)

In this idealized representation of a fractured reservoir, we assign two values for each parameter (e.g., pressure, saturation) within each simulation grid. The equations of motion (Darcy's law) and mass conservation are written independently for each medium. Multiphase mass transfer flow between the two media is shown by a source-sink transfer function. In a DUALPORO simulation (ECLIPSE 100) the communication between producer and injector only happens through the fracture network.

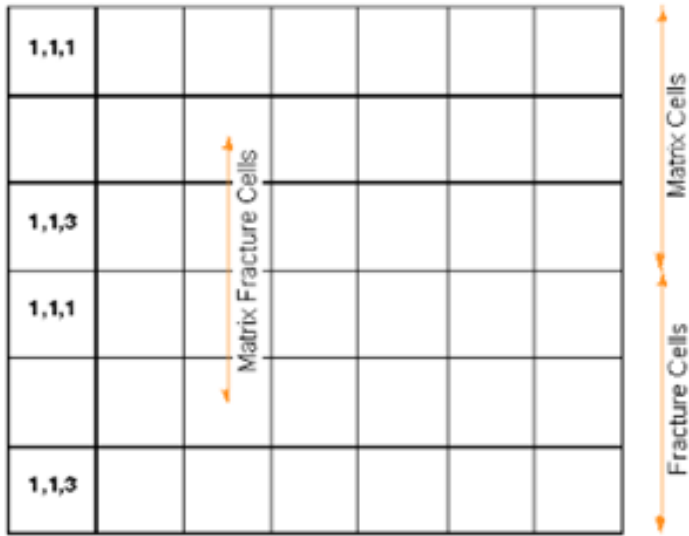


Figure 11: A simple dual porosity, dual permeability system (Eclipse reference manual, 2010)

For such a system in Eclipse (Schlumberger, 2010) the matrix fracture transmissibility is given on the form:

$$TR = CDARCY \cdot K \cdot V \cdot \sigma$$

Where by default:

CDARCY is Darcy's constant in the appropriate units.

K is taken as the X-direction permeability of the matrix blocks.

V is the grid cell bulk volume (not the pore volume, since we have no porosity factor).

σ is a factor of dimensionality, to account for the matrix/fracture interface area per unit volume.

Kazemi (1976) has proposed the following form for σ :

$$\sigma = 4 \left(\frac{1}{l_x^2} + \frac{1}{l_y^2} + \frac{1}{l_z^2} \right)$$

where l_x , l_y and l_z are typical X, Y and Z dimensions of the blocks of material making up the matrix volume. (l_x , l_y and l_z are thus not related to the simulation grid dimensions). Alternatively, as σ (SIGMA) acts as a multiplier on the matrix-fracture coupling, it may simply be treated as a history matching parameter.

To account for gravity, the keyword GRAVDR is used. The total flow between matrix and fracture is then for a gas oil system given by:

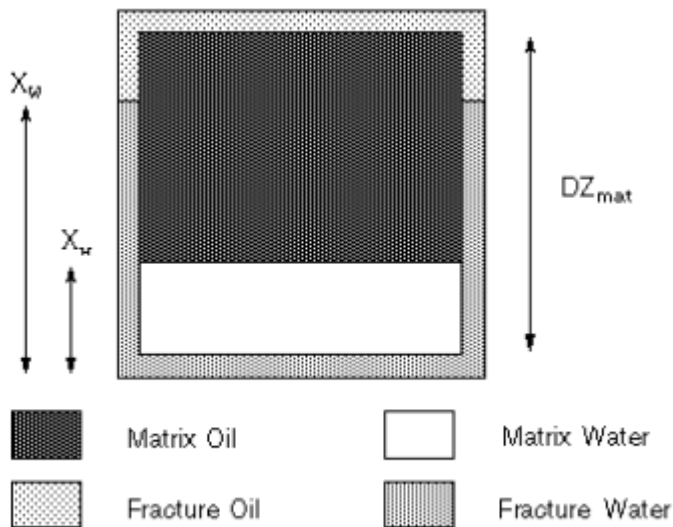


Figure 12: A typical block of matrix material containing oil and water (Eclipse reference manual, 2010)

$$F_g = TR \cdot G_{MOB} \cdot (P_{of} - P_{om} + d_{fm}\rho_g g - P_{cogf} - P_{cogm} + DZ_{mat} (X_G - X_g)) (\rho_o - \rho_g)g/2$$

$$F_o = TR \cdot O_{MOB} \cdot (P_{of} - P_{om} + d_{fm}\rho_o g - DZ_{mat} (X_G - X_g)) (\rho_o - \rho_g)g/2$$

Where

TR is the transmissibility between the fracture and matrix cells,

G_{MOB} is the gas mobility in the (upstream) fracture cell,

O_{MOB} is the oil mobility in the (upstream) fracture cell,

P_{of} is the oil phase pressure in the fracture cell,

P_{om} is the oil phase pressure in the matrix cell,

D_{fm} is the difference in depth between the fracture and matrix cells (usually zero),

ρ_g is the density of gas at reservoir conditions,

ρ_o is the density of oil at reservoir conditions,

g is the acceleration due to gravity,

P_{cogf} is the capillary pressure of gas in the fracture cell (normally zero)

P_{cogm} is the capillary pressure of gas in the matrix cell.

The pictures below show how the connections are made, the arrow in red show matrix – matrix connection in a DUALPERM run. In this model, fluid flow is assumed to happen not only in the fractures, but in the matrix too. Physically this means that we in reality have a continuous oil/gas phase between the blocks, and hence make the gravity drainage (GRAVDR) more efficient.

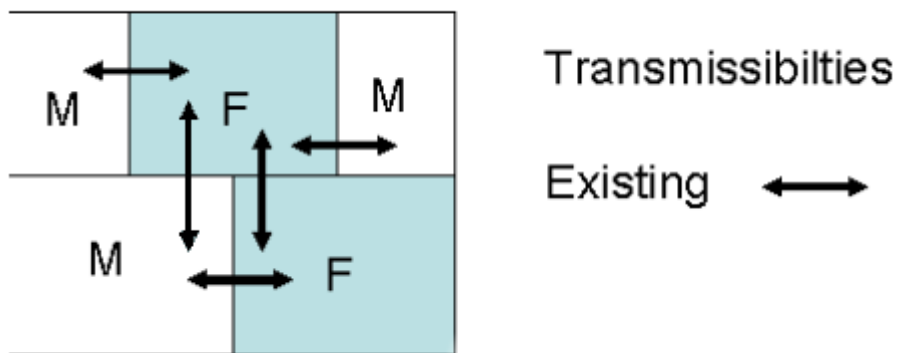


Figure 13: Shows schematic view of matrix fracture connection in a DUALPORO simulation. (Eclipse reference manual, 2010)

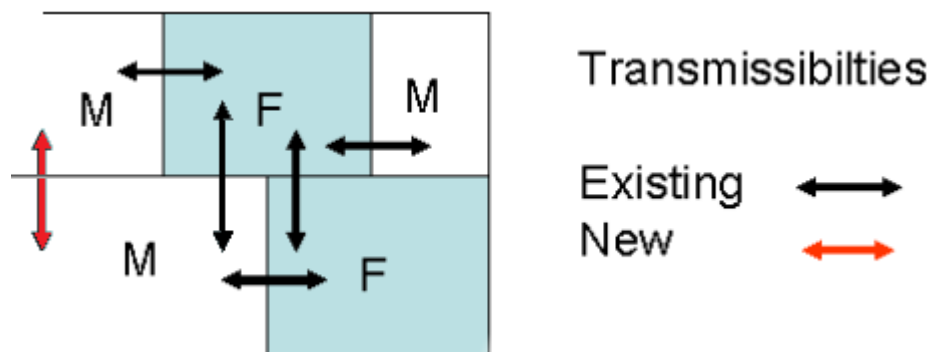


Figure 14: The transmissibility's during a DUALPERM simulation. New is the connection between the two matrix blocks (Kjøsnæs, 2011).

3.3. Possible disadvantages of the dual porosity model

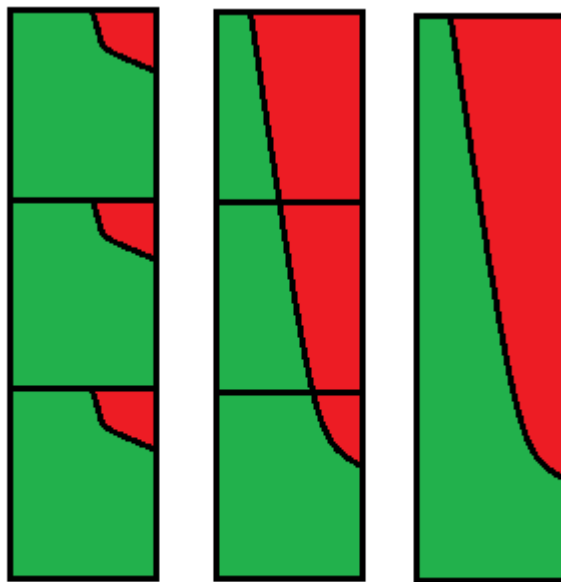
Earlier we looked at how the dual porosity model works, but its disadvantages are not seen clearly. Obviously a fractured reservoir model must model the entire reservoir as realistic as possible. Ole Krogh Jensen (2005) looks at three particular problems that are considered here:

1. Capillary continuity
2. Block to Block interaction (reimbibition)
3. Saturation gradients within matrix blocks

In the next section I will discuss how Eclipse 100 is able to solve the above problems. Failure to solve these problems will lead to the dual porosity model not being valid in reservoirs where the above criteria are present. Eclipse 100 is a widely used simulator, and is used in many big companies like Statoil, NTNU and Schlumberger, among others.

3.3.1 Capillary continuity

As illustrated in the figure below, block height has a great influence on recovery. The same count for capillary continuity.



a) Without capillary continuity

b) With capillary continuity

c) One big block

Figure 15: Effect of capillary continuity (Kjøsnæs, 2011).

In a real reservoir, all three situations might happen, and it could also be that one part of the reservoir is fractured, while the other part is not. In this case you would like to have a simulator that could divide the reservoir up in multiple sections. In the simulations of this thesis there has been no need to divide the reservoir into several sections, but Eclipse is able to do this division with the DPNUM keyword. To divide the reservoir into parts with different matrix heights is also possible.

3.3.2 Block to block interaction

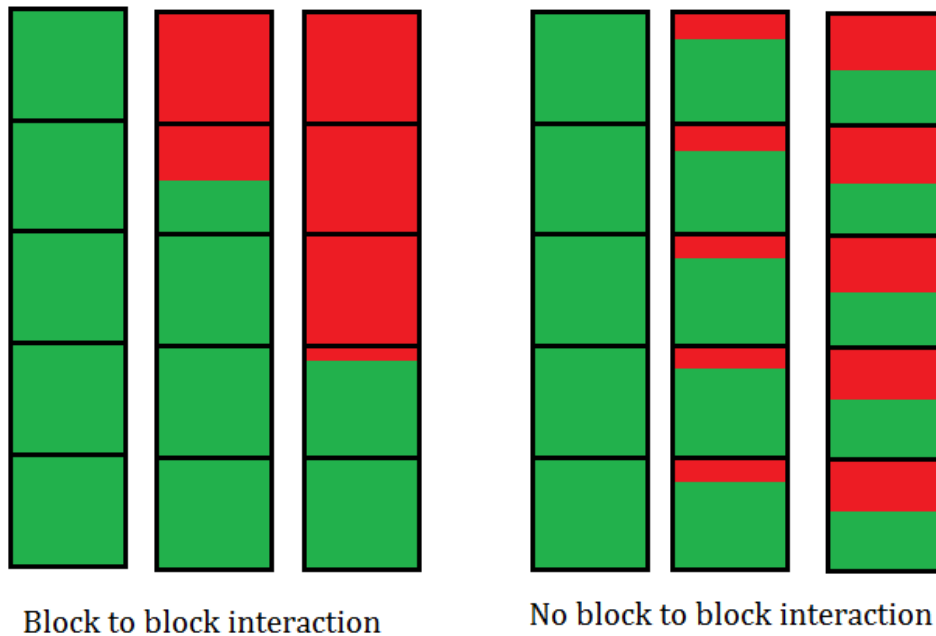


Figure 16: Block to block interaction in gas oil system (Kjøsnes, 2011).

Saidi A.M et al. (1979) showed in his simulations that blocks do not necessarily drain independently. Oil drained from one block has a tendency to reimbibe into the matrix block below, by capillary and gravity forces. Saidi discovered that reinfiltration would result in a lower oil production rate as the oil would travel through all the matrix blocks instead of going directly into the horizontal fractures. Illustrated above are the two different drainage possibilities.

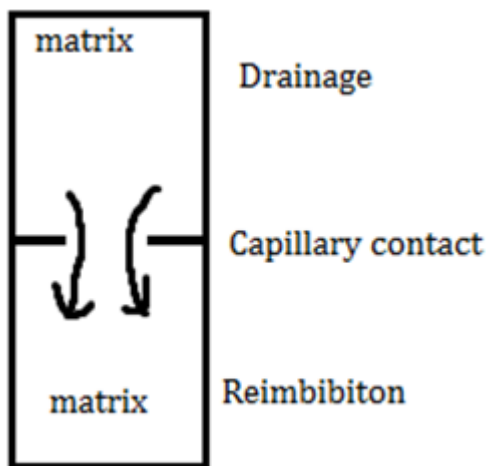


Figure 14: Block to block interaction in oil gas system (Kjøsnes, 2011).

It is sometimes hard to just evaluate how block to block interaction work in a dual porosity system, compared to how it would work in the real life. In such a situation the easiest probability is probably to make a similar single porosity model to see if the dual porosity model models it the same way. My test

simulation (Figure 17) showed that the dual permeability model had a similar behavior as the single porosity model in a case where we have a production well at the top of the reservoir and a water injection well at the bottom. Since it is a water oil system the oil will by gravity segregate upwards, meaning that the block-to-block interaction now happens upwards. In this case we could see that we have higher oil saturation at the top of the blocks, but it is unknown if this is due to a lower capillary pressure or the block interaction. The picture is however taken at an early stage of the imbibition process, where it is normally assumed that water imbibition is the main production mechanism. In that case the results below are an indication of oil flowing upwards, showing that Eclipse model block-to-block interaction correctly in this scenario. A combination of block-to-block interaction and higher capillary forces is however likely to have made the results as shown below.

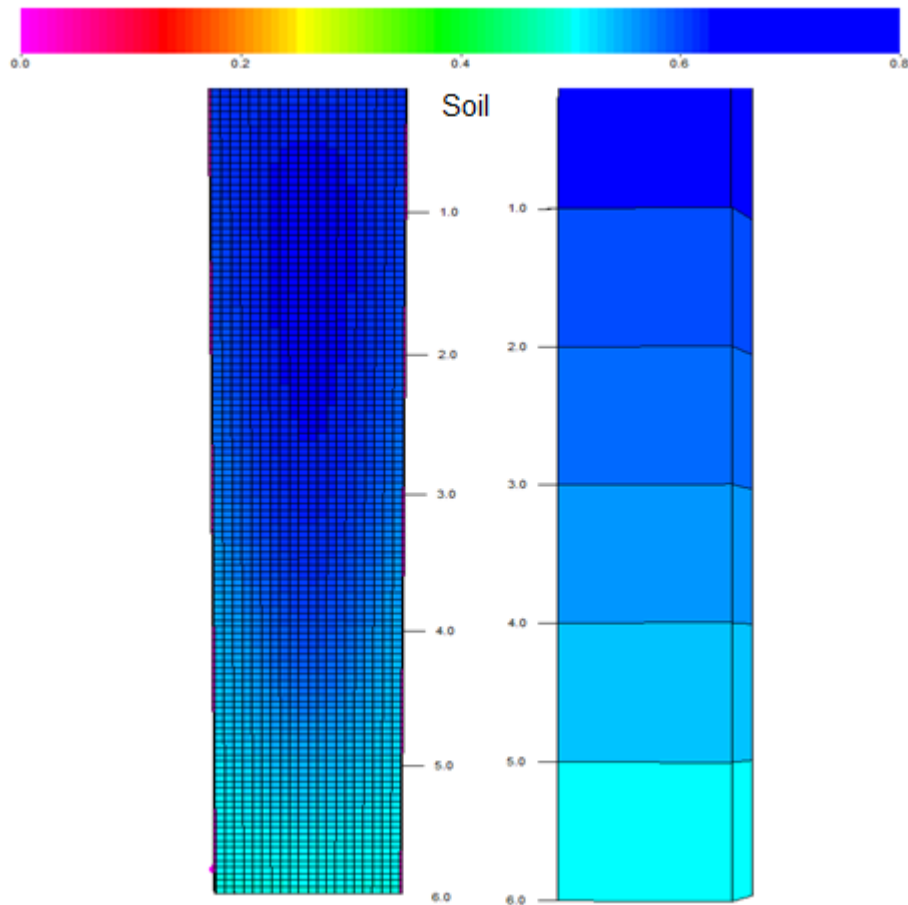


Figure 17: Comparison between the single and dual porosity model to see how block-to-block interaction is measured (Kjøsnæs, 2011).

3.3.3 Sharp saturation gradients in upscaled grid cells

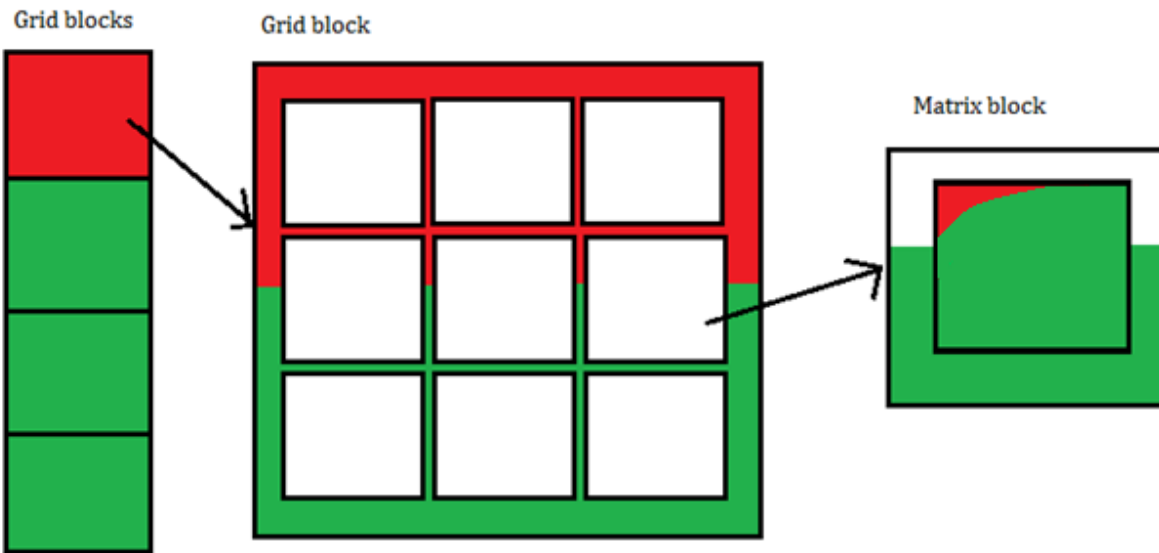


Figure 18: Sharp saturation gradients (Kjøsnes, 2011)

One of the main differences between a conventional model and a dual porosity model is the ability to model the sharp saturation gradients that occur in the reservoir. The dual porosity model is not able to measure saturation gradients since grid blocks span more than one matrix block. Within a grid cell all matrix blocks are treated the same, and it would be natural to believe that this would give some errors in reservoir prediction.

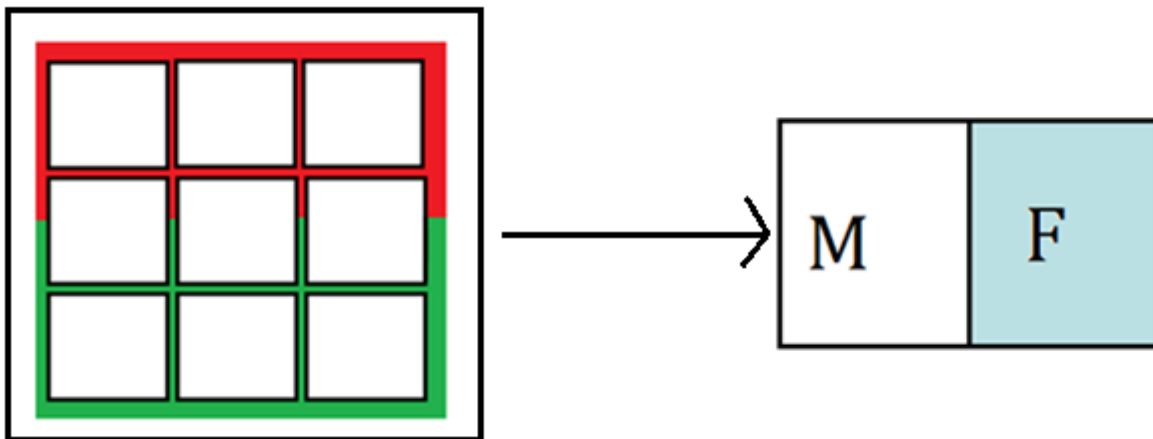


Figure 19: The problem of upscaling is shown when nine matrix blocks are converted to a grid cell (Kjøsnes, 2011).

Illustrated above is what happens when we go from reality to the dual porosity model. As we could understand there will be problems when all the matrix blocks get the same treatment, even though the drainage/imbibition processes are different.

There are mainly two different methods used for upscaling, one use the results from a finer grid simulation and then try to history match the coarser grid results to this one. The other method use well documented upscaling procedures to compute upscaled grids and upscaled effective permeabilities. There are several methods to do both the above methods, which all could give good results. This problem issue is potentially very interesting as block height could be very small, and upscaling is needed in order to be able to solve the simulated issue in an efficient way.

Whatever methodology that is used we seek an investigation which:

- Gives a detailed image of the flow pattern without having to solve the full fine scale system.
- Is robust and flexible with respect to the fine grid and the fine grid solver.
- Is accurate and fast.

To investigate fracture capillary pressure and fracture relative permeability I planned to use the reservoir model from the sixth SPE comparative study (SPE6). The SPE6 reservoir is a full-scale reservoir with dimension of 2000ft*1000ft*250ft divided into 10*1*5 equally sized grid blocks, in x, y and z direction respectively.

The height of the matrix blocks varies between 25 ft. and 5 ft. If we assume cubic formed matrix blocks this will imply that it is between 640 and 80 000 matrix blocks in one grid cell. Ideally, each matrix block should have its own grid cell to do more accurate calculations, but this would have been far too computationally expensive. Because of this uncertainty, I wanted to check if the large grid blocks would affect the simulated reservoir behavior in any way before I started to do my simulations on the SPE6 model.

The experiment and the results I obtained are described in Appendix3. To my surprise, the simulations showed that it was just minimal differences in reservoir behavior when we used smaller grid blocks. The conclusion was that huge grid cells don't play a major difference in the reservoir for a homogenous reservoir. This conclusion made me assured of that the behavior in the SPE6 model was realistic, and that it was no need to plot each matrix block.

4. The test system

To investigate how fracture capillary pressure and nonlinear relative permeability affect the simulation results two different test scenarios were made. One was a small test scenario where a single porosity and dual porosity model was made, the other was a full-scale reservoir. First this thesis will focus on the geometry and results from the test model, then we will use the learning from the test example to understand results from the full-scale model.

4.1 Test model geometry

Both models are made with Cartesian coordinates and contains six matrix blocks, where each block is 1m^3 ($1\text{m} \times 1\text{m} \times 1\text{m}$). In the fine grid model, which is considered as the solution, each matrix block is divided in a $20 \times 1 \times 20$ grid pattern. That means that the matrix block is divided into 400 grid blocks, with a height and width of 5 cm. The six matrix blocks were placed on top of each other, and each matrix block is surrounded by thin fractures. The fractures are made by small grid blocks that are given other values for permeability and porosity.

The dual porosity model was made in order to match the fine grid model as much as possible. The dual porosity model contains one grid block for each matrix block (six in all), and an additional six grid blocks for the fracture cells. This system is made so that each matrix cell has its own associated fracture cell. Figure 10 and Figure 13 shows how this works.

The contact area between the different matrix blocks is varied between full contact and no contact. When the contact point exists in the fine grid model, the grid cells have the properties of a normal matrix cell instead.

In the case where we used water injection we used the following initial conditions: The fractures are initially filled 100% with oil and the matrix blocks contain 75% oil and 25% water. In the case where we use gas injection the reservoir is initially 100% filled with oil.

In order to produce the system, a production well was placed at the top of the system, and a water injection well was placed at the bottom of the six matrix blocks. The production well had a restraint at 270 Bar as BHP. The injection well was set to a constant rate of $0.05 \text{ Sm}^3/\text{day}$. When gas is injected, the production well is placed at the bottom and the injection well at the top.

Figure 17 shows a nice representation of the geometry of the two test systems, both the single porosity and double porosity system.

4.2 Fluid and rock properties

(The PVT data is taken from Ole Torsæters project in fractured reservoirs 2011)

P_i	276	Bar
μ_w	0.35	Cp
μ_o	0.19	Cp
μ_g	0.024	Cp
ρ_w	1000	Kg/m ³
ρ_o	833	Kg/m ³
ρ_g	0.83	Kg/m ³
B_w	1	v/v
B_{oi}	1.5	v/v
B_g	0.0039	v/v
R_{si}	0	v/v
ϕ_m	0.3	fraction
k_m	4	md
ϕ_f	1	fraction
ϕ_f in DUALPORO model	0.006	fraction
k_f	10000	md
C_w	5.29E-05	1/bars
$C_{rm}=C_{rf}$	4.35E-5	1/bars
S_{wir}	0.2	fraction
S_{or}	0.25	fraction
k_{ro} at S_{wir}	1	fraction
K_{rw} at S_{or}	0.23	fraction

Table 5: Basic fluid and rock properties for oil-water imbibition

Imbibition relative permeability and capillary pressure in matrix rock for the water oil system			
S_w	k_{rw}	K_{ro}	P_c [bar]
0.2	0.0	1.000	3.448
0.25	0.005	0.860	0.621
0.3	0.01	0.723	0.138
0.35	0.02	0.600	0.034
0.4	0.03	0.492	0.000
0.45	0.045	0.392	-0.028
0.5	0.06	0.304	-0.083
0.6	0.11	0.154	-0.276
0.7	0.18	0.042	-0.690
0.75	0.23	0.000	-2.758

Table 6: Imbibition relative permeability and capillary pressure in matrix rock

Imbibition relative permeability and capillary pressure in fracture for the water oil system			
S_w	k_{rw}	K_{ro}	P_c [bar]
0	0	1	0
1	1	0	0

Table 7: Imbibition relative permeability and capillary pressure in fracture

Imbibition relative permeability and capillary pressure in matrix rock for the gas oil system			
S_g	k_{rg}	K_{ro}	P_c [bar]
0.05	0.0	0.95	0.007
0.10	0.03	0.90	0.010
0.15	0.05	0.85	0.013
0.20	0.09	0.80	0.015
0.30	0.18	0.723	0.021
0.40	0.28	0.492	0.035
0.50	0.39	0.304	0.052
0.60	0.50	0.154	0.080
0.70	0.64	0.042	0.130

Imbibition relative permeability and capillary pressure in fracture for the gas oil system			
S_g	k_{rg}	K_{ro}	P_c [bar]
0	0	1	0
1	1	0	0

The capillary pressure and relative permeability curve shows us that we have a waterwet/mixed wet reservoir. In such a reservoir both spontaneous imbibition and imbibition forced by gravity will be recovery mechanisms. Traditionally the relative permeability for the fractures is assumed equal to the saturation, and no capillary pressure is assumed, this is in my simulations referred to as the original file.

4.3 Case studies

Three different studies were conducted.

Case 1.1 was to observe how a stack of matrix blocks reacted to nonlinear fracture permeability when water injection was used.

Case 2.1 and Case 2.2 was to observe how a stack of matrix blocks reacted to fracture capillary pressure when water injection and gas injection was used, respectively.

Case 3.1 and Case 3.2 was to observe how a stack of matrix blocks with capillary continuity reacted to fracture capillary pressure, for both gas and water injection.

All this cases were also subjected to a comparison between the fine grid solution and the dual porosity solution.

4.4 Non straight fracture relative permeability

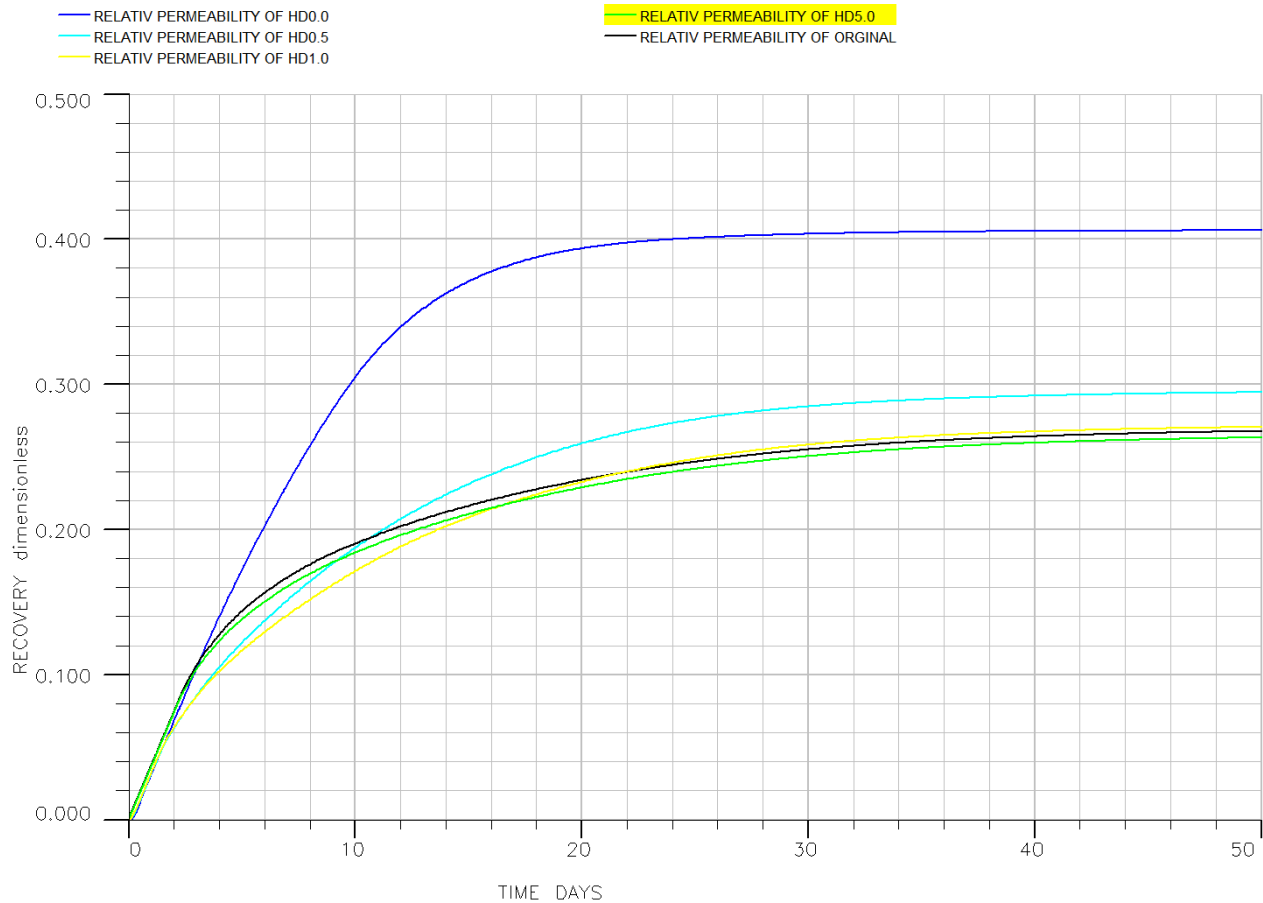


Figure 20: Case1.1 Recovery with a change in the fracture relative permeability curve.

In the above figure we have changed the relative permeability curve of the fractures in the single porosity model. From this figure we could see that the effects of a lower relative permeability in the fractures is that we get a higher recovery, but it is small differences in the recovery when H_D is one, or bigger. A big part of the increased recovery for $H_D=0$ is due to that the viscous forces gets bigger, and therefore gives an increased recovery. When the relative permeability of water is reduced, we will need a bigger force to push the water through the system. This increases the injector BHP and gives us an increment in the viscous forces. In a real fractured reservoir, the production time is expected to be much higher, and the injection rate for a fractured reservoir is not expected to play a major role in the recovery process. Therefore the effect of changed relative permeability may not be so pronounced as these graphs shows. The next graph shows the recovery difference when the same system is exposed to different injection rates and the relative permeability is hold like the one for $H_D=0.5$ (BHP is held the same).

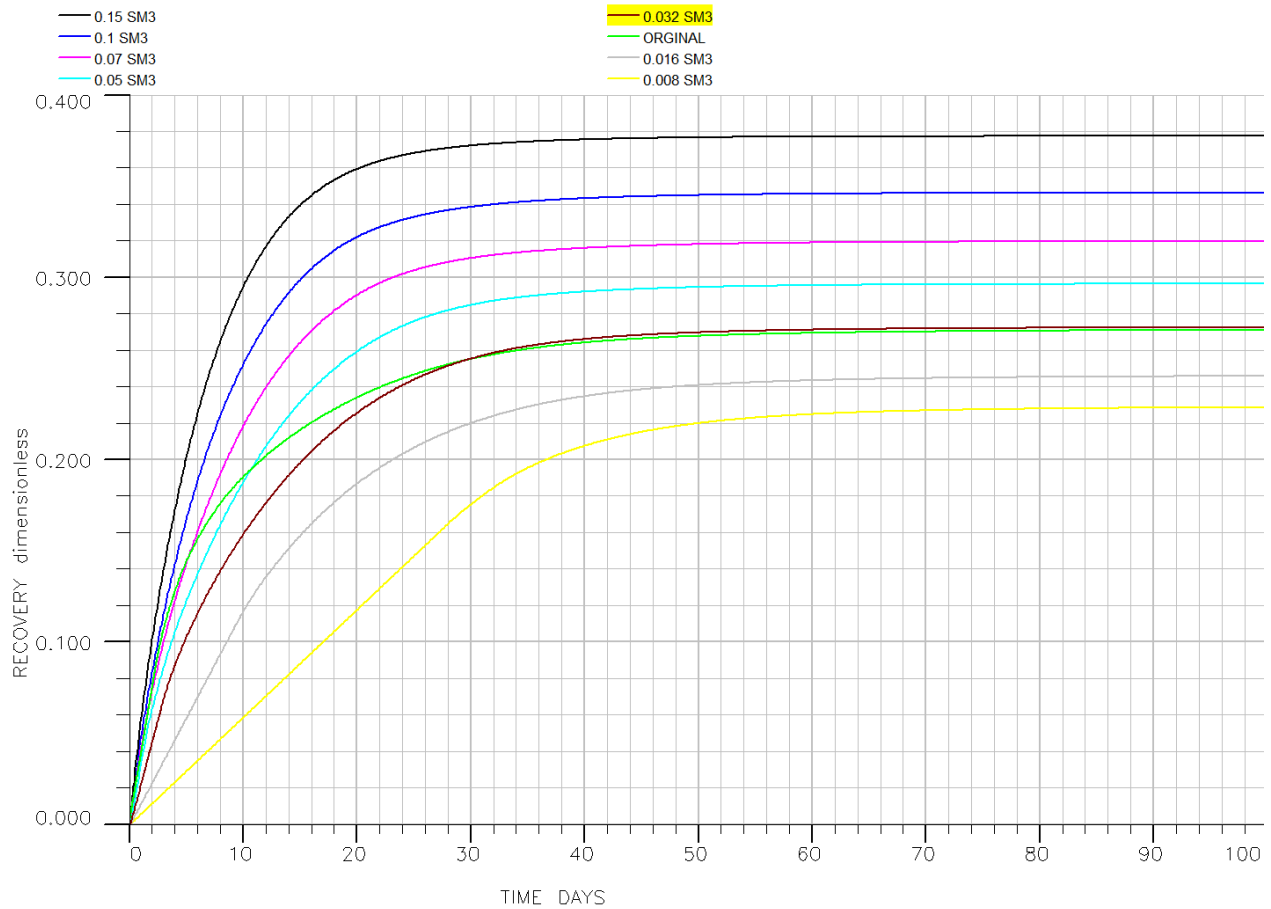


Figure 21: The recovery graph for $H_0=0.5$ and different injection rates for the single porosity system.

In the above figure we have exposed the single porosity model for different water injection rates. This confirms that the injection rate makes a difference in the final recovery. When a high injection rate is applied, this implies a higher pressure gradient for the system and therefore the viscous forces get bigger.

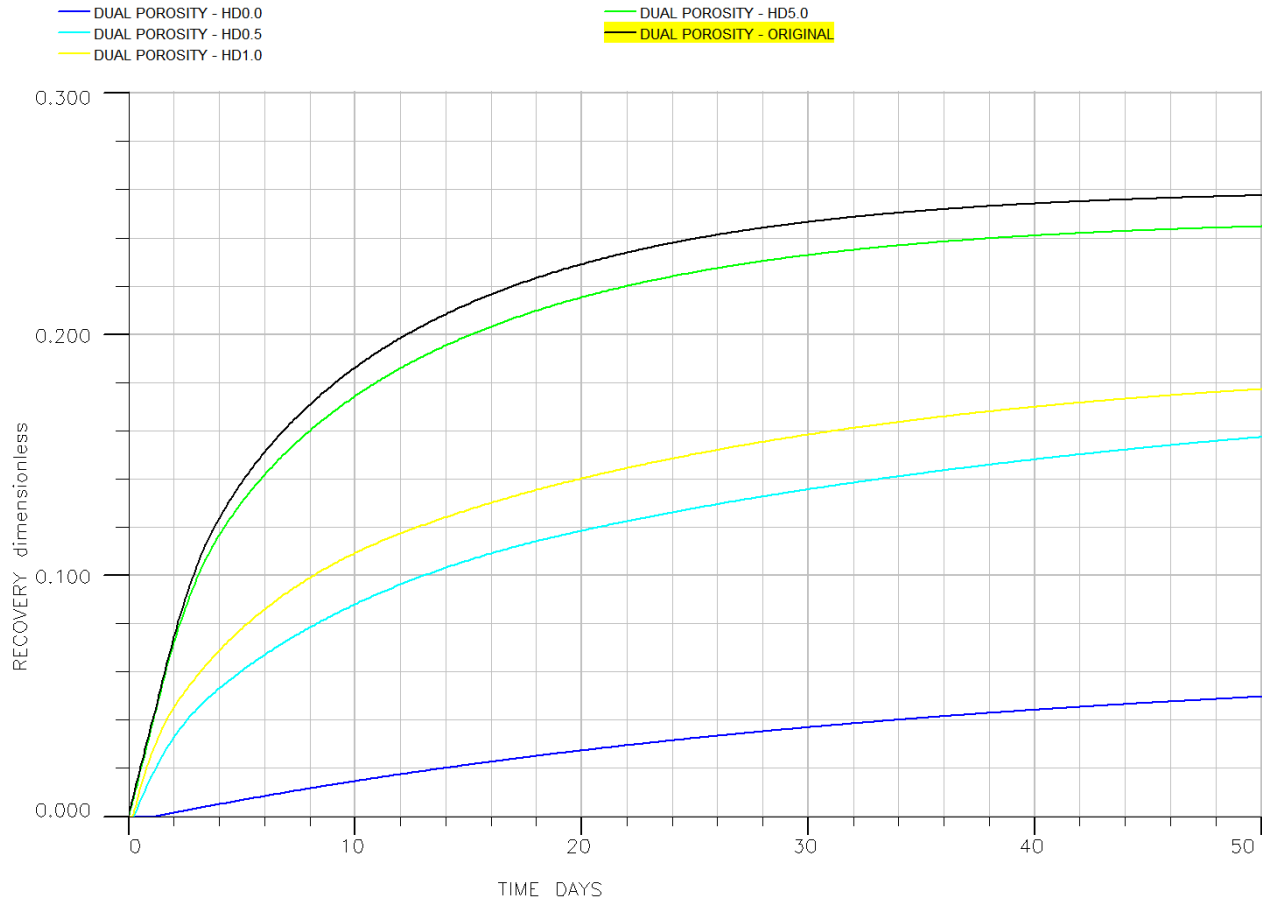


Figure 22: Case 1.1.1: Relative permeability is changed in a dual porosity system.

In this system we have simulated the same as in Case 1.1, but now a dual porosity model is used. In this case the dual porosity system behaves very different from the single porosity system. We get a decrease in recovery for low H_D numbers. This is because that the matrix rock in a dual porosity (DUALPORO) system not is affected by viscous forces. The recovery mechanisms in a DUALPORO run is oil expansion, imbibition and forced imbibition/drainage. Viscous forces are normally not modeled, but there is a possibility to turn this function on (VISCD). The reduced production for low H_D numbers is caused by that we now have irreducible oil saturation in the fractures. Originally we were able to produce all the oil from the fractures, but this irreducible oil saturation makes some of the oil remain. In the next figure we also see the big difference between the dual porosity system and the single porosity system when we look at the sensitivity to injection rate. While the single porosity model is highly affected by the injection rate the dual porosity systems recovery is not affected.

The effect of using the VISCD keyword to measure viscous forces is shown in Figure 41 in Appendix1.

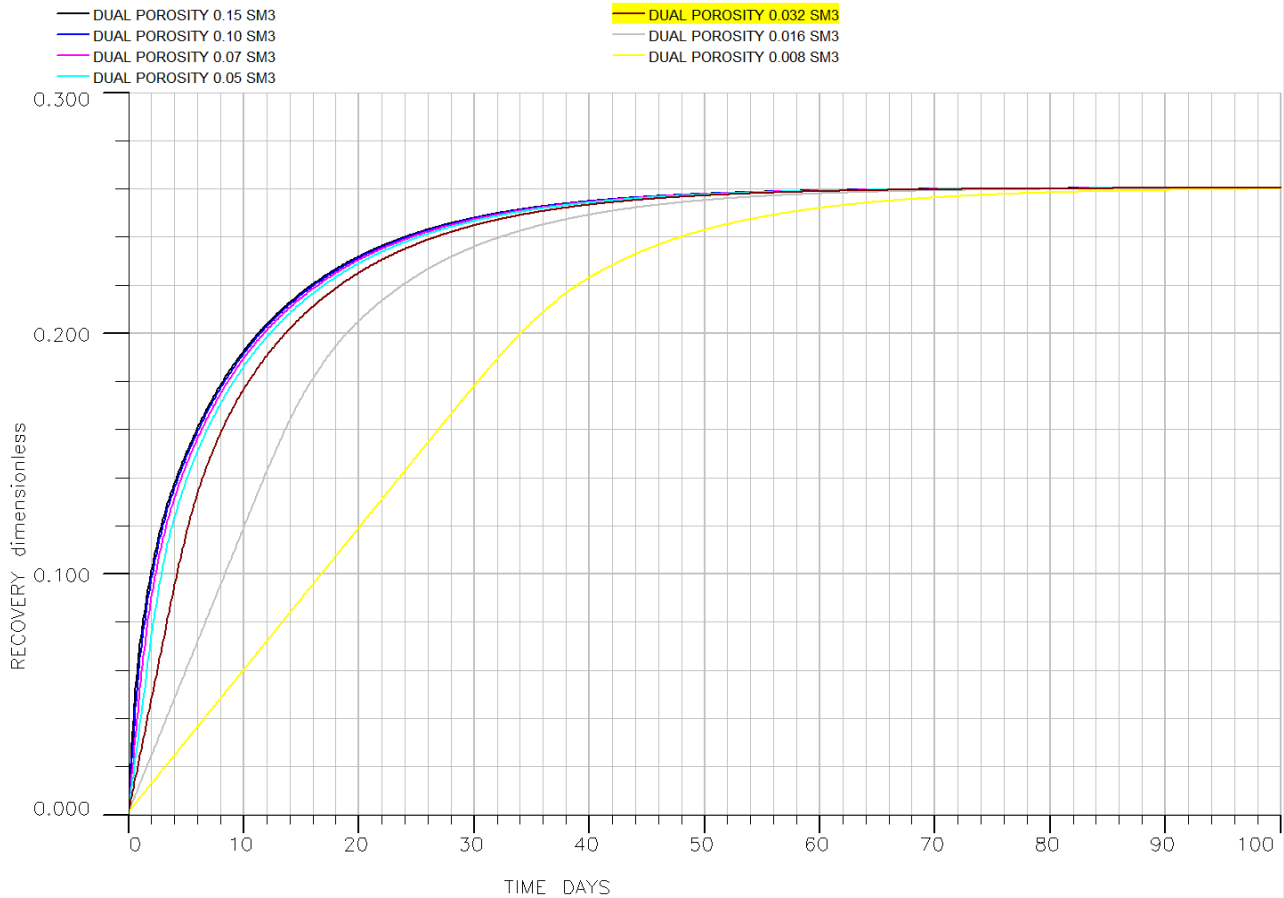


Figure 23: The comparison in injection rate shows us that the dual porosity model does not model viscous forces in matrix blocks.

In Figure 21 we saw that the single porosity model is affected by injection rate. This does not affect a dual porosity system, since recovery here is explained by gravity equilibrium with the fracture cells. Since irreducible oil in the fractures made a decrease in the recovery, it would be interesting to see how much of the oil that is made unrecoverable by changed fracture relative permeabilities. The decreased recovery for low H_D values is also seen in the single porosity model, but only for very low injection rates as viscous forces gets small. Figure 42 in Appendix1 shows this.

Since lowered H_D values makes a bit of the oil in the fractures irreducible we will look into where the reservoir oil is stored to see if we could understand the lowered recovery. The matrix block is 1m^3 , has 30% porosity, original oil saturation of 0.75 and its final saturation is 0.6 (assumed no forced imbibition). This gives each matrix block 0.045m^3 recoverable oil [$1\text{m}^3 \cdot 0.3 \cdot (0.75 - 0.6)$]. The fractures have a porosity of 0.006, which gives a storage capacity of 0.006m^3 . The fraction of recoverable oil in the fractures is therefore 0.12 [$0.006 / (0.045 + 0.006)$]. This is a considerable amount, and if some of the fracture volume is unable to produce, a significant reduction in recovery is expected. In addition, lower relative permeability makes the production go slower, so that final recovery takes longer time to obtain.

4.6 Capillary pressure in fractures

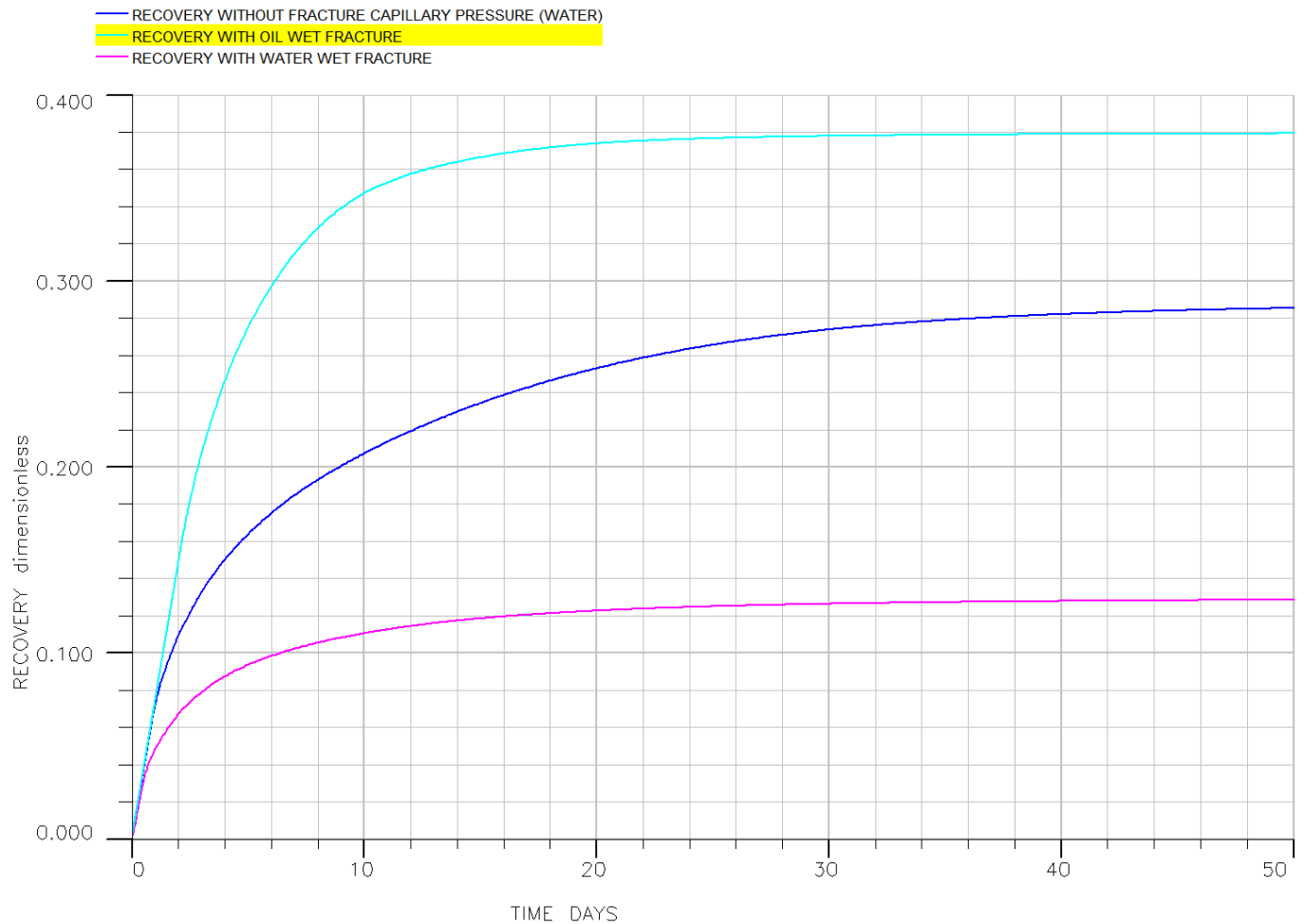


Figure 24: Case2.1 shows recovery with water injection and capillary pressure in the fractures. $P_c = \pm 10$ kPa

In the case of fracture capillary pressure for the water injection case, we could see that the fracture capillary pressure could both increase and decrease the final recovery. The increase in recovery depends on the wettability of the matrix rock and fracture.

In this case the matrix rock was mixed wet, and the recovery could be affected both positively and negatively of fracture capillary pressure. If the fracture were water wet it would prefer water inside, and oil coming from the matrix would have a harder time to enter the fracture. However, if the fracture is oil wet it would prefer oil inside and oil could easier leave the matrix. In this test case the fracture capillary pressure is set to a constant value of either 0.1Bar or -0.1 Bar, this number was somehow randomly chosen, and if a smaller value were chosen it would have been less difference between the three cases. When we set the fracture capillary pressure in the gas injection cases the same value is chosen. A fracture capillary pressure of 10kPa should be well below maximum obtainable fracture capillary pressure, as some authors have realized capillary pressures as high as 275kPa (Firoozabadi, A and Hauge, J, 1990).

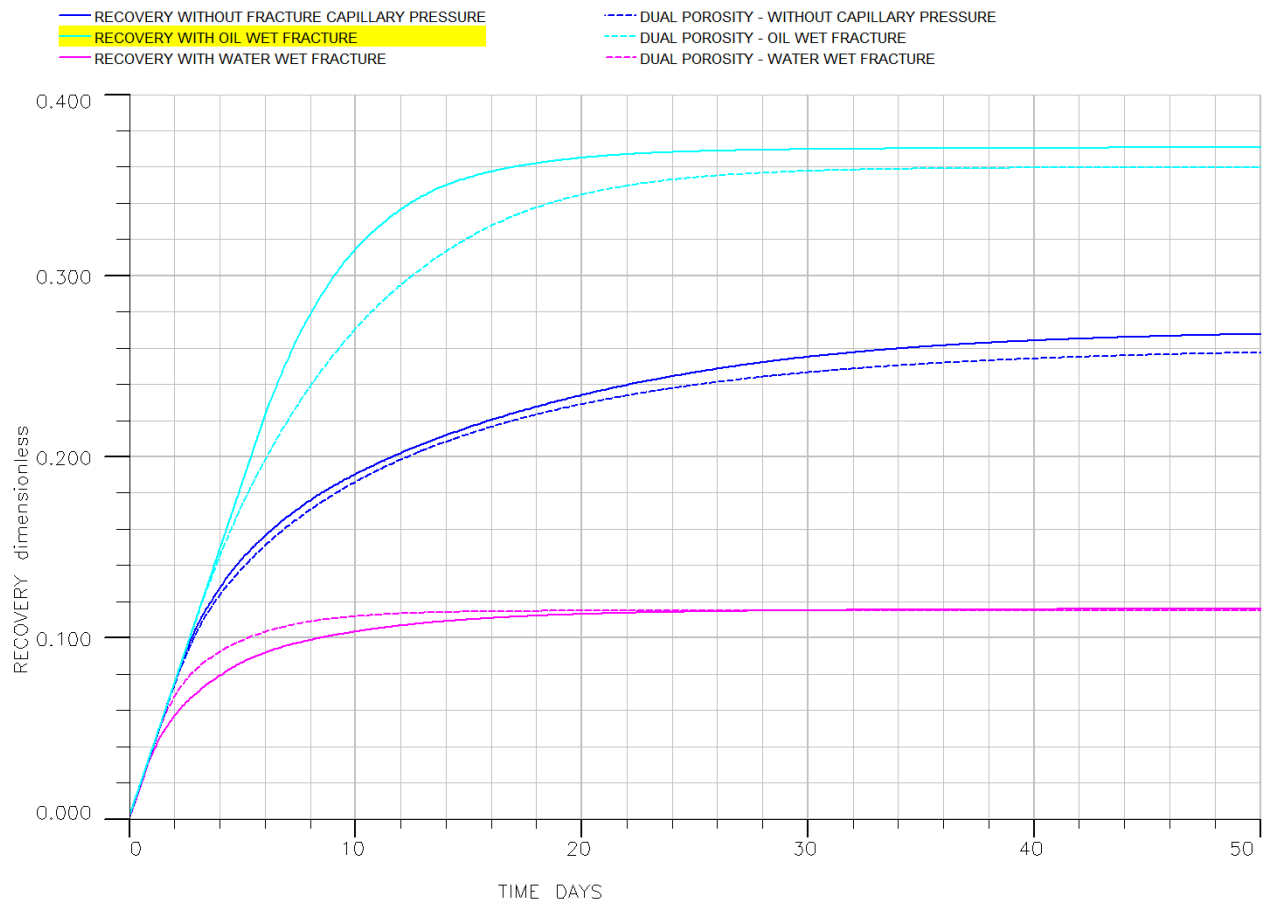


Figure 25: Case1.1.2: Comparison between the dual porosity and single porosity model.

Since full scale fractured reservoirs normally is modeled with a dual porosity system it is important to see how well the dual porosity model is able to fit the single porosity model. In the comparison between the two models we could see that they have a reasonable good agreement and we could conclude that the dual porosity model models fracture capillary pressure correctly in the above case.

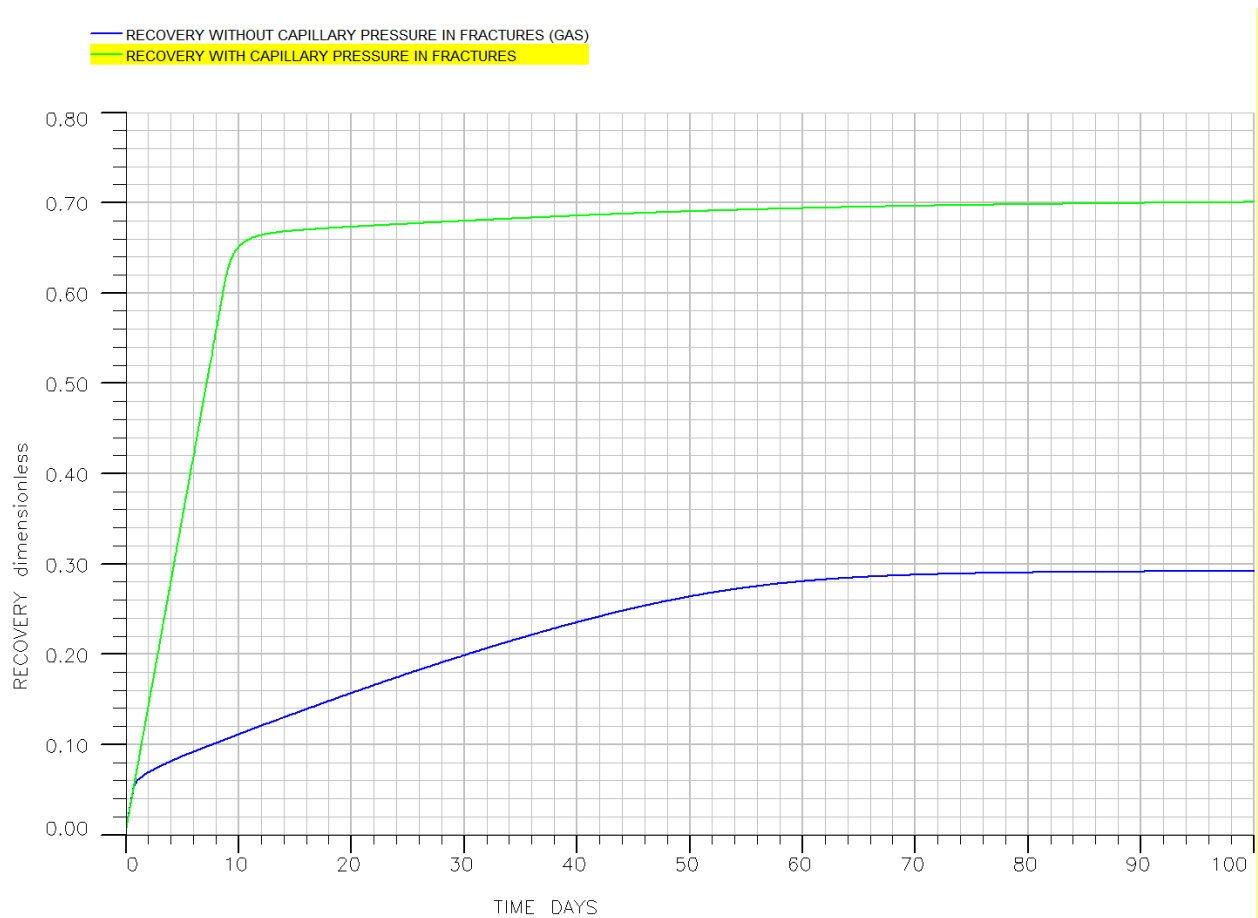


Figure 26: Case2.2 shows recovery with gas injection and fracture capillary pressure in the fractures (10kPa).

In the above figure gas injection is done for a reservoir with and without capillary pressure. In general the fracture capillary pressure plays a more important role in a gas injection case, and in this case, the recovery is more than doubled. The capillary pressure curve of the matrix rock will however affect how important fracture capillary pressure is. In this case, fracture capillary pressure gives a high increase in the final recovery, approximately twice as high as originally. For intermediate high blocks, this case really shows how big difference the capillary pressure in a fractured reservoir could have. The increased recovery is due to the additional capillary pressure that the matrix rock is exposed to when we have the fracture capillary pressure (a fracture capillary pressure of 10kPa is set).

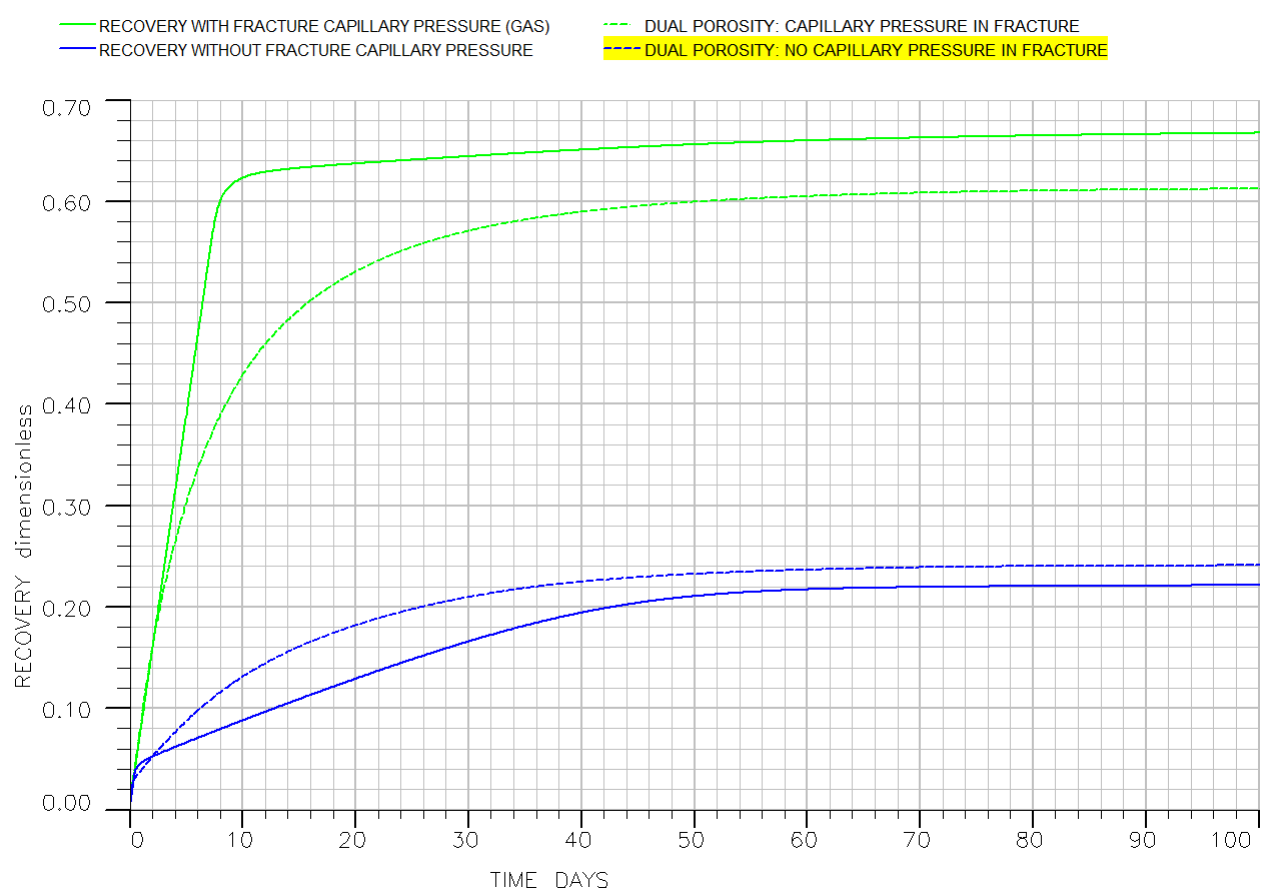


Figure 27: Comparison between the dual porosity model and single porosity model for a gas injection case.

Above we have compared the results for the dual porosity model and the single porosity model for a gas injection case. In the comparison between the two models we could see that they have a good agreement.

Conclusion: The dual porosity simulation gives good results for both water and gas injection, both in the case of fracture capillary pressure and without it.

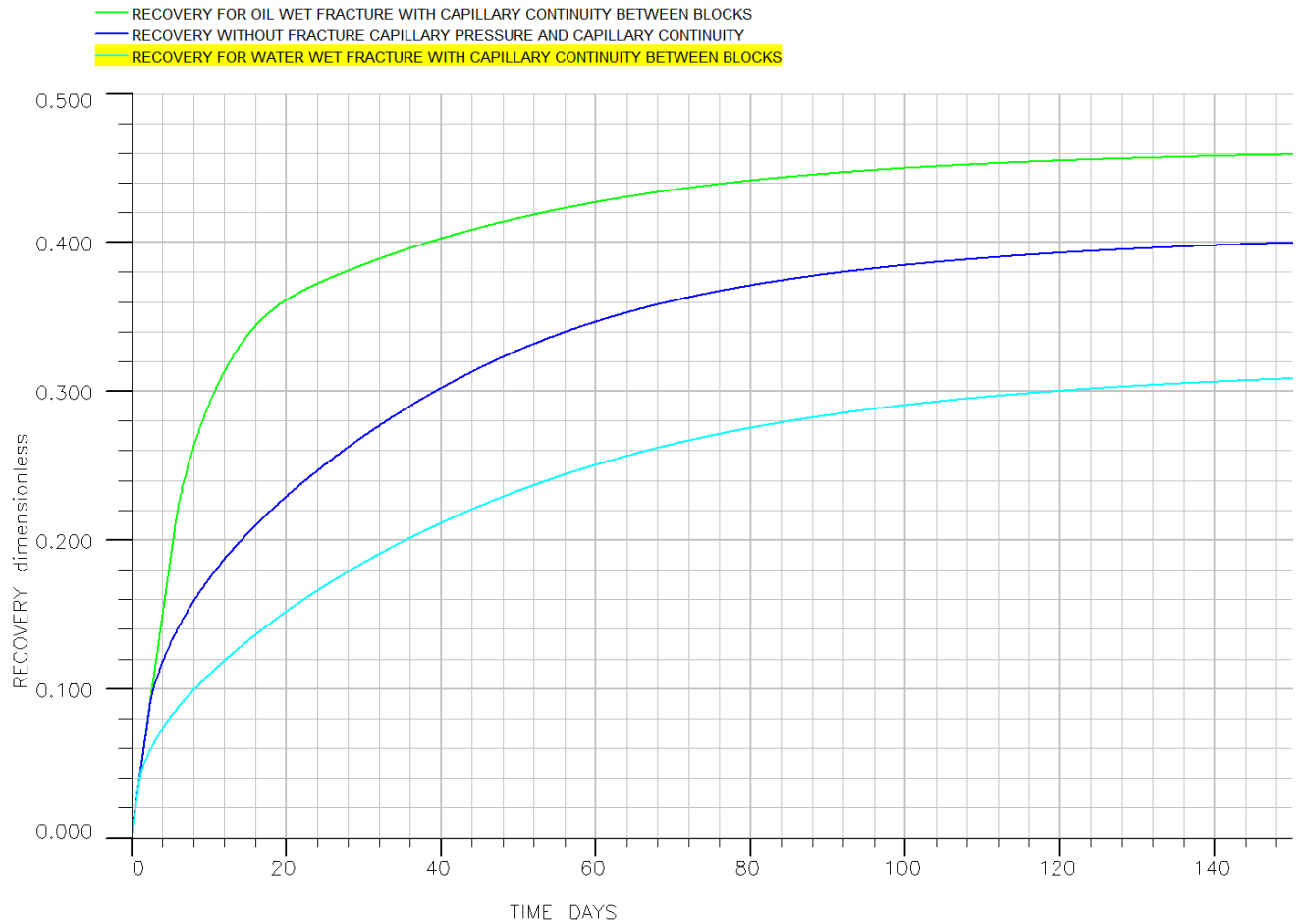


Figure 28: Case 3.1 Recovery for six blocks with capillary continuity, fracture capillary pressure and water injection

This graph shows the recovery for six blocks with capillary continuity in the single porosity model in case of water injection. We could see how fracture capillary pressure affects this system. Six blocks that are 1 meter high with capillary continuity between them could be looked at as a system where block height is six meters. We could see that we have similar tendency as we had in the case of 1 meter high blocks, but now the recovery is higher. This is because the increased capillary pressure will help us to drain more of the oil.

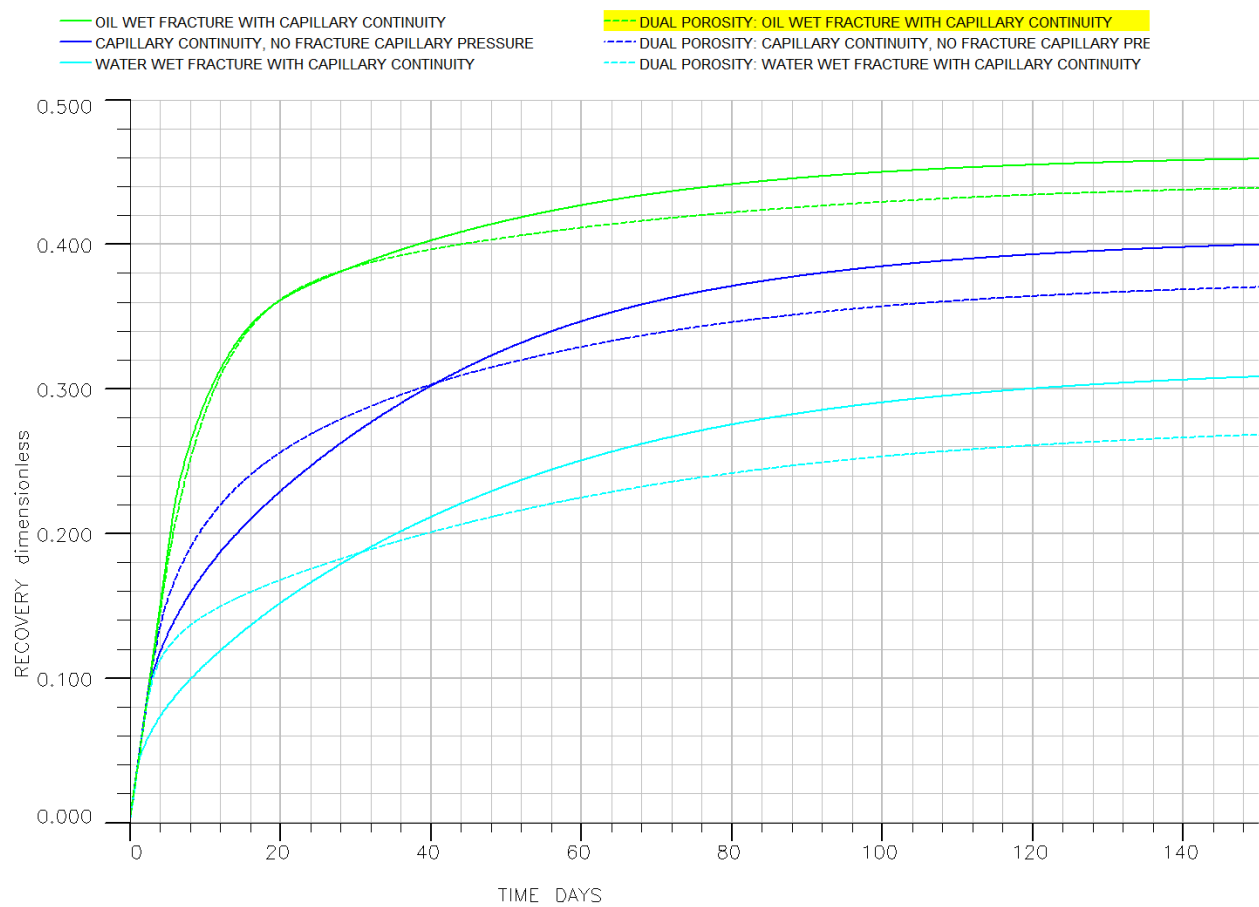


Figure 29: Comparison between the dual porosity model, and single porosity model, when we have water injection and capillary continuity.

Also in the case of capillary continuity the dual porosity model is able to give reasonable good results.

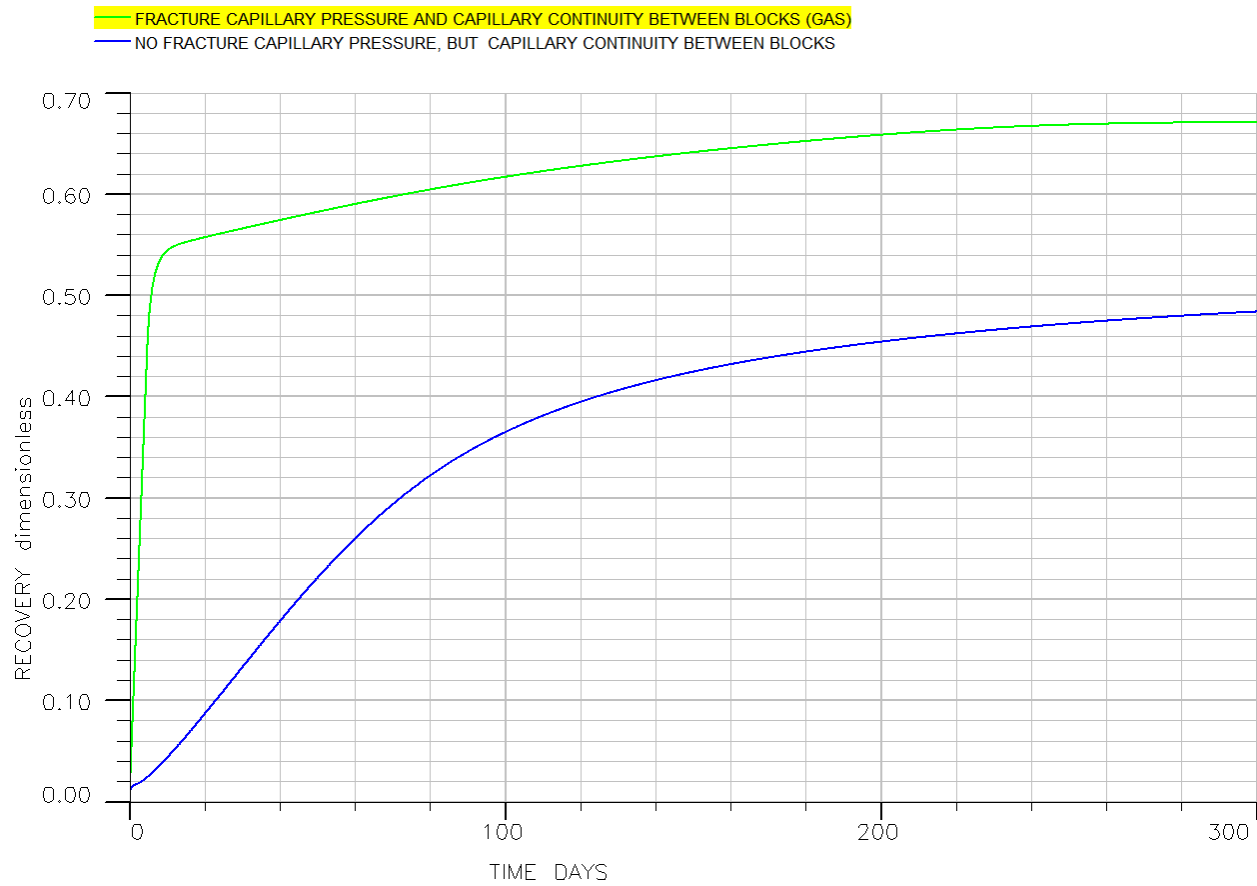


Figure 30: Case 3.2 Recovery for six blocks with capillary continuity, fracture capillary pressure and gas injection

This graph shows the recovery for six blocks with capillary continuity and gas injection. The final recovery in the case of fracture capillary pressure is similar to as if we had only one block, but the final recovery for the case of no fracture capillary pressure is greatly increased when we have capillary continuity.

This shows us that the height of the matrix blocks are important. For tall matrix blocks the effect of fracture capillary pressure is reduced, and the recovery differences between the two scenarios gets smaller. This was also observed in the water injection case.

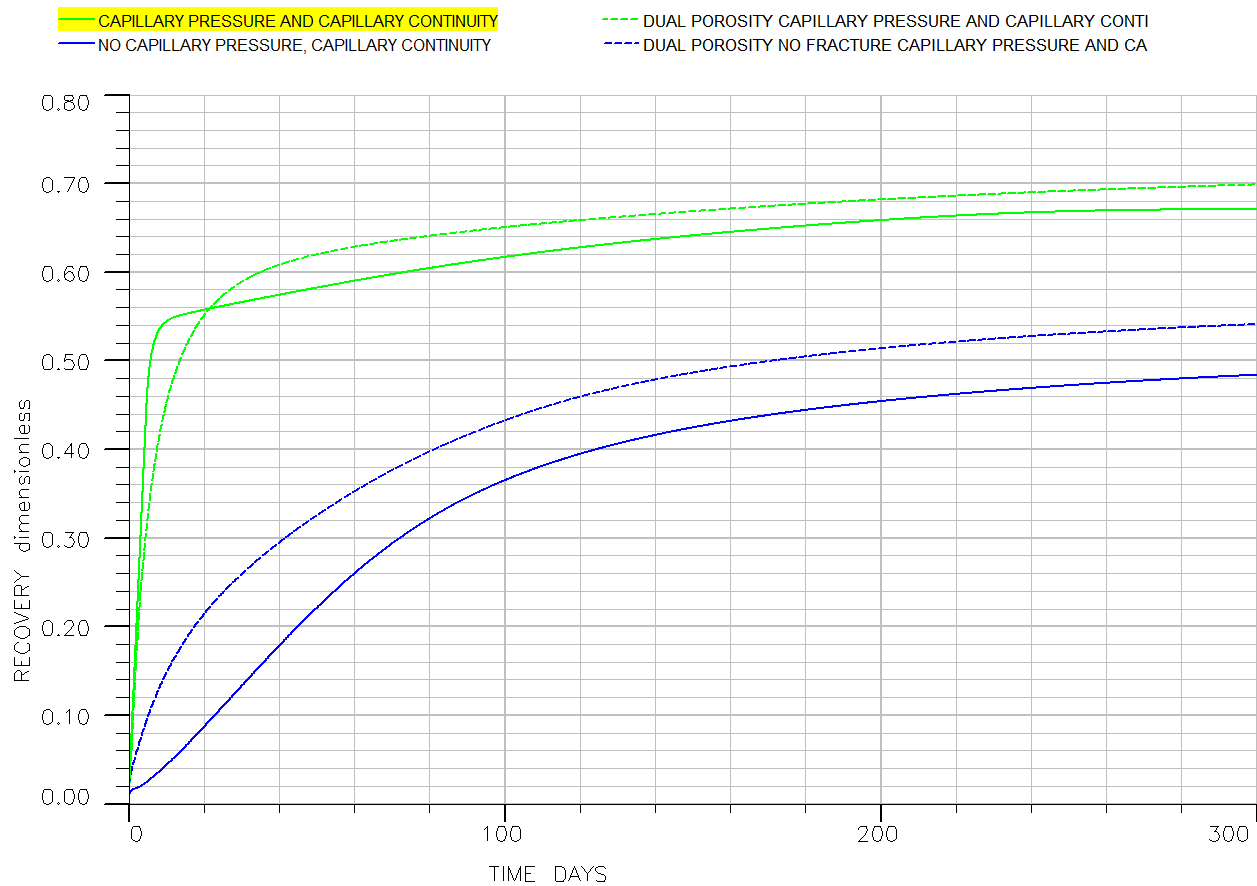


Figure 31: Comparison between the dual porosity model, and single porosity model, when we have gas injection and capillary continuity.

The above figure is a comparison between the dual porosity model and single porosity with gas injection and capillary continuity between blocks. Fracture capillary pressure is on (green plots) or off (blue plots). Once again, the dual porosity model gives a similar result as the single porosity model, which shows that we have a good agreement between the different simulators.

4.7 Summary from test model

In short my test simulations discovered that there is a huge difference in recovery made when we assume a capillary pressure in the fractures, compared to when we not have capillary pressure in them. Both the water injection and the gas injection case get an increase in recovery, but the improvement is more pronounced for the gas injection case. This is because fracture capillary pressure helps drainage by gravity, which is the most important recovery mechanism for a gas injection case.

The difference in relative permeability did not seem to give clear results. For high injection rates it would increase the recovery in the single porosity model, but if we had low injection rates it would lower the recovery because some irreducible oil would be left in the fractures. For the low injection case, the difference in recovery between the different relative permeabilities were however small.

To check if these problems were possible to simulate in a dual porosity model we checked how the results varied when we compared it to the single porosity model. The results were that the dual porosity model was suitable to simulate fracture capillary pressure, but when we had a different relative permeability curve the results were a bit more confusing. Since the dual porosity model (DUALPORO) not take the viscous forces into account we saw that we got erroneous results when we had a high injection rate. For a low injection rate the results is however in agreement. Since the viscous forces in general not play an important role for fractured reservoirs, and low pressure gradients is the most common we could say that the relative permeability modeling with DUALPORO also works acceptable.

In Appendix3 the dual porosity model also showed that it was able to handle upscaling very well. In the case were a homogenous reservoir with 125.000 matrix blocks went from being simulated with 125.000 grid cells to 125 grid cells no mismatch between the cases was observed at all. This is very positive for the dual porosity system, since a real reservoir get simulated with much more than 1 matrix block in each grid cell.

4.8 Conclusion from test system

Based on the literature study and the results of the simulation, the following conclusions are made:

Water-oil system:

The conclusion on non-straight fracture relative permeability curves is confusing, but we are likely to leave more oil in the fractures when we get irreducible oil there. This will reduce recovery, but higher viscous forces in the system might increase recovery. The effect of non-straight fracture relative permeability curves are better seen in a full-scale reservoir, where effects of different layers, heterogeneity and economical values are evaluated.

For the fracture capillary pressure it was shown that fracture capillary pressure could both increase and decrease the recovery, depending on which phase that is preferred in the fractures. The effect is however not as big as for a gas oil system.

Gas-Oil system:

There is acceptable to use straight line relative permeability curves in the fractures, since the high density difference and low interfacial tension is enough to ensure that gravity forces will dominate over capillary forces.

For the fracture capillary pressure it was a huge increase in the recovery. It was shown that fracture capillary pressure helped to overcome the threshold pressure and thereby was able to increase the recovery dramatically.

Capillary continuity:

The water-oil and gas-oil system both positively increased their recovery when they experienced capillary continuity. The effect of capillary continuity reduced the effect of fracture capillary pressure, but the recovery was still larger than without fracture capillary pressure. This is because we get close to irreducible oil saturation at the bottom/top of the matrix column when they have capillary continuity. The effect of capillary continuity is the same as if we had taller matrix blocks, so for reservoirs with very tall blocks fracture capillary pressure might be unimportant.

5. The full sized reservoir

We have now seen how altered fracture properties affected the test system, but we need to see how it affects a full size reservoir. A real reservoir is much more complex than the previous test example, so for a real reservoir we would need to examine and think of other problems that might occur. Important differences between the full-scale reservoir and the test example are that the full-scale reservoir is heterogeneous, contains dissolved gas and that it has other matrix and fracture properties.

The full reservoir that I have chosen to do my simulations on is the reservoir that is used in the sixth SPE comparative study. A full description of this reservoir is given in Appendix2.

Water injection

Design: For all cases when water is injected the injection well is perforated in layer 1-5 while the production well is perforated in layer 1-3. The production well is limited to 1000 STB/D of total liquid(s) production. The injection well is constrained by a maximum injection rate of 1750 STB/D water or 6100psig injection pressure.

If we expect the results of the full-scaled reservoir to be similar to the results we obtained in the test example we might be a bit surprised. In a real reservoir we have many things that we have to consider and unexpected things might happen. In this reservoir the oil contains dissolved gas. This makes a mayor difference from the test case.

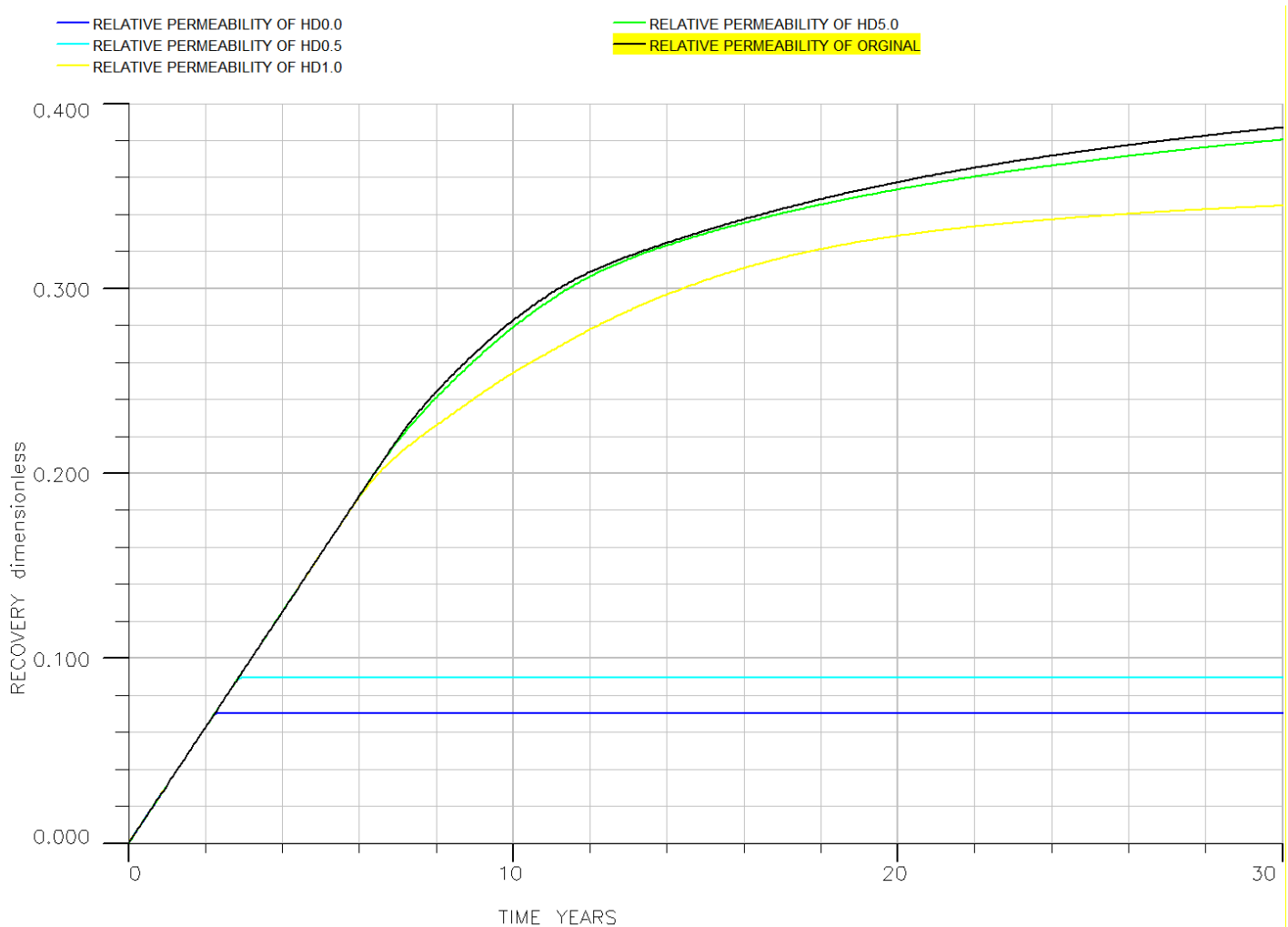


Figure 32: Recovery vs. time in a full-scale reservoir and different HD-values

In Figure 32 we could see a slightly lowered recovery for the cases where H_D is 5.0 or 1.0. This has the same reason behind it as it had in the much smaller test example. In the test case we concluded that the reduced recovery was due to irreducible oil in the fractures. Although most of the porosity is in the matrix, a significant fraction of the recoverable oil is in the fractures. If no forced imbibition happen the

matrix saturation will go from 0.8 to 0.6, and the fracture oil saturation will go from 1 to 0. Since fracture porosity is 0.01 and matrix porosity is 0.29 this means that 15% of the total recoverable oil is in the fractures $[0.01/(0.01+(0.29)(0.8-0.6)]$. If a part of this 15% gets irreducible this would obviously give a reduced final recovery. There are only minor differences between the straight-line relative permeability plots and the one when H_D is 5. This indicates that there is no need to use H_D values bigger than this.

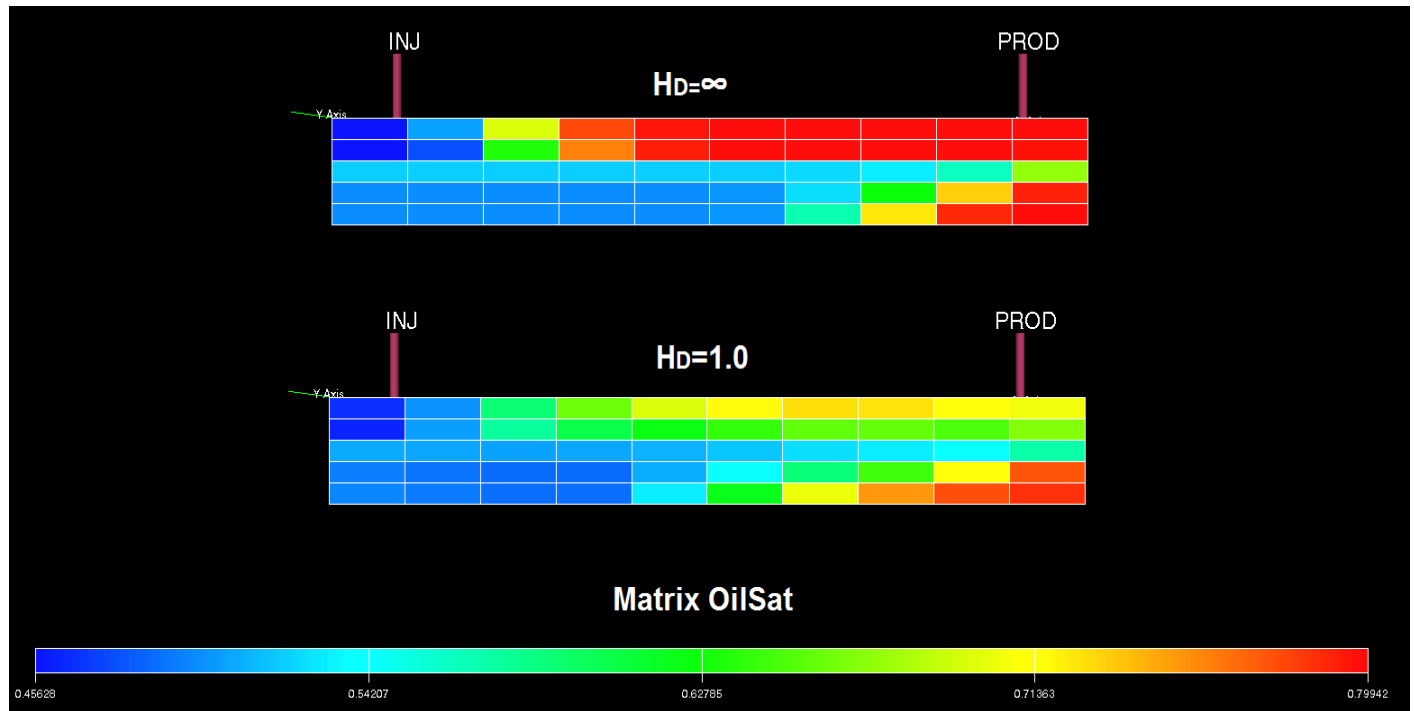


Figure 33: When we look at the recovery in each block after 5 years of production we could see that the sweep for $H_D=1.0$ is improved. This means that the waterfront is moving more equally in all layers in the reservoir.

Above is a picture where we could see how reduced H_D could affect the sweep. Layer 3 is a highly permeable layer, and normally water breakthrough is expected to occur here first. The sweep efficiency is interesting and show other, maybe unexpected, aspects of what could happen when the relative permeability curves is reduced. After 5 years of production, when both the models still have the same recovery, we could see that the sweeps work different from in the original file. When we have a H_D value of 1 we could see that the waterfront moves more evenly. The improved sweep happens as reduced water permeability in the lower layers makes the water flow in the two upper layers. Figure 44 and Figure 45 in Appendix1 shows plots of this.

The recovery for H_D 0.0 or 0.5 is enormously decreased. The production well is set to produce 1000 STB of liquid without any restriction on drawdown, as the case is for the SPE6 paper. This makes a given drawdown, if the flow of liquids is hindered by a decrease in relative permeability we will need a larger drawdown to obtain this rate. This is what happens when $H_D=0.0$ or 0.5. This large drawdown makes gas flow freely into the well and reservoir pressure falls and the set production impossible. This makes a big portion of the oil left unrecovered. Next figure shows what happens to the gas production rate, in this case we get very high gas production rate for low H_D values.

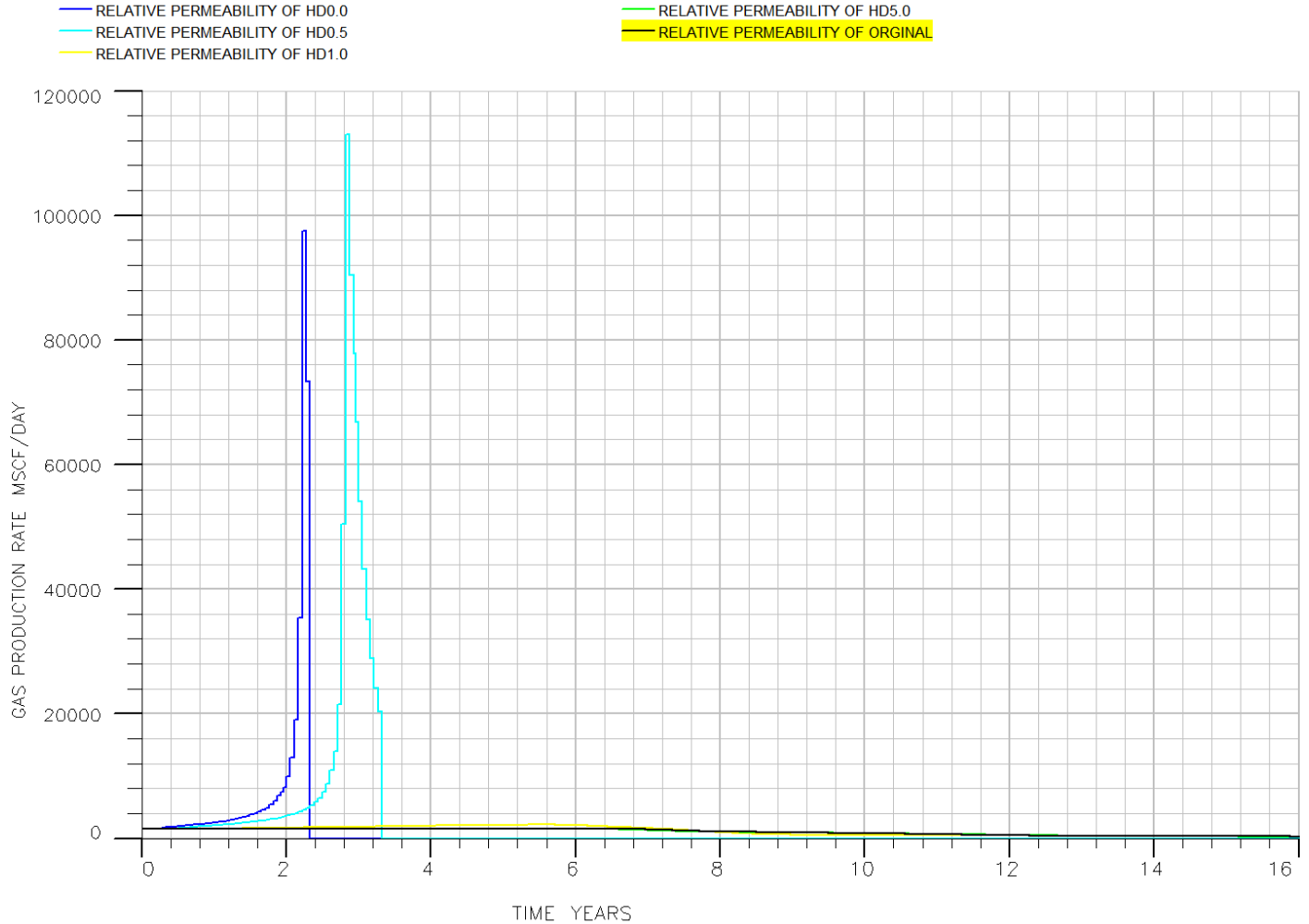


Figure 34: Gas production rate explode when low relative permeabilities applies

The high gas production rates makes the reservoir pressure shrink dramatically and it is impossible to keep the production up. In real life, a realistic way to handle this problem could have been to lower the drawdown or maybe even stop the production completely once they realized that they got a gas breakthrough. In this way we might have been able to avoid a big gas production. This would however mean a big reduction in the production rate, and the economic loss of this could be large. A realistic way to predict this behavior would in any case be preferable, so that a production stop is avoided.

Figure 43 in Appendix1 shows how the reservoir pressure decreases when gas production occurs.

The gas breakthrough happens because we need a big drawdown to produce the given amount of liquid. If the gas breakthrough was caused by the big drawdown that was made, we would expect that the same could happen in a scenario where horizontal permeability is decreased. Figure 46 in Appendix1 shows

the effect of decreasing the horizontal permeability. Originally the K_V/K_H ratio was 0.1, when this ratio increased by decreasing the horizontal permeability (K_H) we saw that the gas breakthrough happened when K_V/K_H was around 1. This shows that a decreased relative permeability could give similar results as decreased fracture permeability.

Natural depletion

Design: In this case we have no injection well and the production well is only perforated in the lowest layer of the reservoir (fifth layer). Production rate is set to a maximum drawdown of 100psi or 500 STB/day.

In the water injection case we saw that it was important to avoid gas production as the reservoir pressure would fall dramatically and oil production would be impossible. In a reservoir without any injection the reservoir pressure would undoubtedly shrink fast. In such a situation it is of paramount importance to avoid water and gas production since this will reduce the reservoir pressure. In this case there is no free water, but dissolved gas would be freed when the pressure decrease below the bubble point. It is important to avoid production of this gas to keep reservoir pressure up.

In the case of natural depletion we will see how reservoir behavior changes when we have fracture capillary pressure or non-straight fracture relative permeability curves.

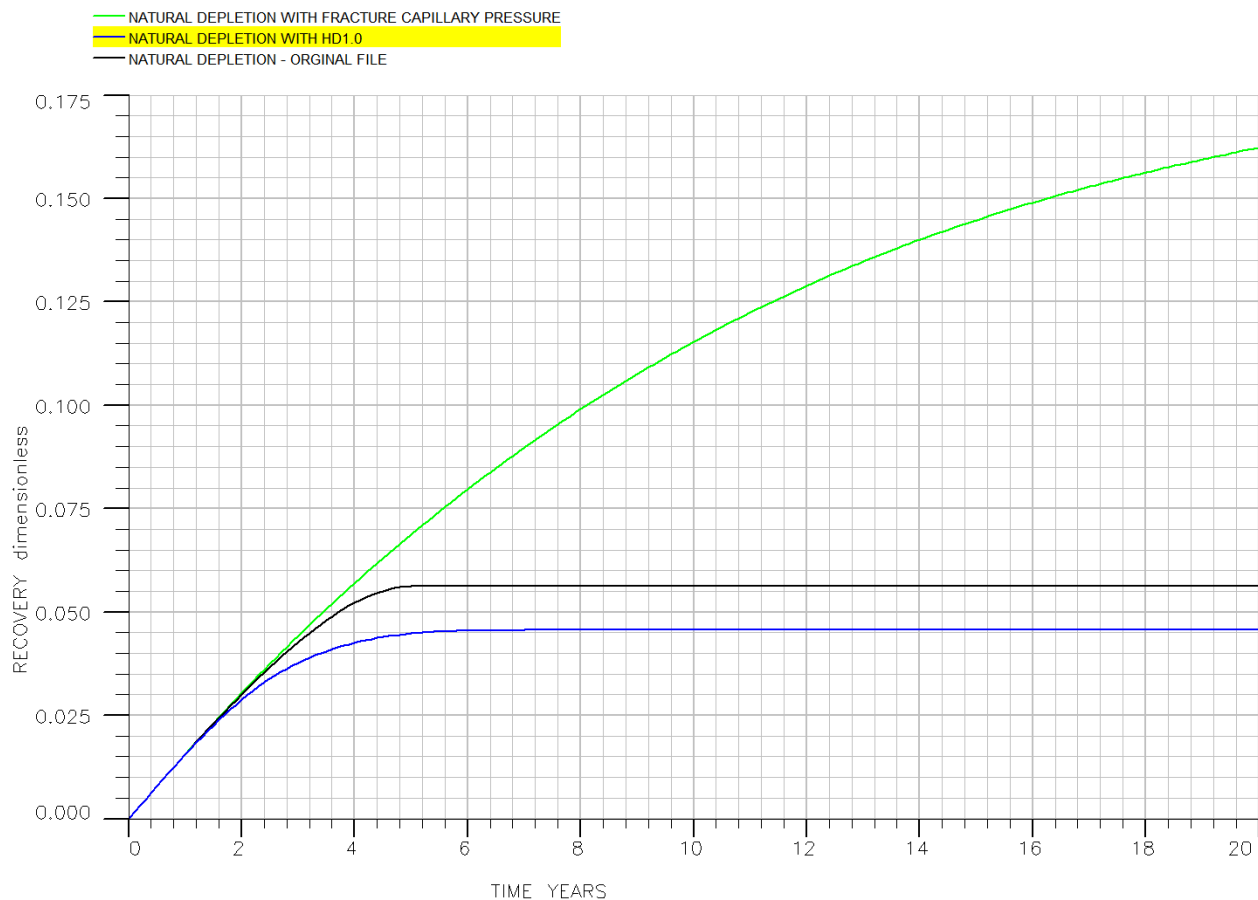


Figure 35: Recovery is shown for different natural depletion situations. All three situations get low recoveries.

In the above figure we could see that we have very low recoveries for all three cases when we don't have any injection. Only in the case where we have fracture capillary pressure (Table 9 in Appendix2) we get an acceptable final recovery of about 18%, but this is still just about half of what we recovered when we had water injection.

The situations where we get the lowest recovery is when we have a fracture relative permeability reduction ($H_D=1$), and the second lowest is when we have straight-line permeabilities without fracture capillary pressure (original file). Both this situations gives however very small final recoveries of around 5%. In the below figure we try to investigate why the recovery get so small. It is clear that the production life in case of fracture capillary pressure is very large compared to the two other cases. While we could produce oil for more than 20 years with fracture capillary pressure, the production will end after only 5 years if we don't have that.

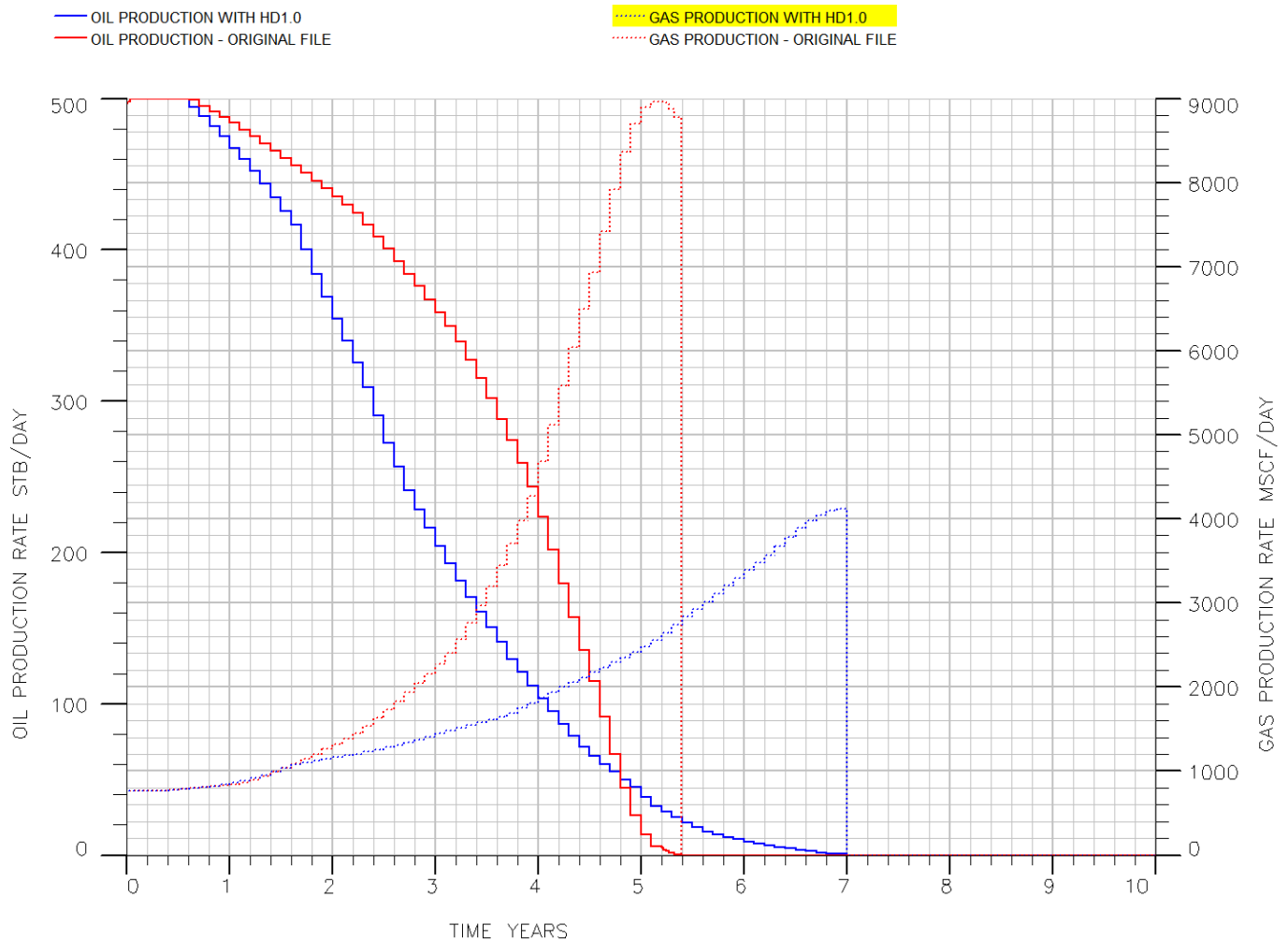


Figure 36: Oil and gas production rate.

In the above figure we observe that the oil production rate falls when the gas production rate increase. We learned from the water injection case that a high production rate makes a high drawdown and we could expect that the gas production would happen of the same reason in a natural depleted reservoir.

Figure 37 show how much the recovery increase when the maximum production rate is set from 500 STB/D to 300 STB/D. If production occur with 500STB/D we get a higher oil recovery in the beginning of

production life, but final recovery is lower and for the original file the final recovery increase as much as 30% with this reduced rate. The most favorable production rate is decided upon which rate that seems to be most beneficial economically. It is however clear that it is huge differences between the three cases in general. The increase in recovery for Figure 37 show how important well planning and reservoir understanding is. The three cases are very different from each other, and the oil production may be very different from what we predicted if we wrongly choose to simulate the reservoir without for example the use of fracture capillary pressure.

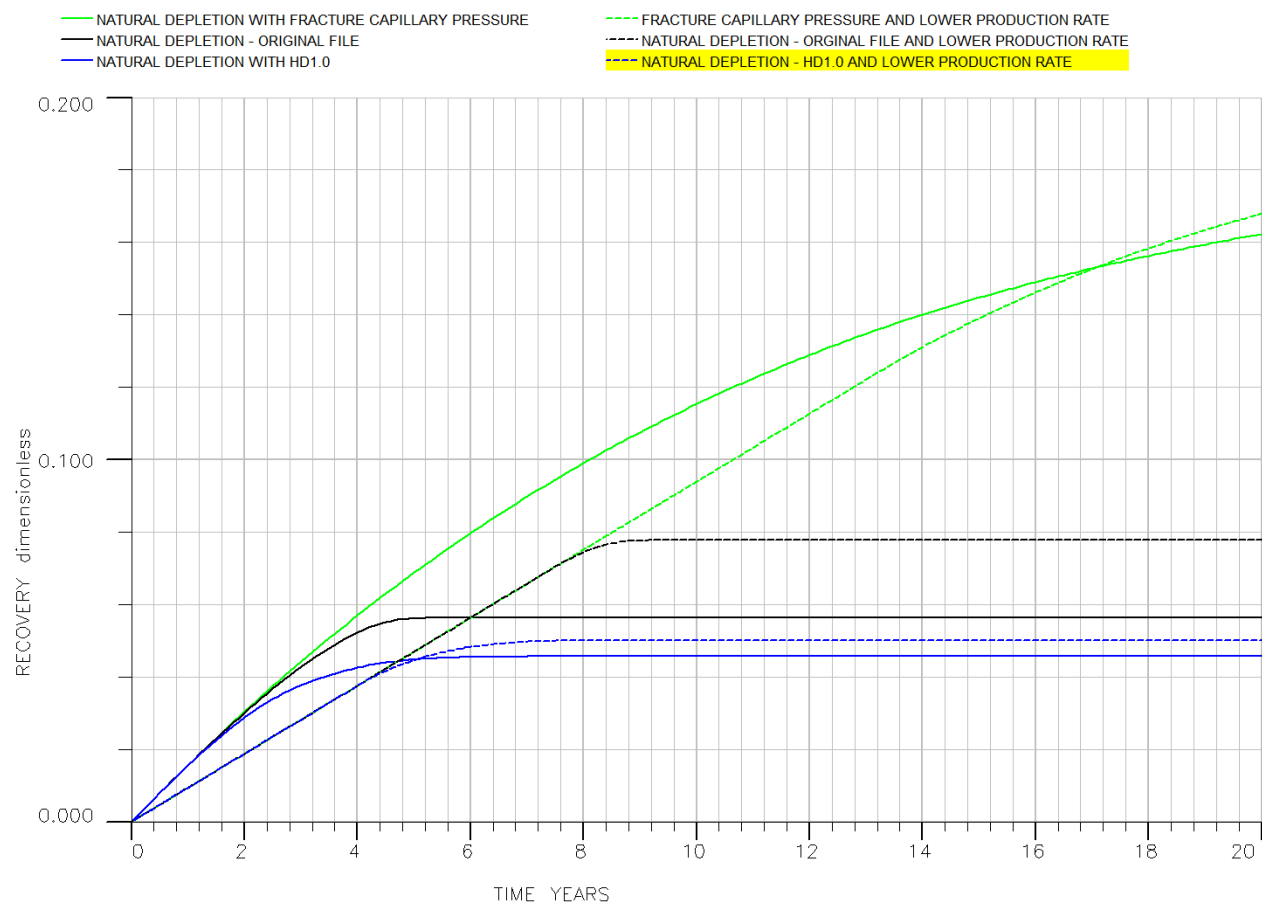


Figure 37: A comparison of recovery in the reservoir with natural depletion under different production rates.

In this graph the final recovery increase with around 30% for the original file when changing production rate from 500STB/D to 300STB/D.

Gas injection

Design: In this case the injection well is perforated in layer 1-3, and the production well is perforated in layer 4-5. The production well is restricted by 100 psi drawdown or a maximum production rate of 1000 STB/D. To retain reservoir pressure 90% of the produced gas is injected back to the reservoir. In the water and depletion case there has been no minimum production rate. This is unrealistic, since a well need a certain production rate to be economical valuable. In the gas injection case the minimum production rate is set to 100 STB/day.

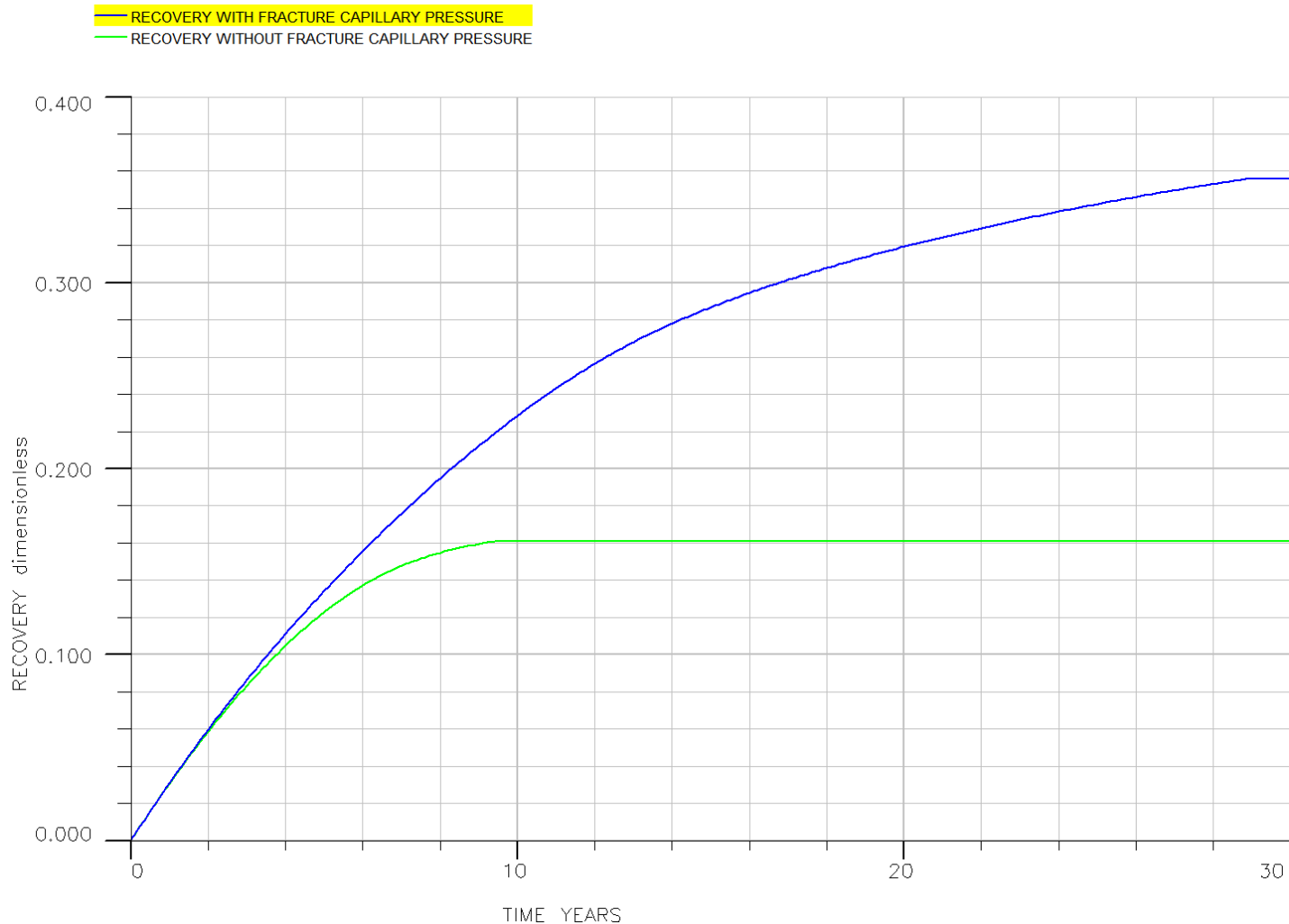


Figure 38: This plot shows the recovery vs. time for the gas injection case. When fracture capillary pressure is assumed, we get a highly increased recovery.

The above graph shows recovery for the gas injection case with and without fracture capillary pressure. The graph is easy to understand; fracture capillary pressure increase the recovery tremendously. The final recovery change from about 16% to 36%. This is 2.25 times higher ultimate recovery, and similar to results obtained in the test example. The enormously increase in recovery shows how important fracture capillary pressure could be. The production time is however much higher.

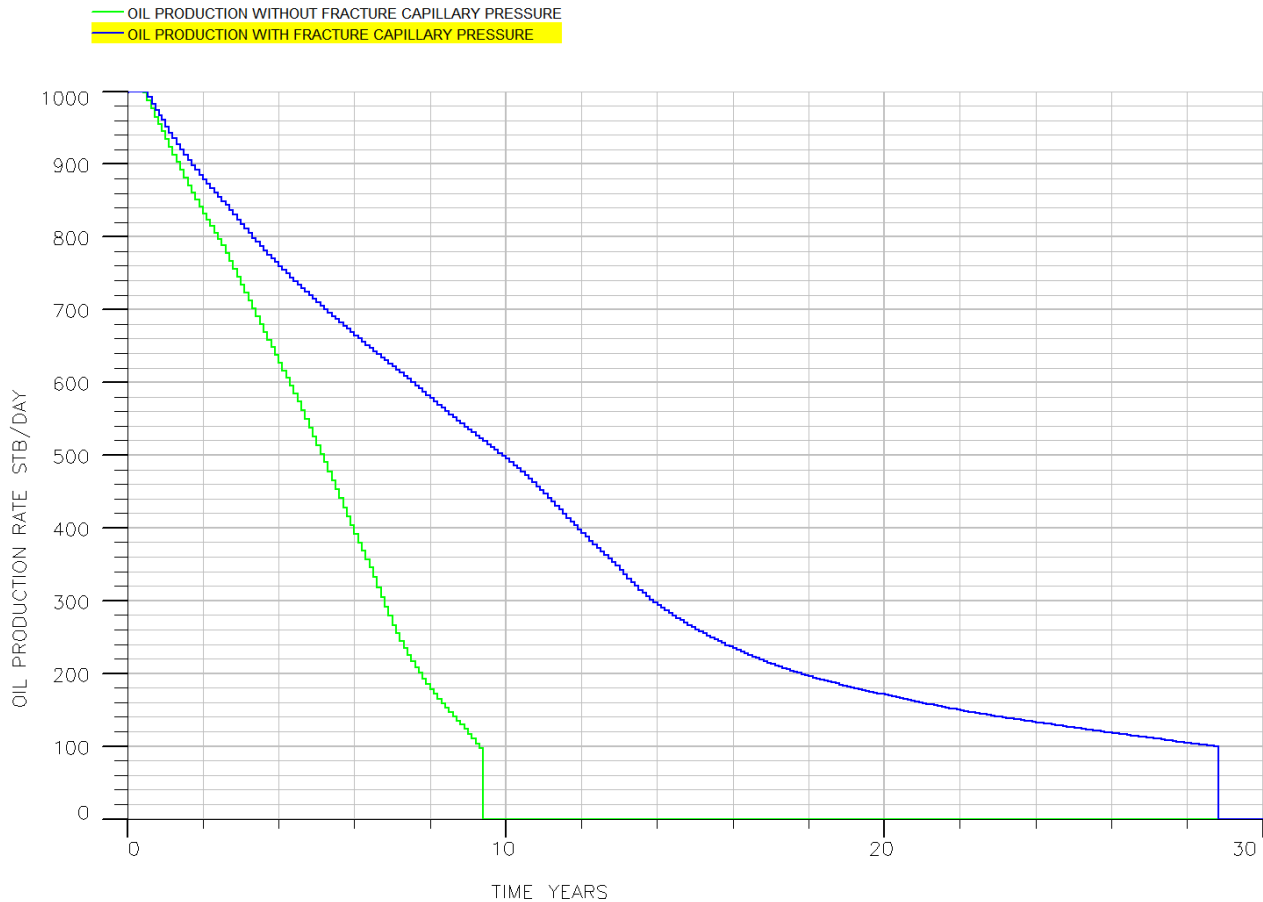


Figure 39: The oil production rate when gas is injected.

In the above plot we look at the production rate when we have gas reinjection. We already know that we get a higher recovery with capillary pressure, but from this plot it is obvious that the extra production time is quite big as well. With fracture capillary pressure the reservoir will produce for 29 years, but without fracture capillary pressure it would only produce 9 years. Indirectly this could be seen in the recovery vs. time plot, but it is easier observed here. When we have fracture capillary pressure the production time is increased 3.2 times while final recovery increases 2.25 times. This means that the average production rate has gone down, which again mean slower production mechanisms. This could be caused by that a bigger percentage of the recovery comes from gravity drainage, which is considered to be a slow recovery mechanism compared to the viscous displacement of fracture oil.

As a part of the sensitivity study, we checked how an increased block height would affect the production rate and final recovery. The results here were in order with results from the test case, and showed that tall blocks reduced the recovery difference between the cases of fracture capillary pressure, and those without. The increased block height makes a stronger gravity drainage, and as a result both final recovery and production time increase. Figure 47 and Figure 48 in Appendix 1 shows how recovery and oil production rate change with tall matrix blocks (50ft.).

Conclusion from full scale reservoir

Water injection:

The general conclusion is that we need to use non-straight fracture permeability lines for any reservoir where H_D is smaller than 5. Reduced fracture relative permeability curves will change the flow behavior in the reservoir, and sweep is likely to be different, as well as an increased drawdown makes reservoir gas cap production more likely. The error that is done by using straight-line permeability for small H_D values could be huge in all results, and economical prediction.

A low H_D value corresponds to reservoirs with very narrow fractures, low density difference and high interfacial tension between the phases or high fracture density (small matrix blocks).

Natural depletion:

It is big differences in reservoir behavior depending on fracture properties. E.g. the reservoir lifetime could vary between 5 to 20 years depending on fracture capillary pressure. Depending on which fracture properties we have we saw that we could increase the reservoir recovery between 5% and 30% only by changing the production rate from 500 STB/D to 300 STB/D.

Gas injection:

The conclusions from the full-scale reservoir are much the same as for the test system. The importance of fracture capillary pressure is proven another time. We also saw that capillary continuity had similar effect in this reservoir as it had in the test case.

6. Conclusion

The final conclusions of this thesis are as follow:

Single porosity model vs. the dual porosity model:

When we compared the results with fracture capillary pressure the dual porosity model matched the fine grid model very well, and we could say that fracture capillary pressure was modeled perfectly. For non-straight relative permeability lines the results were however more unclear. The single porosity model showed that we were very dependent on the injection rate, but this is not considered to be important in a fractured reservoir. Based on this we declared that the dual porosity model is well suited to match non-straight permeability curves.

Water oil systems with water injection into the fractures:

When H_D values are lower than 5 (narrow fracture openings, small block size, low fluid density difference and/or high interfacial tension between the phases) we need to use non-straight fracture relative permeability curves. The reduced fracture relative permeability will change the movement of water and the sweep could become more efficient since we could get a more stable and less segregated waterfront. The ultimate recovery in a dual porosity model is however lower when we have a reduced fracture relative permeability, this is since some of the fracture oil will become irreducible. We should also be more careful with possible gas production as lower relative permeability curves could imply a higher drawdown at the production well.

In the test system it was shown that fracture capillary pressure could both decrease and increase recovery, depending on the wettability of the fractures, the effect is however more important in a gas injection case.

Natural depletion with no injection into the fractures:

It is big differences in reservoir behavior depending on fracture properties. E.g. the reservoir lifetime could vary between 5 to 20 years depending on fracture capillary pressure. Depending on which fracture properties we have we saw that we could increase the reservoir recovery between 5% and 30% only by changing the production rate from 500 STB/D to 300 STB/D.

Gas-Oil system with gas injection into the fractures:

From H_D calculations it was shown that it was acceptable to use straight relative permeability curves in the fractures, as gravity forces will dominate compared to capillary forces.

In case of fracture capillary pressure it was shown that we could dramatically increase the recovery, and from both the reservoir systems we were able to increase the final recovery with a factor two! The

fracture capillary pressure would help the gas to overcome the threshold pressure and this is why the recovery increase so much.

Capillary continuity:

The water-oil and gas-oil system both positively increased their final recovery when they experienced capillary continuity. When fracture capillary pressure was applied to blocks with capillary continuity we saw that the recovery increased, but not so much as when we not had capillary continuity. As the effect of capillary continuity is the same as if we have taller matrix blocks, this implies that for very high matrix blocks fracture capillary pressure might be unimportant. One the other hand, for small matrix blocks fracture capillary pressure becomes more important.

7. Further work

The simulation results in this thesis show that both fracture capillary pressure and non-straight fracture relative permeability lines could affect the recovery a lot. The future work with these two parameters should be to develop a method that easy find a way to predict the true properties of these parameters in the reservoir.

Fracture capillary pressure is shown to have very big impact on the recovery, especially for small matrix blocks. In the future it will be important to be able to make the fracture capillary curve with the same accuracy as we today could measure the matrix capillary curve.

References

- Bird R.B., Steward W.E. and Lightfoot E.N. (2002). *Transport Phenomena, second edition*. John Wiley & Sons, Inc. New York.
- Bourbiaux and Leonnier. (2010). Simulation of naturally fractured reservoirs: State of the art.
- Chimá, A. and Geiger, S. (2012). *An Analytical Equation to Predict Gas-Water Relative Permeability Curves in Fractures*. paper SPE 152252, presented at Caribbean Petroleum Engineering Conference, Mexico City.
- Chimá, A., Chávez, E. and Calderón, Z. (2010). *An equation to Predict Two-Phase Relative Permeability Curves in Fractures*. paper SPE 138282.
- Dershowitz. W. (1996). A Stochastic Approach For Fracture Set Definition. *Document ID 96-1809*. American Rock Mechanics Association.
- Diomampo, G.P. (2001). *Relative Permeability Through Fractures*. MS thesis, Stanford University, California. .
- Firoozabadi, A and Hauge. J. (1990). Capillary pressure in fractured porous media. *SPE 18747*. Society of Petroleum Engineers.
- Firoozabadi, A and Thomaset L.K. (1989). *Sixth SPE comparative solution project: a comparison of dual porosity simulators, SPE18741*.
- Firoozabadi, A., Horie, T. and K. Ishimoto. (1990). *Laboratory studies of Capillary Interaction in Fracture/Matrix Systems*. paper SPE 18282.
- Fourar M., Piquemal, J. and Bories, S. (1992). *Experimental Study of Two-Phase Flow in Rough Fractures*. presented at Seventeenth Stanford Geothermal Workshop, Stanford University.
- Fourar, M and Bories, S. (1995). *Experimental study of Air-Water Two-Phase Relative Permeability Curves in Fractures (Narrow Channal)*. Int. J., Multiphase Flow pp 621-637.
- Jensen, Ole Krogh. (2005). Lecture material (compendium) of "Carbonate reservoir engineering".
- Kasiri. N and Bashiri A. (2011). *Status of Dual-Continuum Models for Naturally Fractured Reservoir Simulation*. Petroleum Science and Technology.
- Kazemi H, Gilman J.K, Elsharkawy A.M. (1992). Analytical and numerical solution of oil recovery from fractured reservoirs with empirical transfer functions. *SPE Reserv. Eng.*
- Kazemi. H. (1976). Numerical Simulation of Water Oil Flow in Naturally Fractured reservoirs. *SPE 5719*.
- Kjøsnæs, V. (2011). Semester Project: Comparison between dual porosity simulators and single porosity simulators. Norwegian University of Science and Technology.

- Lian, P.Q and Ma. C.Y. (2012). *The Characteristics of Relative Permeability Curves in Naturally Fractured Carbonate Reservoirs*. Canadian Petroleum Technology.
- Lim K.T and Aziz K. (1995). *Matrix fracture transfer shape factors for dual porosity simulators*. J.Petrol.Sci. Engi.
- Noroozi, M.M, Moradi, B., and Bashiri, G. (2010). *Effects of Fracture Properties on Numerical Simulation of a Naturally Fractured Reservoir*. paper SPE 132838 presented at the Trinidad and Tobago Energy Resources Conference.
- Persoff, P and Pruess, K. . (1995). *Two-phase Flow Visualization and Relative Permeability measurement in Natural Rough-walled Rock Fractures*. Water Resour. Res., 31, 1175-1186.
- Pieters, D. A. and Graves, R.M. (1994). *Fracture Relative Permeability: Linear or Non-linear Function* |. paper SPE 28701.
- Porte J.J., Kossack C.A., Zimmerman R.W. (2005). *The Effect of Fracture Relative Permeabilities and Capillary Pressures on the Numerical Simulation of Naturlally Fractured Reservoirs*. paper SPE 95241.
- Rangel-German and Kovscek. (2003). Time dependent matrix fracture shape factors for partially and completely immersed fractures. *SPE 84411 presented at the SPE annual technical conference and Exhibition. Denver Colorado*.
- Romm, E.S. (1966). *Fluid Flow in Fractures*. Nedra Publishing House, Moscow.
- Rossen, W.R and Kumar, A.T. (1994). *Effect of Fracture Relative Permeabilities on Performance of Naturally Fractured Reservoirs*. paper SPE 28700.
- Saidi A.M. and Tehrani D.H. (1979). *Mathematical Simulation of fractured Reservoir Perfomance, based on Physical Model Experiments. Presented at 10th World Petroleum Congress*.
- Schlumberger. (2010). Eclipse reference manual.
- Torsæter, Ole. (2010). Lecture material of "Fractured reservoir Engineering", TPG4225.
- Vaan Golf-Racht. (1982). *Fundamentals of Fracture Reservoir Engineering*. Elsevier.
- Warren, J.E. and Root,P.J. (1963). *The Behavior of Naturally Fractured reservoirs, SPEJ 245-255*.
- Welge, H.J. (1952). A Simplified Method for Computing Oil Recoveries by Gas or Water Drive.

Nomenclature

P_{initial}	Pressure initially
P_{cog}	Oil gas capillary pressure
P_{cf}	Fracture capillary pressure
Φ_{m}	Porosity of matrix
Φ_{f}	Porosity of fractures
k_{m}	Permeability of matrix
k_{f}	Fracture permeability
k_{fh}	Fracture horizontal permeability
$k_{\text{rg,o,w}}$	Relative permeability of gas, oil or water
$\mu_{\text{g,o,w}}$	Viscosity of gas, oil or water
$\rho_{\text{g,o,w}}$	Density of gas, oil or water
$B_{\text{g,o,w}}$	Gas, oil or water formation volume factor
B_{oi}	Initial oil formation volume factor
R_{s}	Solution gas oil ratio
S_{wir}	Irreducible water saturation
$S_{\text{g,o,w}}$	Saturation of gas, oil or water
C_{w}	Water compressibility
$C_{\text{rm}}=C_{\text{rf}}$	Matrix and fracture compressibility
$n_{\text{x,y,z}}$	Number of grid blocks in x -,y- or z - direction
Δx	Matrix block length in x direction
Δy	Matrix block length in y direction
Δz	Matrix block length in z direction
b_{o}	Half mean fracture aperture
H	Block height
γ	Interfacial tension/surface tension

Appendix1: Figures from simulations and equations

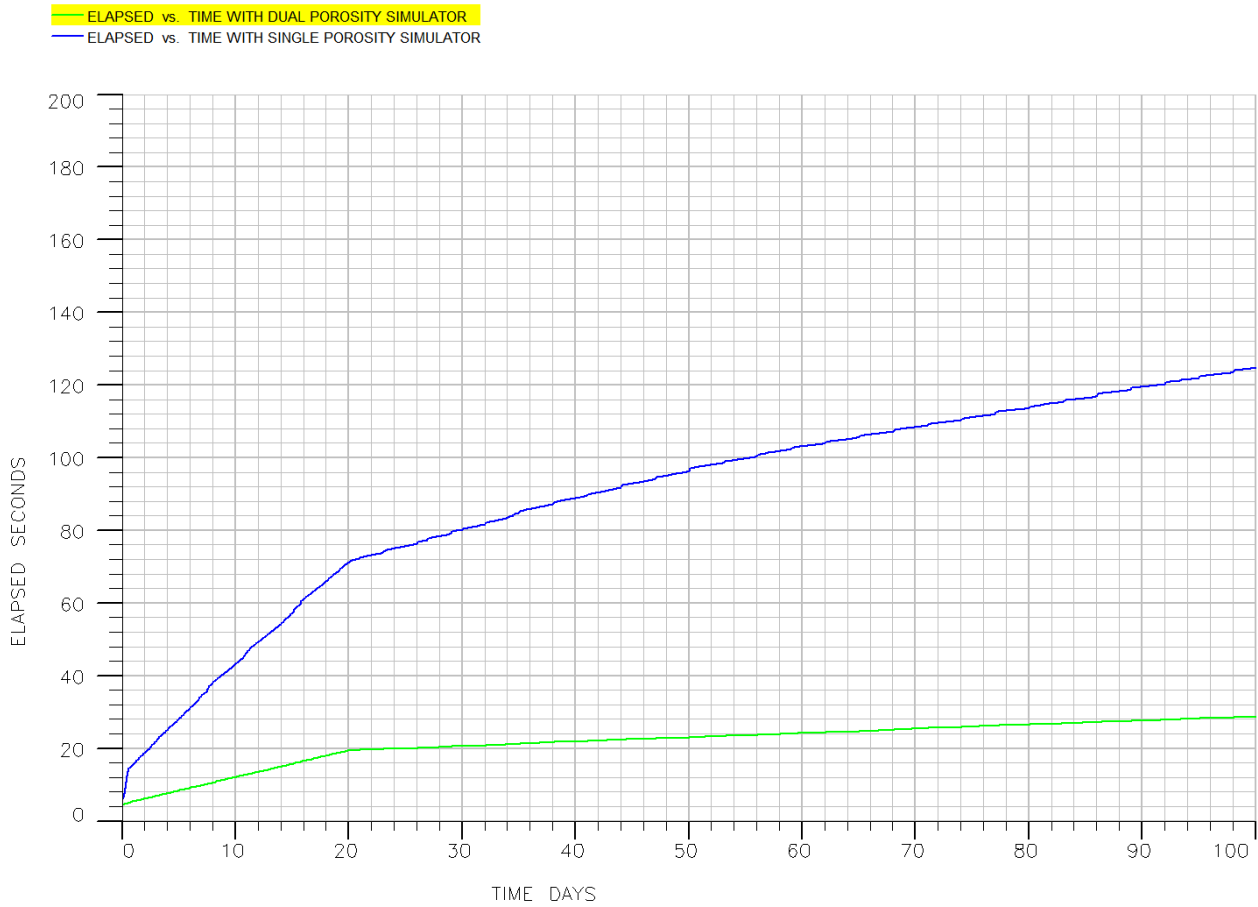


Figure 40: This is the time difference with the single porosity model and dual porosity model for the test system. This is a very small system, and if the simulation model were bigger, the single porosity model would have been even slower.

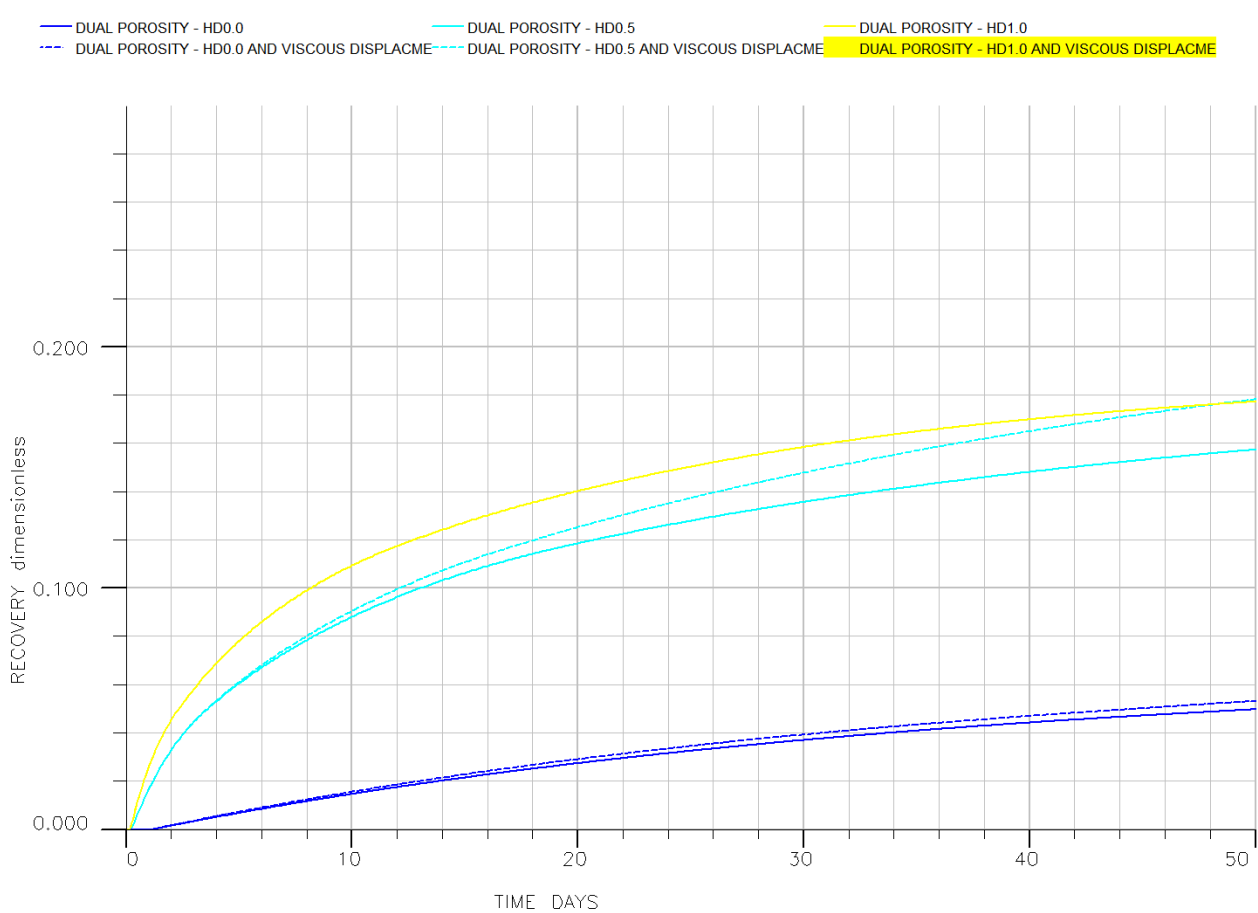


Figure 41: Recovery for dual porosity model when viscous displacement is included (VISCD).

We could see a small increment when the dual porosity model includes the viscous forces, but the increment is only when the H_D values are small (0.0 or 0.5). For the other H_D values, there is no difference in recovery and therefore the plots for $H_D = 5$ or ∞ is not included. The effect of the viscous forces is still much smaller than for the single porosity model, but with history matching this could be changed (i.e. by changing L_x , L_y and L_z values). But since viscous displacement not is considered to be an important recovery mechanism in fractured reservoirs, this may be dropped.

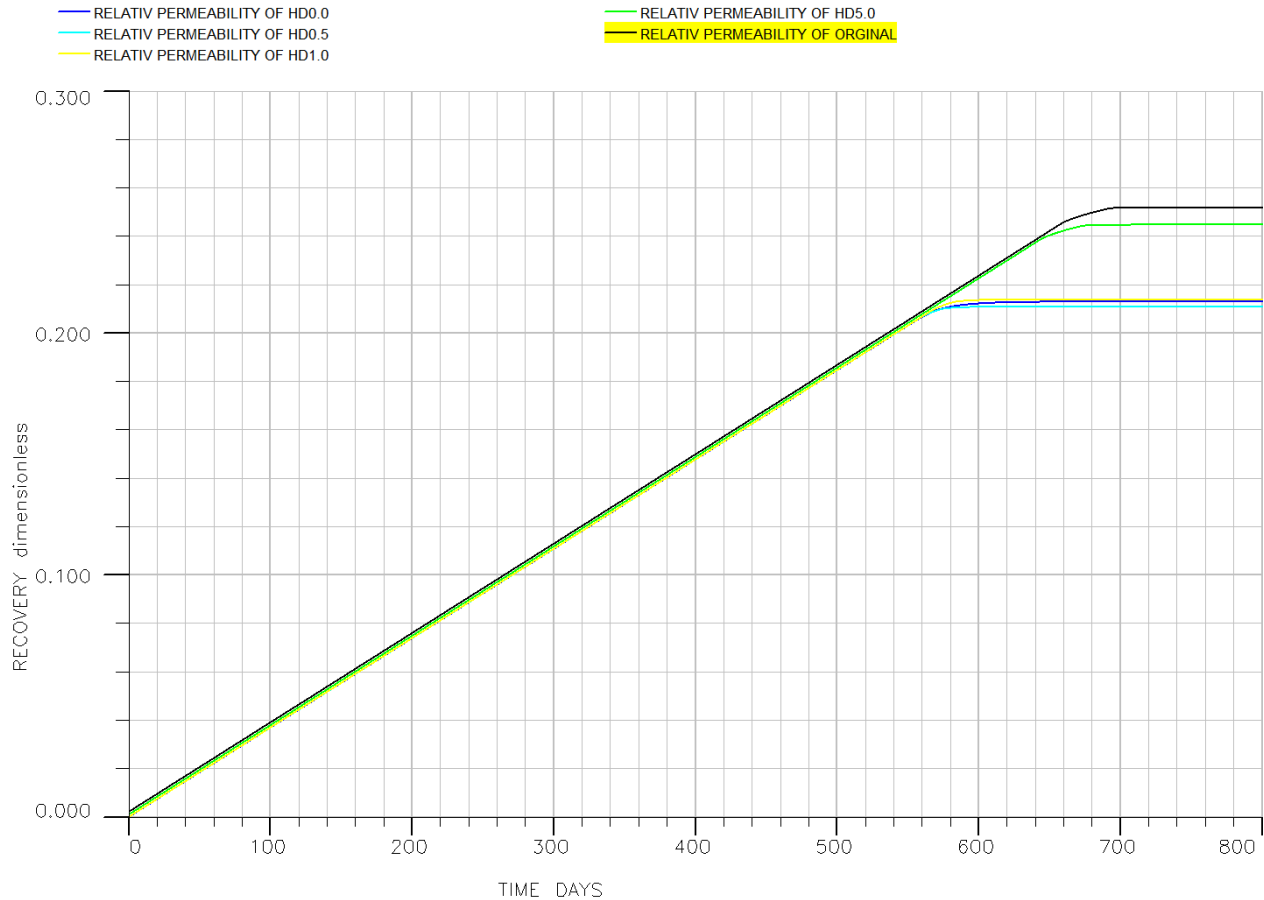


Figure 42: Low H_D values decrease the recovery for the single porosity model as well, but only for very small injection rates.

The above figure is interesting; here we see that the single porosity model gets the same tendency for recovery as the dual porosity model gets. Low H_D values give low recoveries when the viscous forces not are taken into account. To minimize the viscous forces an extremely low injection rate at $0.0005 \text{ m}^3/\text{day}$ is chosen. The total production time while using this injection rate is however still much less then for an average reservoir, which gives credibility to that it not is necessary to simulate a reservoir with viscous forces. In fact the reservoir injection rate may not be so low as it first might have appeared, an injection rate of $0.0005 \text{ m}^3/\text{day}$ is equivalent with injecting the total reservoir pore volume in 3600 days, a rate which may be reality in many reservoirs [$0.3 \cdot 6 \cdot 1 \text{ m}^3 / 0.0005 \text{ m}^3/\text{day} = 3600 \text{ days}$].

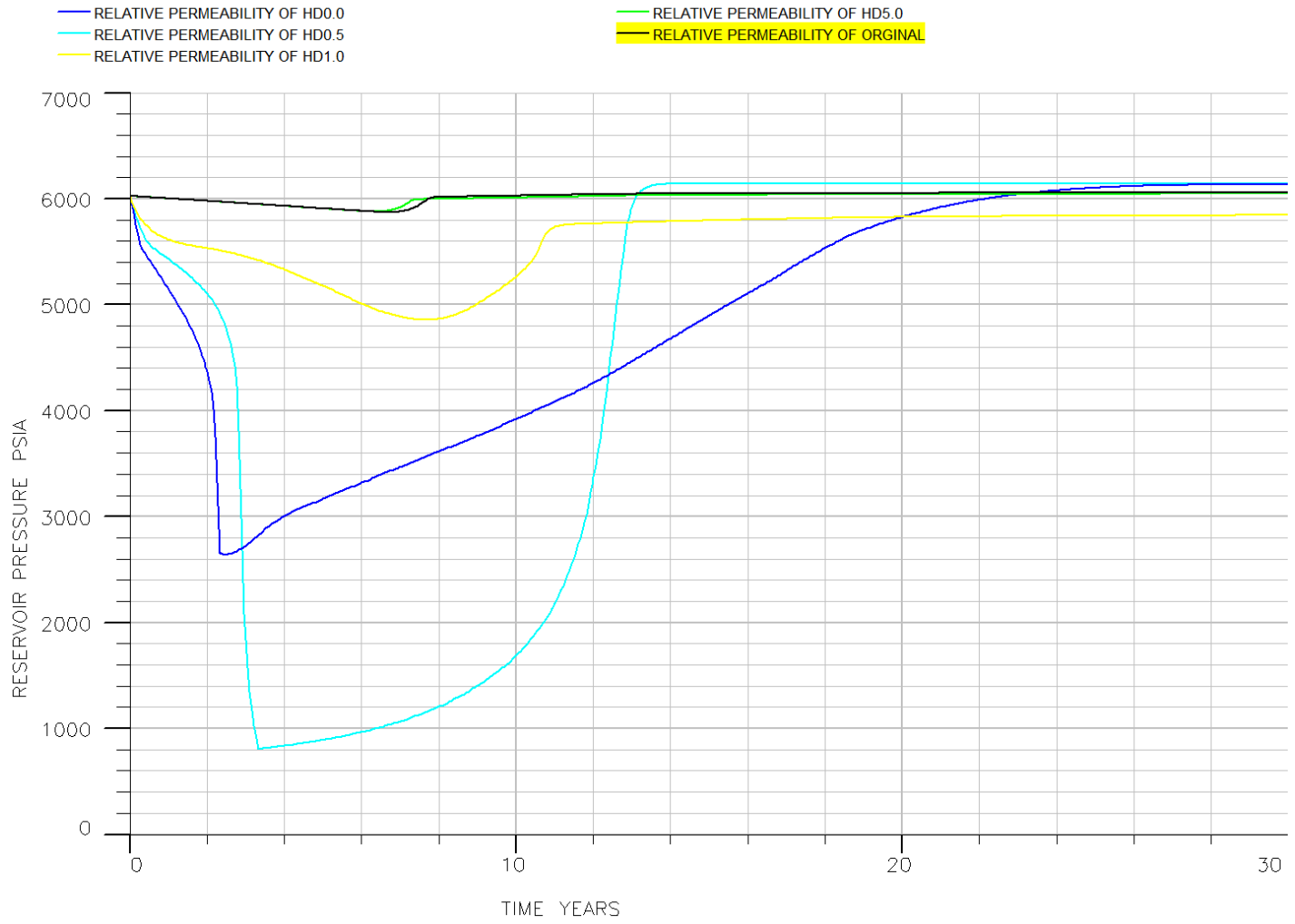


Figure 43: Reservoir pressure for full field reservoir with water injection and different HD values.

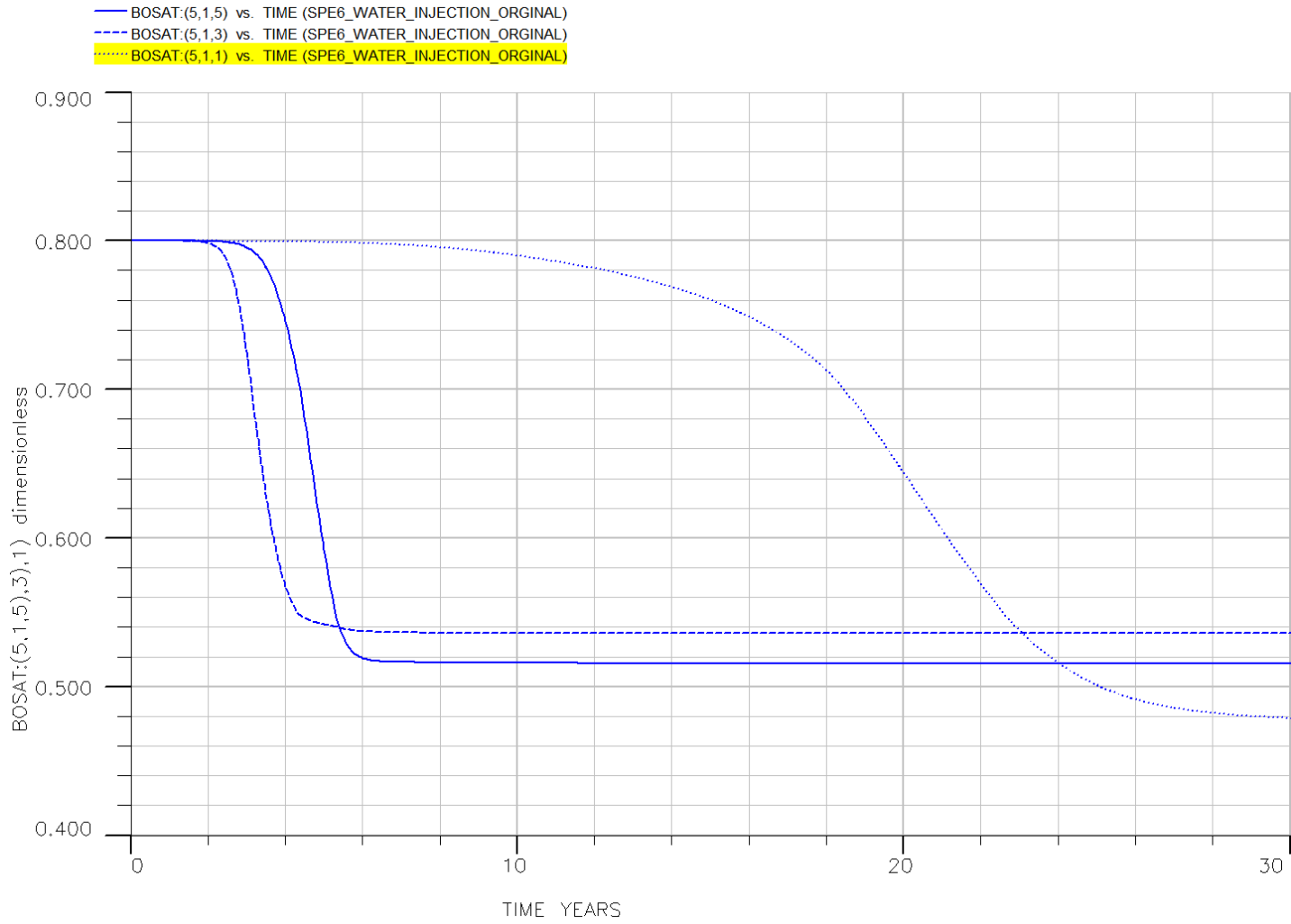


Figure 44: Different layers drains at different times in the original file.

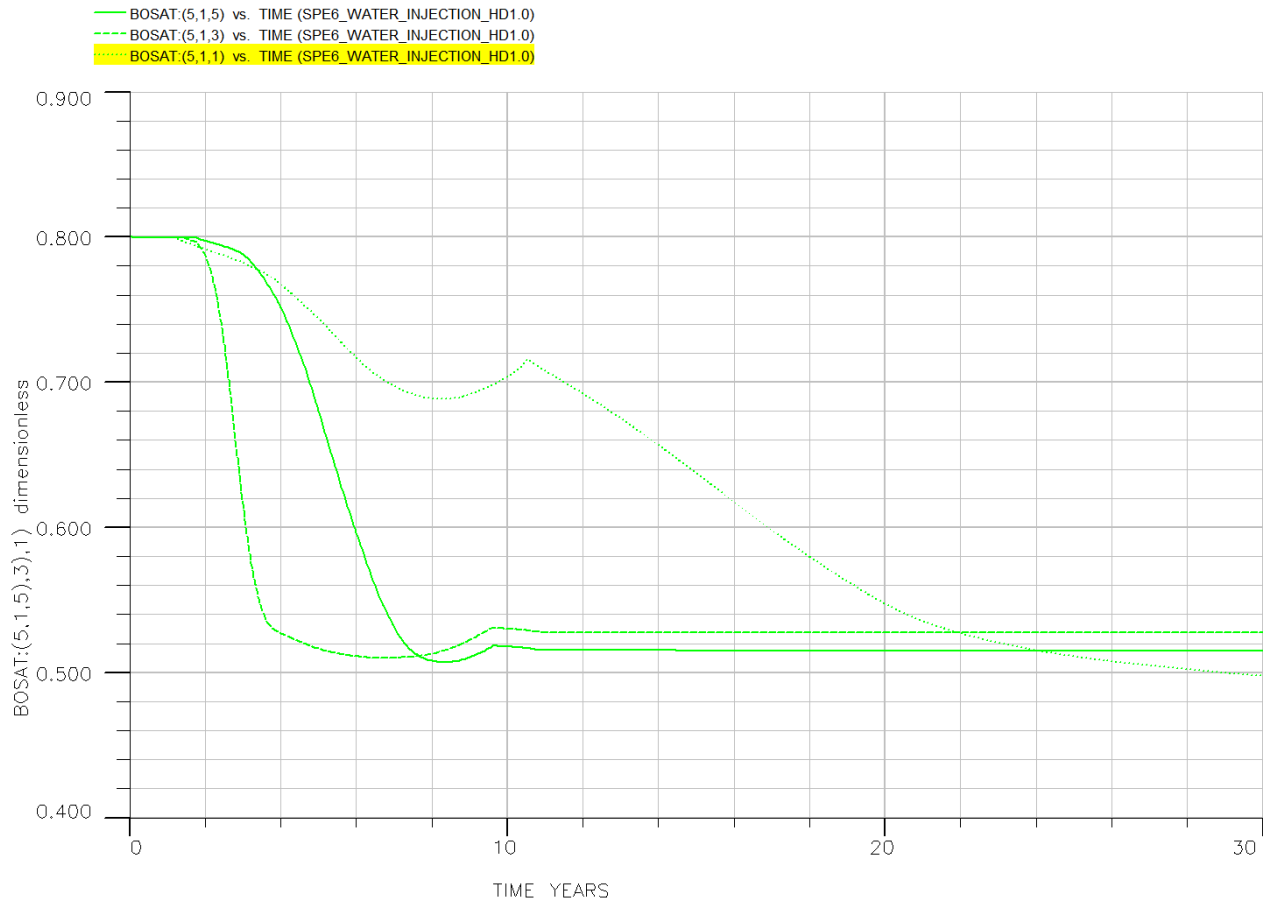


Figure 45: When we have HD equal to 1 we get a more evenly drainage of the matrix fracture cells. If we compare this result with Figure 44 we could see that this model drains the matrix blocks more evenly, that again mean a better sweep for low HD values.

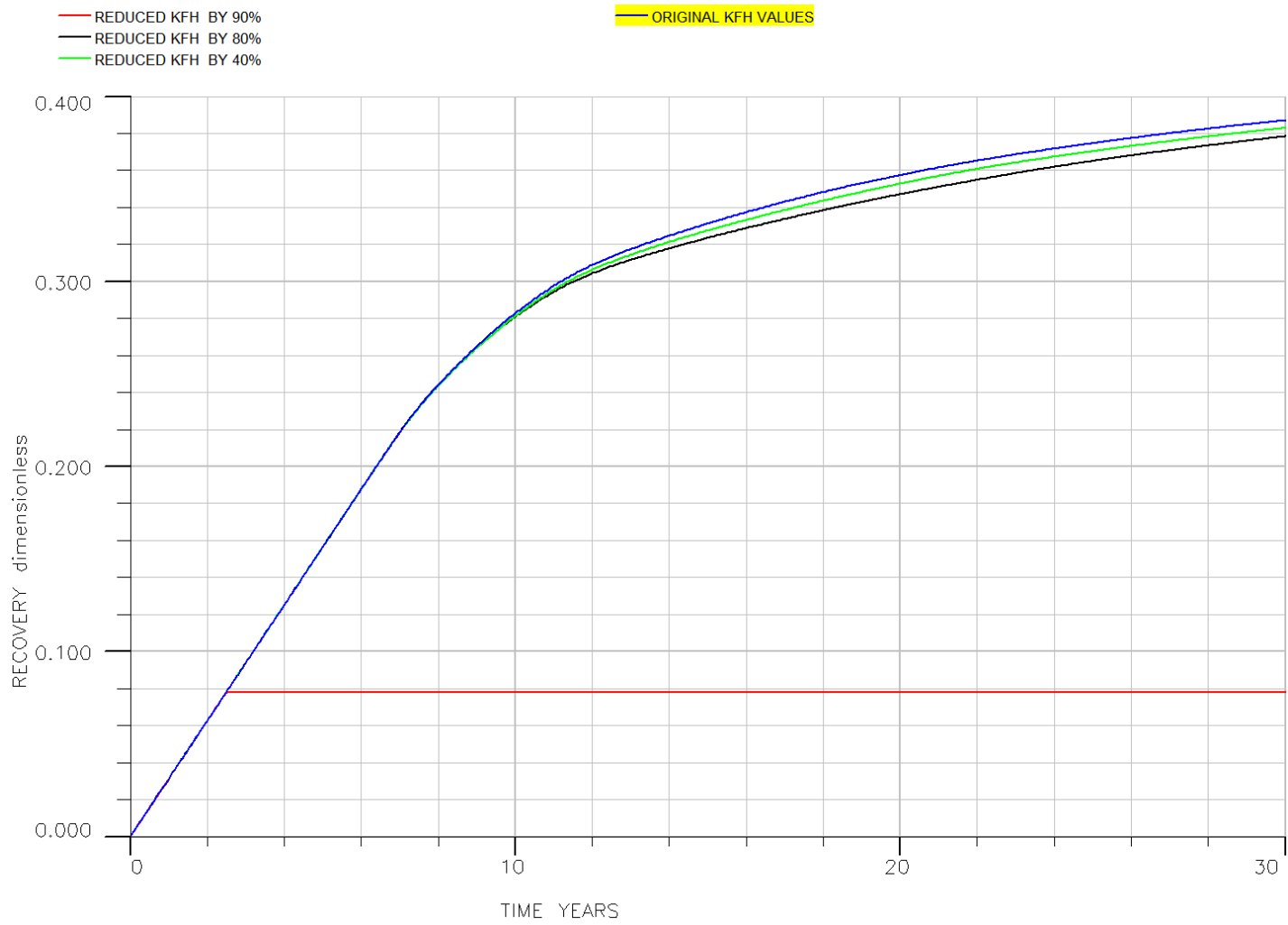


Figure 46: We reduced the horizontal fracture permeability and saw that this made a gas breakthrough when Kfh was reduced by 90%.

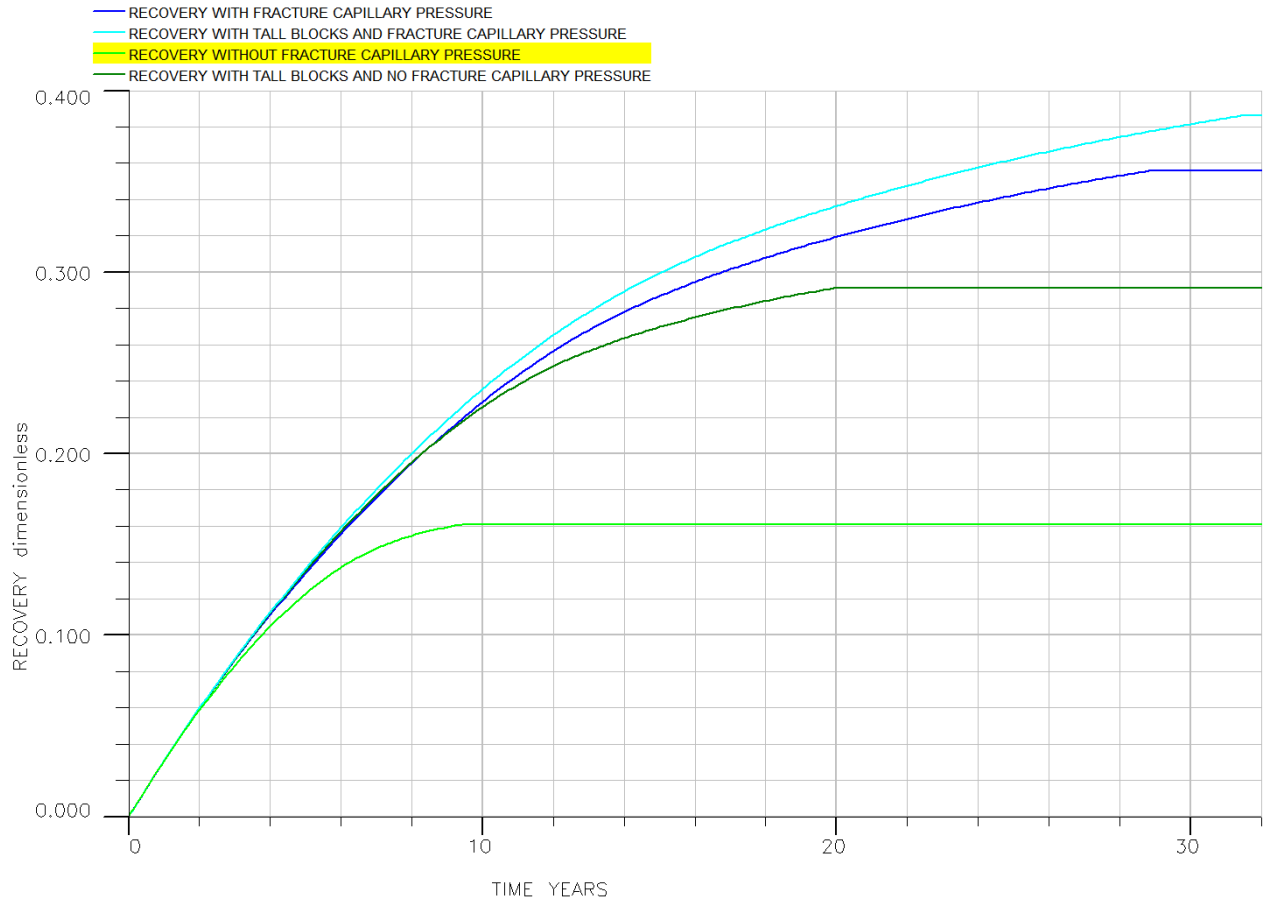


Figure 47: Comparison of recovery for the original reservoir and the same reservoir with tall matrix blocks (50ft).

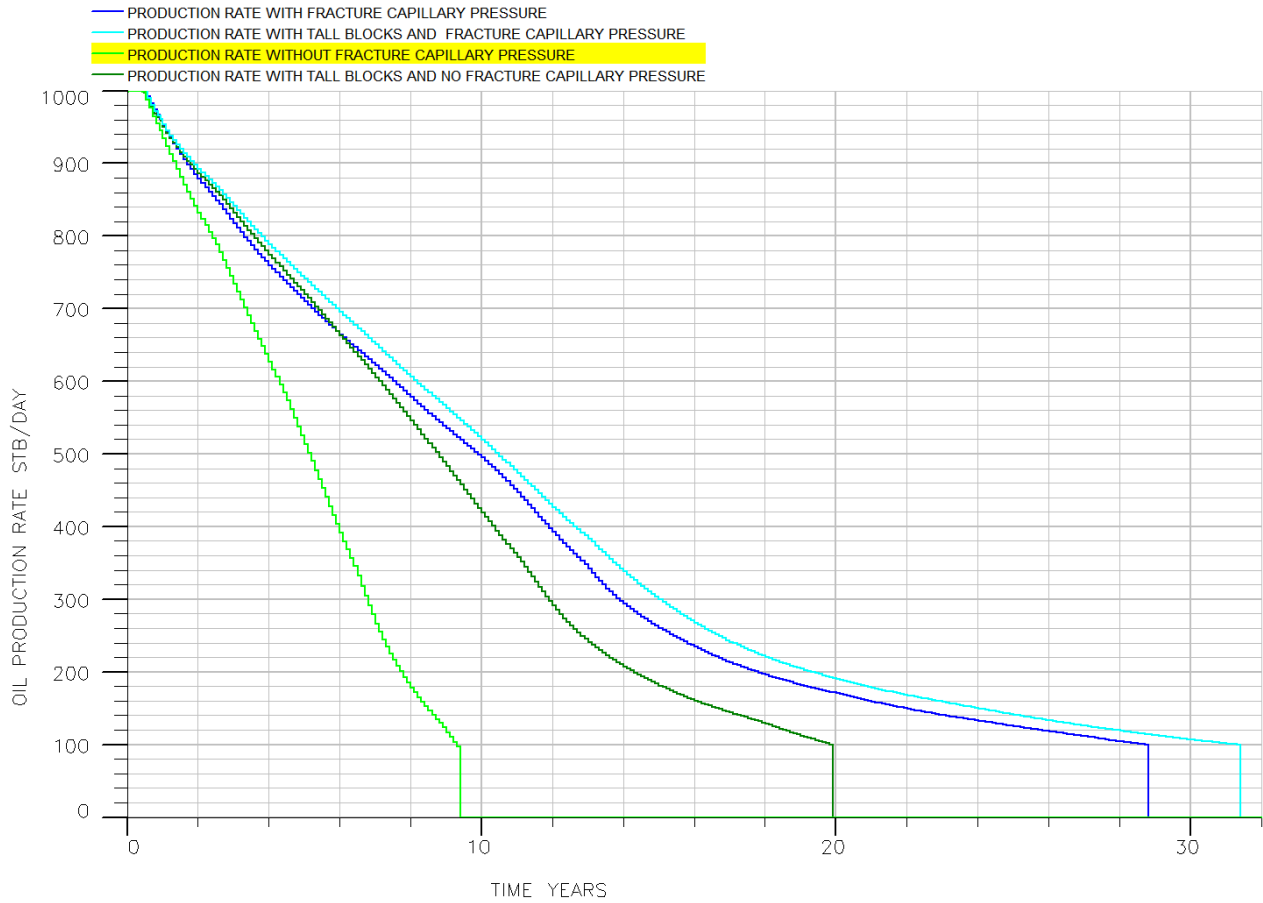


Figure 48: Comparison of oil production rate for the original reservoir and the same reservoir with tall matrix blocks (50ft).

$$K_{rF} = \left[\frac{S_W^5 (\mu_O - \mu_W) + S_W^3 \mu_W (3 - 2S_W)}{S_W (\mu_O - \mu_W) + \mu_W} \right]$$

$$K_{rO} = \left[\frac{S_O^5 (\mu_W - \mu_O) + S_O^3 \mu_O (3 - 2S_O)}{S_O (\mu_W - \mu_O) + \mu_O} \right]$$

Figure 49: Equations to calculate fracture relative permeability assuming gravity segregation (Chimá, A., Chávez, E. and Calderón, Z., 2010).

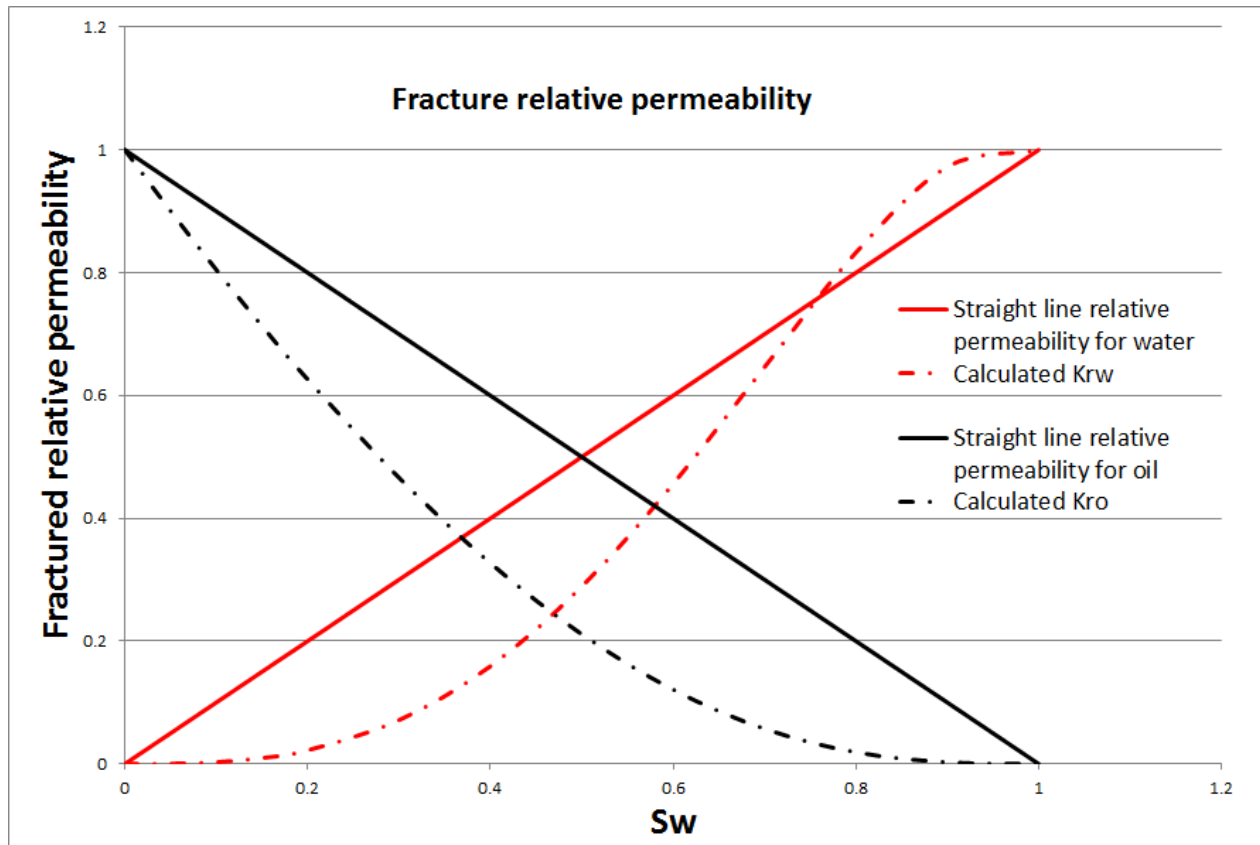


Figure 50: Fracture relative permeability calculated with viscosities at bubble point conditions compared to the straight permeability lines.

Appendix2: Reservoir and fluid description of the full-scaled reservoir.

The full-scale reservoir that I have chosen to do my simulations on is the same reservoir as they have in the sixth SPE comparative solution project (SPE6). The SPE6 reservoir is made in a dual porosity simulator. The reservoir consists of 50 matrix cells and an additional 50 associated fracture cells. The reservoir has five layers vertically and is divided into 10 cells in the x direction and 1 cell in the y direction.

Initially the matrix cells are saturated with 80% oil and 20% water. The fractures are 100% oil saturated.

The well perforation will vary depending on what injection type we have, but the injection and production well is always vertical, and perforated in block (1,1,Z) and (10,1,Z) respectively.

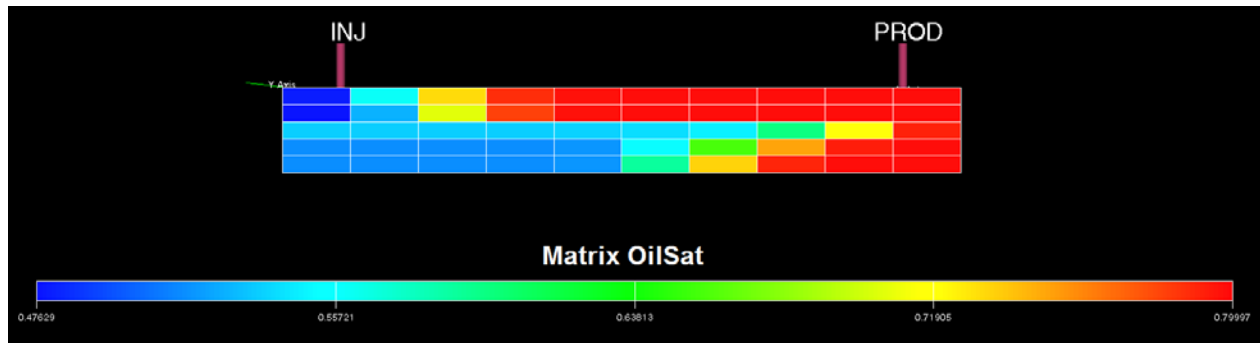


Figure 51: Above the full-scaled reservoir is shown during water injection. The perforations for the two wells vary, but they always have the same placement

Matrix water/oil capillary pressure data and relative permeability (given no free gas in place)			
S_w	K_{ro}	K_{rw}	P_c [psi]
0.20	1.000	0.000	1.00
0.25	0.860	0.005	0.50
0.30	0.723	0.010	0.30
0.35	0.600	0.020	0.15
0.40	0.492	0.030	0.00
0.45	0.392	0.045	-0.20
0.50	0.304	0.060	-1.20
0.60	0.154	0.110	-4.00
0.70	0.042	0.180	-10.0
0.75	0.000	0.230	-40.0

Matrix gas/oil capillary pressure and relative permeability data		
S_g	K_{rg}	P_c [psi]
0.00	0.000	0.0375
0.10	0.015	0.085
0.20	0.500	0.095
0.30	0.103	0.115
0.40	0.190	0.145
0.50	0.310	0.255
0.55	0.420	0.386

Table 8: The capillary pressure curves and relative permeability curves for the full-scale reservoir is from SPE6 own data.

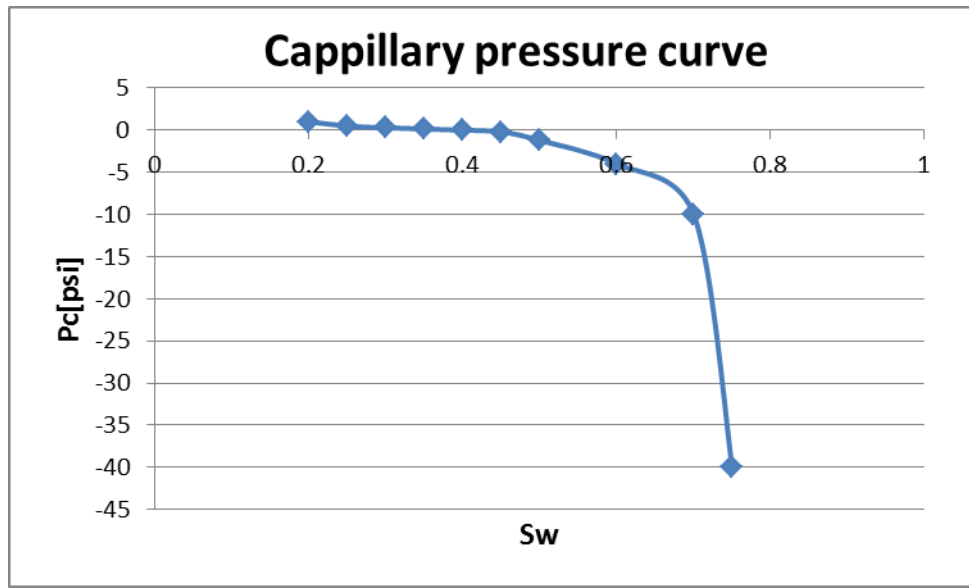


Figure 52: Imbibition capillary curve in matrix for oil-water.

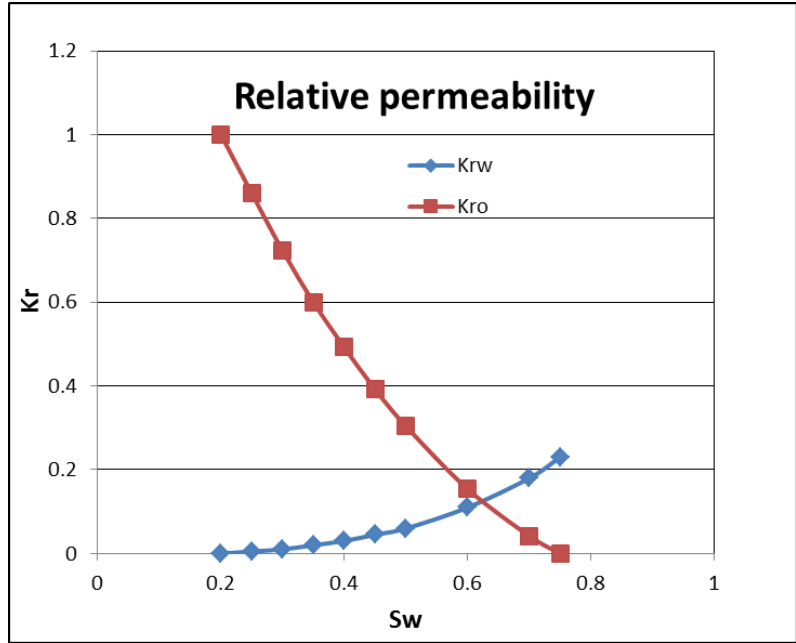


Figure 53: Imbibition relative permeability curve in matrix rock

The capillary pressure and relative permeability curve shows us that we have a water/mixed wet reservoir. In such a reservoir both spontaneous imbibition and imbibition forced by gravity will be recovery mechanisms. The relative permeability for the fractures is assumed equal to the saturation, and no capillary pressure is assumed in the ORIGINAL file.

Fracture gas/oil capillary pressure and relative permeability data		
S_g	K_{rg}	P_c [psi]
0.00	0.00	0.0375
0.10	0.10	0.0425
0.20	0.20	0.0475
0.30	0.30	0.0575
0.40	0.40	0.0725
0.50	0.50	0.0880
0.70	0.70	0.1260
1.00	1.00	0.1930

Table 9: Fracture capillary pressure and gas fracture relative permeability (when fracture capillary pressure is applied).

Layer data			
Layer	Effective fracture permeability (md)	Block height (ft.)	Matrix block shape factor (ft ⁻²)
1	10	25	0.040
2	10	25	0.040
3	90	5	1.000
4	20	10	0.250
5	20	10	0.250

Table 10: Layer data.

Basic fluid and rock properties		
$P_{initial}$	6000	Psi
$P_{bubble\ point}$	5545	Psi
$R_s @\ bubble\ point$	1.53	Mscf/stb
ϕ_m	0.29	fraction
k_m	1	md
ϕ_f	0.01	fraction
n_x	10	number
n_y	1	number
n_z	5	number
Δx	200	ft.
Δy	1000	ft.
Δz	50	ft.
$\rho_o @\ surface\ conditions$	51.14	lb./ft ³
$\rho_w @\ surface\ conditions$	65.00	lb./ft ³
$\rho_g @\ surface\ conditions$	0.058	lb./ft ³
$\rho_o @\ bubble\ point$	36.2	lb./ft ³
$\rho_w @\ bubble\ point$	62.0	lb./ft ³
$\rho_g @\ bubble\ point$	15.0	lb./ft ³
$\mu_o @\ bubble\ point$	0.21	cP

μ_w @ bubble point	0.35	cP
C_w	0.35E-05	1/psi
$C_{rm}=C_{rf}$	0.35E-05	1/psi
z-direction transmissibility	multiply calculated values by 0.1	

Table 11: Basic fluid and rock properties for oil-water imbibition

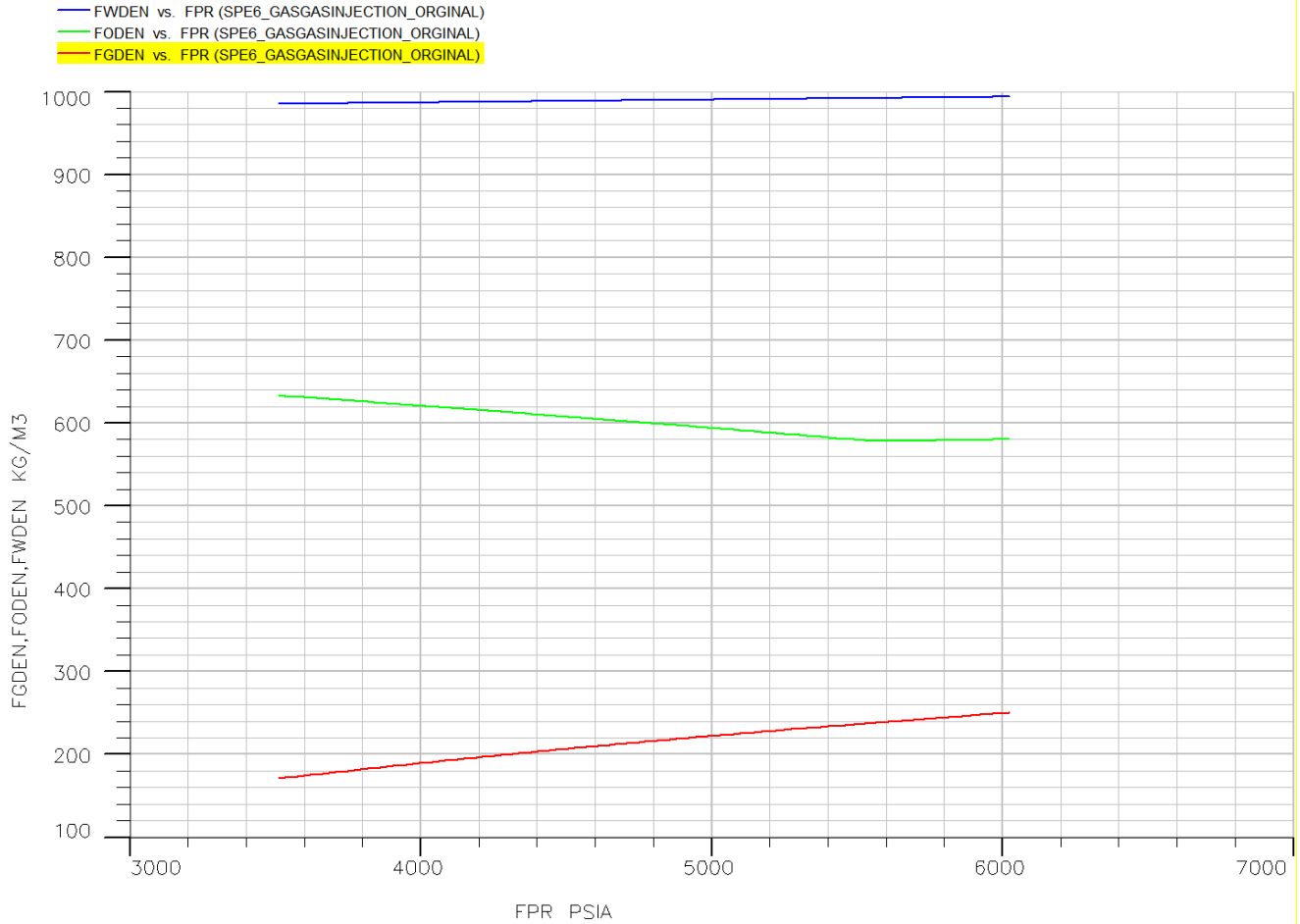


Figure 54: Full field reservoir density during production life.


```

--
STOG
--
-- REFERENCE PRESSURE
--
5545 /
--
-- PRESSURE SURFACE TENSION
--
1674 6.0
2031 4.7
2530 3.3
2991 2.2
3553 1.28
4110 0.72
4544 0.444
4935 0.255
5255 0.155
5545 0.090
7000 0.050 /

```

Figure 55: Surface/interfacial tension from eclipse file.

Note! Even if this values are from the eclipse data file they are not in use, as they only works as a scaling factor from the reference pressure as shown below. The P_{cog} at reference pressure is not specified and the reservoir is operated at no surface tension between gas oil phases as shown in Figure 57. Even if the table above not is used in the simulation, I have chosen to use the above values for H_D evaluation in dynes/cm.

$$P_{cog}(\text{oil pressure}) = P_{cog}(\text{input by user}) \frac{ST(\text{oil pressure})}{ST(\text{reference pressure})} \quad [\text{EQ 3.197}]$$

Note The surface tension is only used as a ratio in the SURFTENS option, and hence the units used does not affect the results of the calculation.

Figure 56: Explanation to how the STOG keyword works from the eclipse reference manual (Schlumberger, 2010).

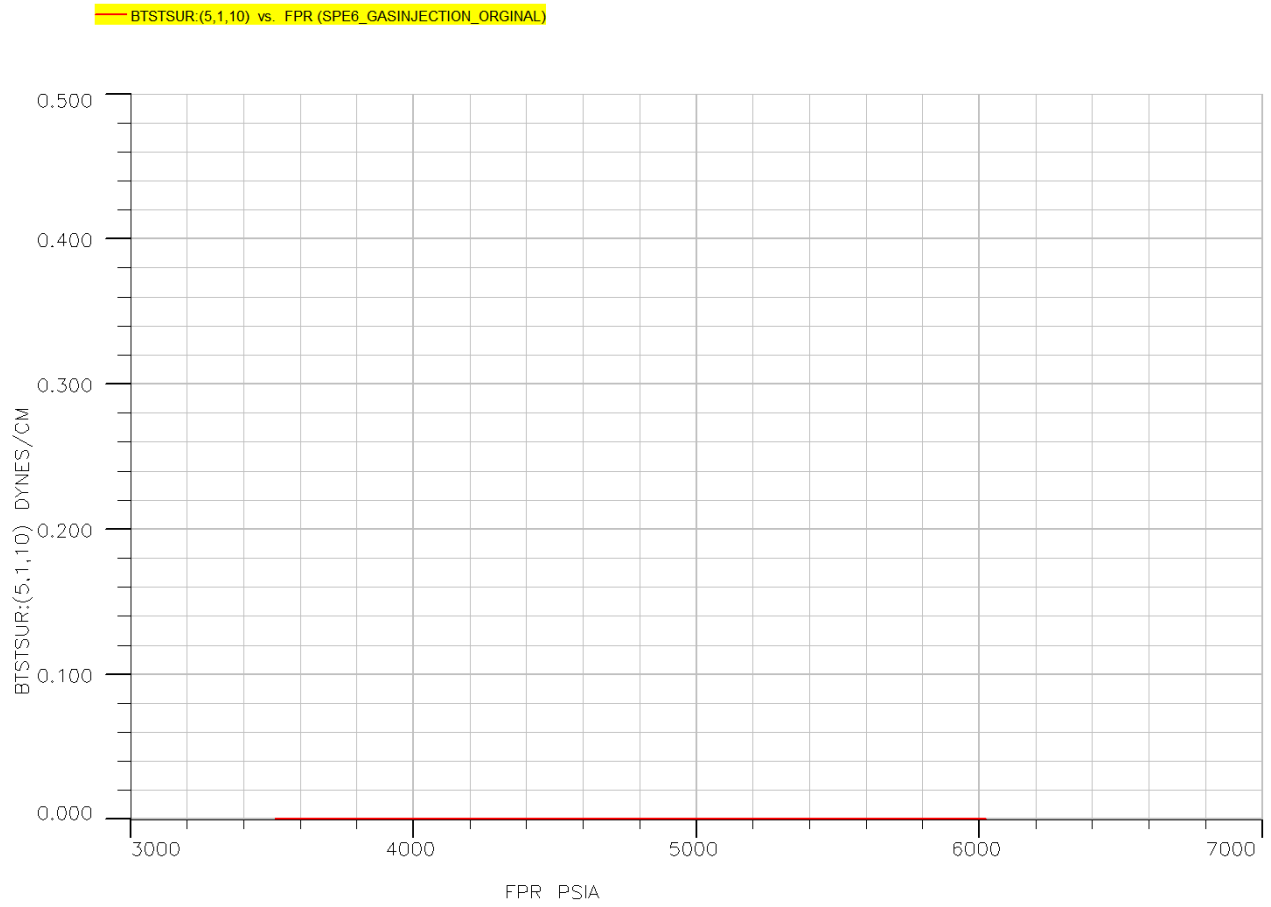


Figure 57: Surface tension is not modeled in the reservoir.

Appendix3: Upscaling

As I explained in the thesis, I was not sure of how correct the results from the SPE6 model would be, due to the many matrix blocks each grid cell spanned. To check this a 50m*50m*50m homogenous reservoir was made and this was divided into 5, 10 or 50 grid cells in each direction. The reservoir properties were the same as in the water test system.

The figure below shows that all the three cases have a perfect match on the recovery vs. time graph.

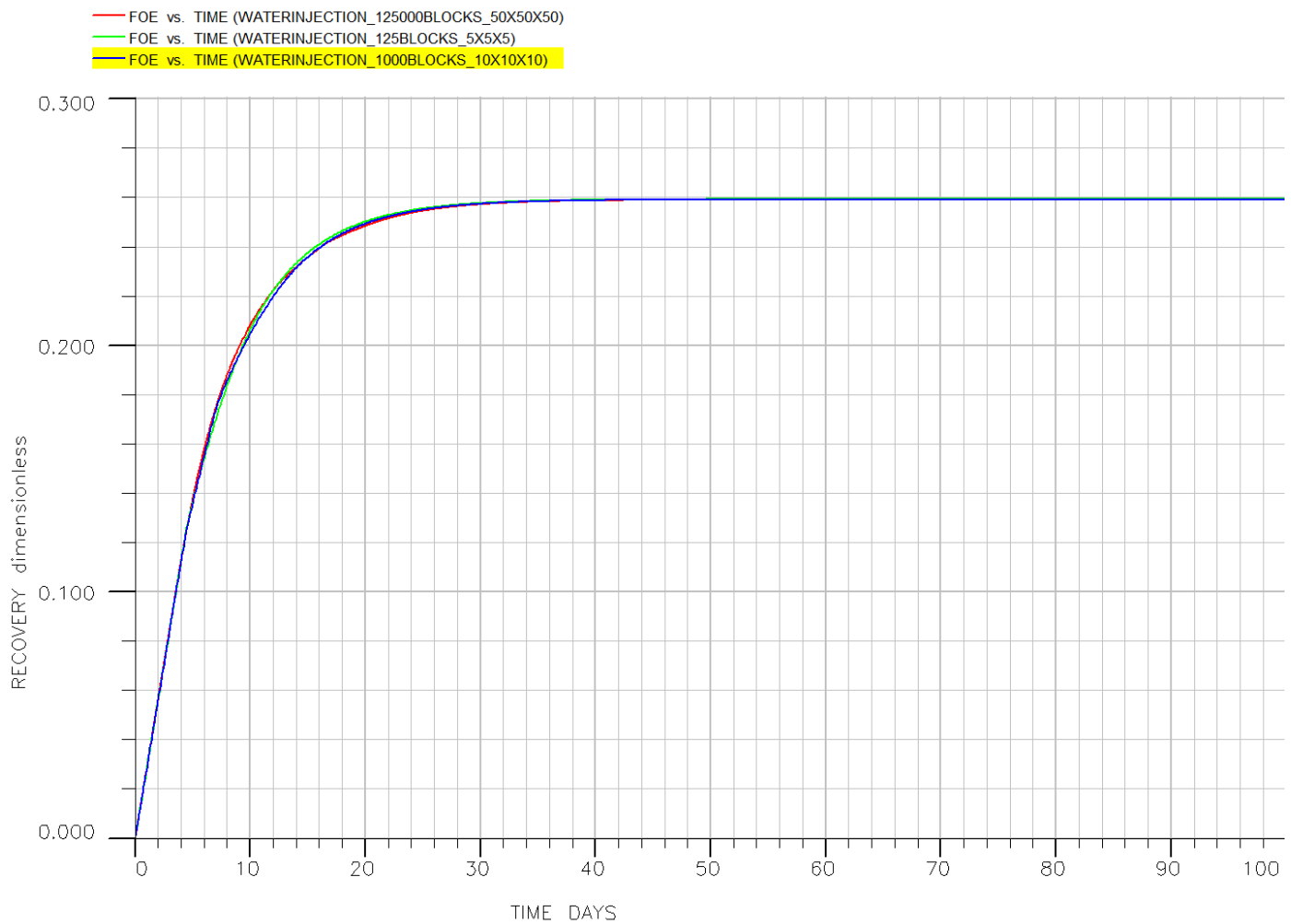


Figure 58: For all grid block sizes the recovery is perfectly similar.

The oil production plots below are also very close to each other.

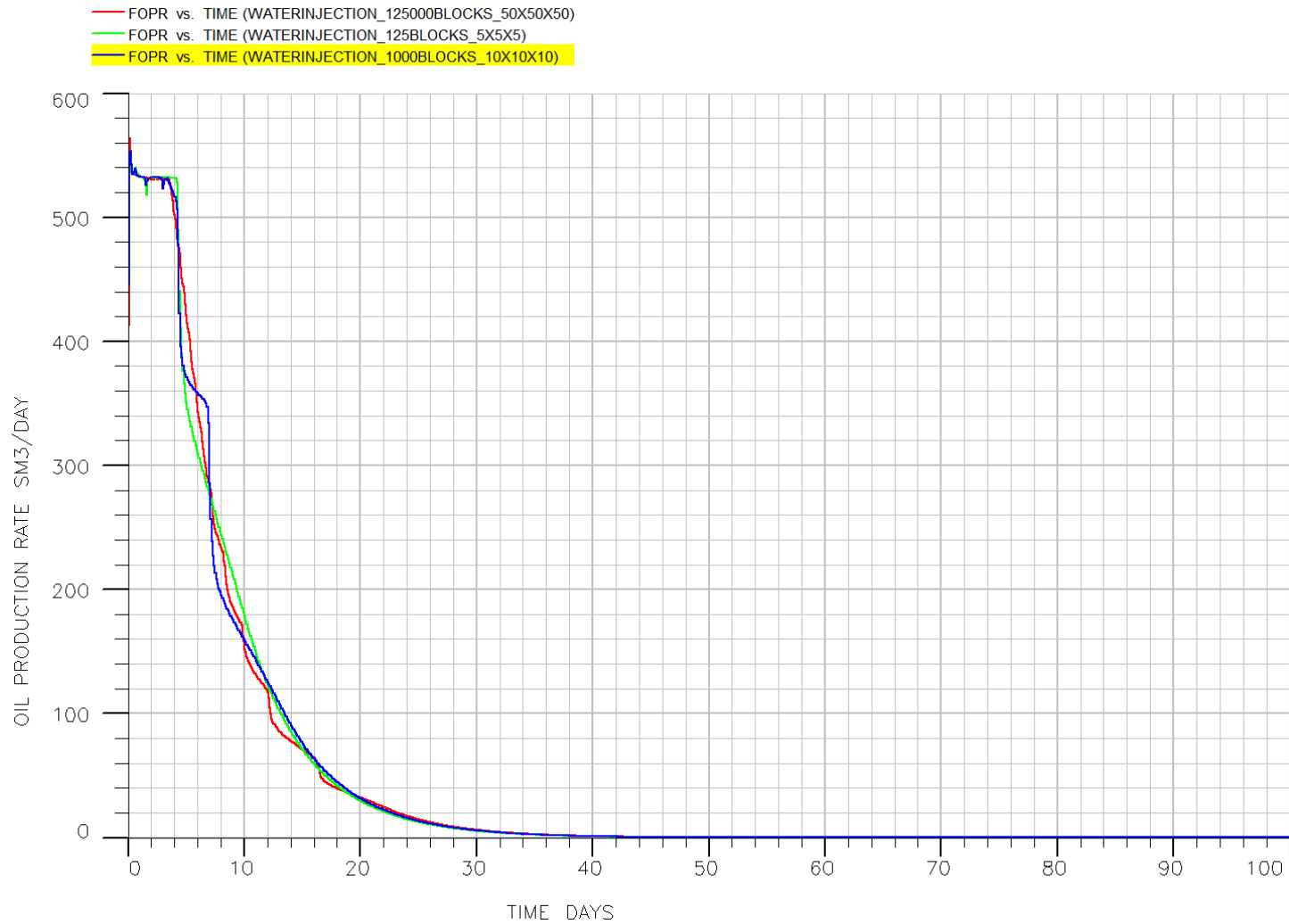


Figure 59: Oil production rate is similar for all grid block sizes.

The only thing that differed a lot was the time spent for the three models. The large model with 50 grid blocks in each direction used much more time than the much smaller models. The huge model used 4.4 hours, while the smaller models only used around 2 and 1 minute to run.

The conclusion was that it was not associated with a big error to make large grid cells. If each matrix blocks had other properties from each other we would have gotten other results, but in a heterogeneous system it was hassle free that the grid block spanned many matrix blocks.

The same study was done while gas was injecting instead, but since the results was similar they are not shown.

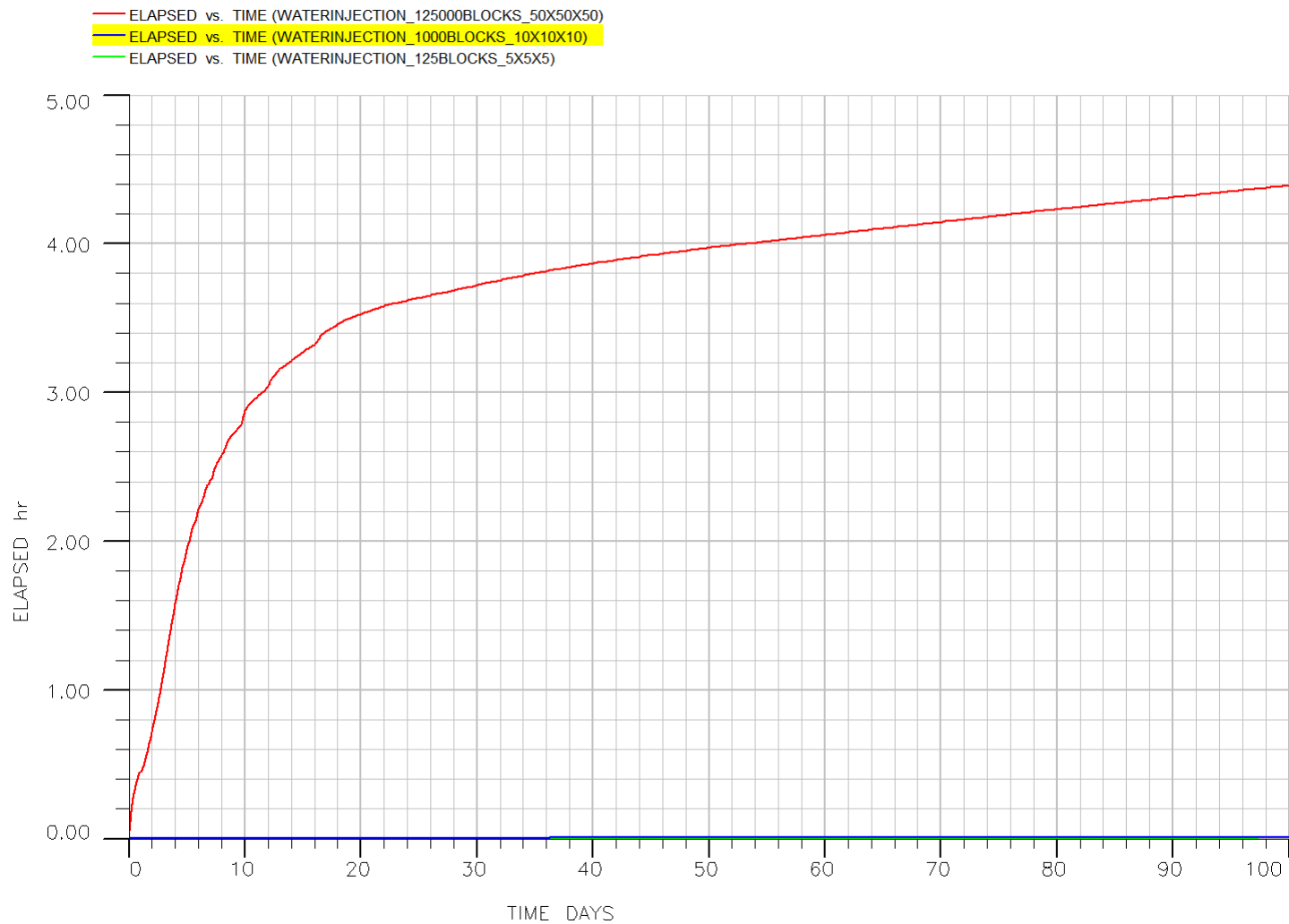


Figure 60: Time consumption (ELAPSED) is incredible much smaller when we have many matrix blocks in one grid cell.

Appendix4: Eclipse files

Water injection -- original file

Water injection for the fine grid test system

RUNSPEC

TITLE

SIMULATION OF WATER/OIL IMBIBITION IN A NATURALLY FRACTURED RESERVOIR

DIMENS

22 1 127/

OIL

WATER

METRIC

TABDIMS

2 1 20 20 1 20/

WELLDIMS

2 106 2 2/

--HWELL/

START

1 'OCT' 2002 /

NSTACK

190/

NUPCOL

12 /

--FMTOUT

--FMTIN

UNIFOUT

UNIFIN

--NOSIM

GRID =====

INCLUDE

P:\MASTER\INCLUDE\FINEGRID.DATA /

--- include files are at the end of the thesis. .

PROPS =====

```
INCLUDE

P:\MASTER\INCLUDE\PROPS.DATA /

REGIONS =====
INCLUDE

P:\MASTER\INCLUDE\REGIONS.DATA /

--- REGIONS.DATA when we use capillary continuity is also included below

SUMMARY =====

INCLUDE

P:\MASTER\INCLUDE\SUMMARY.DATA /

SCHEDULE =====

INCLUDE

P:\MASTER\INCLUDE\TSTEPWAT.DATA /

END
```

Water injection for the dual porosity test system

RUNSPEC

TITLE

TENTH SPE SYMPOSIUM : CROSS SECTION DEPLETION : (PCGO = 0 in fracture

DIMENS

1 1 12 /

DUALPORO

OIL

WATER

METRIC

--SATOPTS

-- 'SURFTENS' /

--EQLDIMS

-- 1 100 20 1 1 /

TABDIMS

2 1 20 20 2 20 /

GRAVDR

--REGDIMS

-- 2 1 0 0 /

--WELLDIMS

-- 2 5 2 2 /

NUPCOL

12 /

START

1 'OCT' 2002 /

UNIFOUT

UNIFIN

--NOSIM

GRID

INIT

--NODPPM KEYWORD USED : THIS PERMITS INPUT OF EFFECTIVE PERMEABILITIES

-- FOR THE FRACTURE

NODPPM

-- USED FOR GRAVITY DRAINAGE CALCULATIONS

DZMTRX

1.0 /

DPGRID

EQUALS

'TOPS ' .0000 1 1 1 1 1 1 / MATRIX


```

'DX ' 1.0000 1 1 1 1 1 6 /
'DY ' 1.0000 1 1 1 1 1 6 /
'DZ ' 1.0000 1 1 1 1 1 6 /
'PERMX ' 4.0000 1 1 1 1 1 6 /
'PERMY ' 4.0000 1 1 1 1 1 6 /
'PERMZ ' 4.0000 1 1 1 1 1 6 /
'PORO ' .3000 1 1 1 1 1 6 /
'PORO ' 0.006 1 1 1 1 7 12 / FRACTURE
'PERMX ' 10000 1 1 1 1 7 12 /
'PERMY ' 10000 1 1 1 1 7 12 /
'PERMZ ' 10000 1 1 1 1 7 12 /
/

--MULTZ
-- 100*0.1 /

RPTGRID
1 1 1 1 1 1 1 0 0 0 0 0 0 0 0 0 0 0 0 0 /

SIGMAV
6*0.9/

PROPS =====
INCLUDE
P:\MASTER\INCLUDE\PROPS.DATA /

--DPKRMOD
--1 2* /
---1 1* YES /

REGIONS =====
--divided the computational grid into region
--saturation function region numbers
EQUALS
'SATNUM' 1 1 1 1 1 6 /
'SATNUM' 2 1 1 1 1 7 12 /
/

RPTREGS
'SATNUM' /

SOLUTION =====
--EQUIL
--6 276 100 0 -100 0 /
RPTSOL
--control output from solution section
-- 1 0 1
'RESTART=2' 'SOIL' 'SWAT' /

SWAT
6*0.25
6*1.
/

```

```

PRESSURE
12*276/

SUMMARY
INCLUDE
P:\MASTER\INCLUDE\SUMMARY.DATA /
SCHEDULE
--name goup I J Ref.Depth Phase Well radius /

WELSPICS
'INJ' 'G' 1 1 -1 'WAT' 0.005 /
'PROD' 'G' 1 1 -1 'OIL' 0.005 /
/

COMPDAT
--name I J K1 K2 open/shut 7-8 Wradius 10-12 com.direction /
'INJ' 1 1 12 12 OPEN 2* 0.005 1* 5 1* 'Z' /
'PROD' 1 1 7 7 OPEN 2* 0.005 1* 20 1* 'Z' /
/

RPTSCHED

1 0 1 0 0 0 1 0 0 0 0 2 0 0 0 0 0
0 0 0 0 0 0 0 0 0 0 0 0 0 0 0 0 0
0 0 0 0 0 0 0 0 0 0 0 0 0 0 0 0 /

RPTSCHED

'SOIL' 'SWAT' 'PWAT' 'KRW' 'KRO' 'SUMMARY=2' /

TUNING
0.0001 0.1 0.001 0.01/

/

2* 100/

WCONPROD
PROD AUTO ORAT 0.5 4* 270/
/
-- BHP ORIGINALT 270
WCONINJE
INJ WAT AUTO RESV 1* 0.05 300/
/
TSTEP
100*0.2
100*3
50*50
/
END

```

Gas injection – original file

Gas injection for the fine grid test

---DETAILED SIMULATION RUN FOR STACK OF FIVE BLOCKS

---OIL DISPLACED BY WATER IN A FRACTURED RESERVOIRS

```
RUNSPEC
TITLE
SIMULATION OF WATER/OIL IMBIBITION IN A NATURALLY FRACTURED RESERVOIR
DIMENS
  22 1 127/
OIL
GAS
METRIC
TABDIMS
  2 1 20 20 1 20/
WELLDIMS
  2 106 2 2/
--HWELL/
START
  1 'OCT' 2002 /
NSTACK
  200/
--FMTOUT
--FMTIN
UNIFOUT
UNIFIN
--NOSIM
GRID =====

INCLUDE
P:\MASTER\INCLUDE\FINEGRIDGAS.DATA /
PROPS =====
--INCLUDE
-- P:\MASTER\INCLUDE\PROPSGAS.DATA /

SGFN
--SG  KRG  PCOW
0.05  0.00  0.007
0.10  0.03  0.010
.15   0.05  0.013
0.2   0.09  0.015
0.3   0.18  0.021
0.4   0.28  0.035
0.5   0.39  0.052
0.6   0.50  0.080
0.7   0.64  0.130
/
0.00  0.000  0.00
1.00  1.00  0.0
/
```

SOF2 1 TABLES 20 NODES IN EACH

-- SO KRO

0.25 0.0

0.3 0.042

0.4 0.154

0.5 0.304

0.55 0.392

0.6 0.492

0.65 0.6

0.7 0.723

0.75 0.86

0.8 1.0

/

0.00 0.00

1.00 1.00

/

PVDG

---GAS PVT FUNCTIONS

--PREF BG(PREF) UG

325 0.0044 0.022

350 0.0042 0.023

375 0.0039 0.024

/

PVDO

--PVT PROPERTIES OF DEAD OIL

--OIL (PRE) BO UO control output from section

325 1.52 0.18

350 1.5 0.19

375 1.48 0.2

/

ROCK

--rock compressibility

--(pref) Cr

350 5.29E-05 /

DENSITY

--fluid density at surface conditions

--oden wden gden

850 1000 0.83 /

RPTPROPS

--control output from prop section

--2*0

--1 2 0 4 5 9/

'SOF2' 'SWFN' 'PVTW' 'PVDO' 'PCW' /

REGIONS =====

```
INCLUDE  
P:\MASTER\INCLUDE\REGIONSGAS.DATA /
```

```
SUMMARY =====
```

```
INCLUDE  
P:\MASTER\INCLUDE\SUMMARY.DATA /
```

```
SCHEDULE =====
```

```
INCLUDE  
P:\MASTER\INCLUDE\TSTEPGAS.DATA /
```

```
END
```

UPSCALING

UPSCALING – SIMULATIONS WITH 50 GRID BLOCKS

RUNSPEC

TITLE

TENTH SPE SYMPOSIUM : CROSS SECTION DEPLETION : (PCGO = 0 in fracture

DIMENS

50 50 100 /

DUALPORO

OIL

WATER

METRIC

--SATOPTS

-- 'SURFTENS' /

--EQLDIMS

-- 1 100 20 1 1 /

TABDIMS

2 1 20 20 2 20 /

GRAVDR

--REGDIMS

-- 2 1 0 0 /

--WELLDIMS

-- 2 5 2 2 /

NUPCOL

12 /

START

1 'OCT' 2002 /

UNIFOUT

UNIFIN

NSTACK

50 /

GRID

INIT

NODPPM

DZMTRX

1.0 /

DPGRID

EQUALS

```

'TOPS ' .0000 1 50 1 50 1 1 / MATRIX
'DX ' 1.0000 1 50 1 50 1 50 /
'DY ' 1.0000 1 50 1 50 1 50 /
'DZ ' 1.0000 1 50 1 50 1 50 /
'PERMX ' 10.000 1 50 1 50 1 50 /
'PERMY ' 10.000 1 50 1 50 1 50 /
'PERMZ ' 10.000 1 50 1 50 1 50 /
'PORO ' .3000 1 50 1 50 1 50 /
'PORO ' 0.030 1 50 1 50 51 100 / FRACTURE
'PERMX ' 10000 1 50 1 50 51 100 /
'PERMY ' 10000 1 50 1 50 51 100 /
'PERMZ ' 10000 1 50 1 50 51 100 /
/

--MULTZ
-- 100*0.1 /

RPTGRID
1 1 1 1 1 1 1 0 0 0 0 0 0 0 0 0 0
0 0 0 0 0 0 0 /

SIGMA
0.9 /

PROPS =====

INCLUDE
P:\MASTER\INCLUDE\PROPS.DATA /

REGIONS =====
--divided the computational grid into region
--saturation function region numbers

EQUALS
'SATNUM' 1 1 50 1 50 1 50 /
'SATNUM' 2 1 50 1 50 51 100 /
/

RPTREGS
'SATNUM' /

SOLUTION =====
RPTSOL
--control output from solution section
-- 1 0 1
'RESTART=2' 'SOIL' 'SWAT' /

SWAT
125000*0.25
125000*1.
/

PRESSURE

```

250000*276/

SUMMARY =====

INCLUDE

P:\MASTER\INCLUDE\SUMMARY.DATA /

SCHEDULE =====

--name goup I J Ref.Depth Phase Well radius /

WELSPECS

'INJ' 'G' 1 1 -1 'WAT' 0.005 /

'PROD' 'G' 1 1 -1 'OIL' 0.005 /

/

COMPDAT

--name I J K1 K2 open/shut 7-8 Wradius 10-12 com.direction /

'INJ' 1 1 100 100 OPEN 2* 0.005 3* 'Z' /

'PROD' 46 45 51 60 OPEN 2* 0.005 1* 5 1* 'Z' /

/

INCLUDE

P:\MASTER\INCLUDE\TSTEPWAT.DATA /

END

UPSCALING – SIMULATIONS WITH 10 GRID BLOCKS

RUNSPEC

TITLE

TENTH SPE SYMPOSIUM : CROSS SECTION DEPLETION : (PCGO = 0 in fracture

DIMENS

10 10 20 /

DUALPORO

OIL

WATER

METRIC

--SATOPTS

-- 'SURFTENS' /

--EQLDIMS

-- 1 100 20 1 1 /

TABDIMS

2 1 20 20 2 20 /

GRAVDR

--REGDIMS

-- 2 1 0 0 /

--WELLDIMS

-- 2 5 2 2 /

NUPCOL

12 /

START

1 'OCT' 2002 /

UNIFOUT

UNIFIN

NSTACK

50 /

--NOSIM

GRID

INIT

--NODPPM KEYWORD USED : THIS PERMITS INPUT OF EFFECTIVE PERMEABILITIES

-- FOR THE FRACTURE

NODPPM

-- USED FOR GRAVITY DRAINAGE CALCULATIONS

DZMTRX

1.0 /

DPGRID

EQUALS

```
'TOPS' .0000 1 10 1 10 1 1 / MATRIX
'DX' 5.0000 1 10 1 10 1 10 /
'DY' 5.0000 1 10 1 10 1 10 /
'DZ' 5.0000 1 10 1 10 1 10 /
'PERMX' 10.000 1 10 1 10 1 10 /
'PERMY' 10.000 1 10 1 10 1 10 /
'PERMZ' 10.000 1 10 1 10 1 10 /
'PORO' .3000 1 10 1 10 1 10 /
'PERMX' 10000 1 10 1 10 11 20 /
'PERMY' 10000 1 10 1 10 11 20 /
'PERMZ' 10000 1 10 1 10 11 20 /
/
```

--MULTZ

-- 100*0.1 /

RPTGRID

```
1 1 1 1 1 1 1 0 0 0 0 0 0 0 0 0
0 0 0 0 0 0 0 /
```

-- Sigma calculated from Kazemi formula = $4 \cdot (1/lx.lx+1/ly.ly+1/lz.lz)$

SIGMA

0.9 /

PROPS =====

INCLUDE

```
--X \home\2008\vegardal\MASTER\INCLUDE\PROPS.DATA /
P:\MASTER\INCLUDE\PROPS.DATA /
```

REGIONS =====

--saturation function region numbers

EQUALS

'SATNUM' 1 1 10 1 10 1 10 /

'SATNUM' 2 1 10 1 10 11 20 /

/

RPTREGS

'SATNUM' /

SOLUTION =====

RPTSOL

--control output from solution section

-- 1 0 1

'RESTART=2' 'SOIL' 'SWAT' /

SWAT

1000*0.25

1000*1.

/

PRESSURE
2000*276/

BOX
1 1 1 1 1 10/

SUMMARY =====

INCLUDE
P:\MASTER\INCLUDE\SUMMARY.DATA /

SCHEDULE =====

--name goup I J Ref.Depth Phase Well radius /

WELSPECS

'INJ' 'G' 1 1 -1 'WAT' 0.005 /

'PROD' 'G' 1 1 -1 'OIL' 0.005 /

/

COMPDAT

--name I J K1 K2 open/shut 7-8 Wradius 10-12 com.direction /

'INJ' 1 1 20 20 OPEN 2* 0.005 3* 'Z' /

'PROD' 10 10 11 12 OPEN 2* 0.005 1* 5 1* 'Z' /

/

INCLUDE

P:\MASTER\INCLUDE\TSTEPWAT.DATA /

END

UPSCALING – SIMULATIONS WITH 5 GRID BLOCKS

RUNSPEC

TITLE

TENTH SPE SYMPOSIUM : CROSS SECTION DEPLETION : (PCGO = 0 in fracture

DIMENS

5 5 10 /

DUALPORO

OIL

WATER

METRIC

--SATOPTS

-- 'SURFTENS' /

--EQLDIMS

-- 1 100 20 1 1 /

TABDIMS

2 1 20 20 2 20 /

GRAVDR

--REGDIMS

-- 2 1 0 0 /

--WELLDIMS

-- 2 5 2 2 /

NUPCOL

12 /

START

1 'OCT' 2002 /

UNIFOUT

UNIFIN

NSTACK

50 /

--NOSIM

GRID

INIT

--NODPPM KEYWORD USED : THIS PERMITS INPUT OF EFFECTIVE PERMEABILITIES

-- FOR THE FRACTURE

```

NODPPM
-- USED FOR GRAVITY DRAINAGE CALCULATIONS

DZMTRX
1.0 /

DPGRID
EQUALS
'TOPS ' .0000 1 5 1 5 1 1 / MATRIX
'DX ' 10.000 1 5 1 5 1 5 /
'DY ' 10.000 1 5 1 5 1 5 /
'DZ ' 10.000 1 5 1 5 1 5 /
'PERMX ' 10.000 1 5 1 5 1 5 /
'PERMY ' 10.000 1 5 1 5 1 5 /
'PERMZ ' 10.000 1 5 1 5 1 5 /
'PORO ' .3000 1 5 1 5 1 5 /
'PORO ' 0.030 1 5 1 5 6 10 / FRACTURE
'PERMX ' 10000 1 5 1 5 6 10 /
'PERMY ' 10000 1 5 1 5 6 10 /
'PERMZ ' 10000 1 5 1 5 6 10 /
/

--MULTZ
-- 100*0.1 /

RPTGRID
1 1 1 1 1 1 0 0 0 0 0 0 0 0 0 0
0 0 0 0 0 0 0 /

-- Sigma calculated from Kazemi formula = 4.(1/lx.lx+1/ly.ly+1/lz.lz)

SIGMA
0.9 /

PROPS =====

INCLUDE
P:\MASTER\INCLUDE\PROPS.DATA /

REGIONS =====

EQUALS
'SATNUM' 1 1 5 1 5 1 5 /
'SATNUM' 2 1 5 1 5 6 10 /
/

RPTREGS
'SATNUM' /

SOLUTION =====

RPTSOL

--control output from solution section

```

```

-- 1 0 1

'RESTART=2' 'SOIL' 'SWAT' /

SWAT

125*0.25

125*1.

/

PRESSURE

250*276/

SUMMARY =====

INCLUDE
P:\MASTER\INCLUDE\SUMMARY.DATA /

SCHEDULE =====

--name goup I J Ref.Depth Phase Well radius /

WELSPecs
'INJ' 'G' 1 1 -1 'WAT' 0.005 /
'PROD' 'G' 1 1 -1 'OIL' 0.005 /
/

COMPDAT
--name I J K1 K2 open/shut 7-8 Wradius 10-12 com.direction /
'INJ' 1 1 10 10 OPEN 2* 0.005 3* 'Z' /
'PROD' 5 5 6 6 OPEN 2* 0.005 1* 5 1* 'Z' /
/

INCLUDE

P:\MASTER\INCLUDE\TSTEPWAT.DATA /

END

```

FULL SCALE RESERVOIR -- THE SPE6 MODEL

WATER AND GAS INJECTION

RUNSPEC

TITLE

TENTH SPE SYMPOSIUM : CROSS SECTION DEPLETION : (PCGO = 0 in fracture

DIMENS

10 1 10 /

DUALPORO

OIL

WATER

GAS

DISGAS

FIELD

SATOPTS

'SURFTENS' /

EQLDIMS

1 100 20 1 1 /

TABDIMS

2 1 20 20 2 20 /

GRAVDR

REGDIMS

2 1 0 0 /

WELLDIMS

4 5 3 3 /

NUPCOL

12 /

START

1 'JAN' 1988 /

UNIFOUT

UNIFIN

--NOSIM

GRID

INIT

--NOGGF

NODPPM

DZMTRXV

10*25.0

10*25.0

10*5.0
10*10.0
10*10.0 /

DPGRID

EQUALS FIELD 09:47 1 AUG 88

'TOPS ' .00000000 1 10 1 1 1 1 / MATRIX
'DX ' 200.000000 1 10 1 1 1 10 /
'DY ' 1000.000000 1 10 1 1 1 10 /
'DZ ' 50.00000000 1 10 1 1 1 10 /
'PERMX ' 1.00000000 1 10 1 1 1 5 /
'PERMY ' 1.00000000 1 10 1 1 1 5 /
'PERMZ ' 1.00000000 1 10 1 1 1 5 /
'PORO ' .29000000 1 10 1 1 1 5 /
'PORO ' .01000000 1 10 1 1 6 10 / FRACTURE
'PERMX ' 10.00000000 1 10 1 1 6 7 /
'PERMY ' 10.00000000 1 10 1 1 6 7 /
'PERMZ ' 10.00000000 1 10 1 1 6 7 /
'PERMX ' 90.00000000 1 10 1 1 8 8 /
'PERMY ' 90.00000000 1 10 1 1 8 8 /
'PERMZ ' 90.00000000 1 10 1 1 8 8 /
'PERMX ' 20.00000000 1 10 1 1 9 10 /
'PERMY ' 20.00000000 1 10 1 1 9 10 /
'PERMZ ' 20.00000000 1 10 1 1 9 10 /
/

MULTZ
100*0.1 /

RPTGRID FIELD 14:29 5 AUG 88

1 1 1 1 1 1 1 0 0 0 0 0 0 0 0 0
0 0 0 0 0 0 0 /

-- Sigma calculated from Kazemi formula = $4 \cdot (1/lx + 1/ly + 1/lz)$

SIGMAV FIELD 09:59 1 AUG 88

10*0.0192
10*0.0192
10*0.48
10*0.12
10*0.12 /

PROPS

-- Pcg=0

--

-- Data from Table 3

SGFN 2 TABLES 20 NODES IN EACH FIELD 11:55 1 AUG 88

.0000 .0000 0.075
.1000 .0150 0.085
.2000 .0500 0.095
.3000 .1030 0.115


```

.4000 .1900 0.145
.5000 .3100 0.255
.5500 .4200 0.386
/
.0000 .0000 .0000
.1000 .1000 .0000
.2000 .2000 .0000
.3000 .3000 .0000
.4000 .4000 .0000
.5000 .5000 .0000
.7000 .7000 .0000
1.0000 1.0000 .0000
/

```

-- CHANGE THE RED ABOVE TO CHANGE FRACTURE CAPILLARY PRESSURE IN THE SYSTEM

- MULTIPLIER ON THE GAS CAPILLARY PRESSURE

-- REFERENCE PRESSURE AT 4000 PSIG

--

STOG

--

-- REFERENCE PRESSURE

5545 /

-- PRESSURE SURFACE TENSION

```

1674 6.0
2031 4.7
2530 3.3
2991 2.2
3553 1.28
4110 0.72
4544 0.444
4935 0.255
5255 0.155
5545 0.090
7000 0.050 /

```

ROCK 1 TABLES 20 P NODES 20 R NODES FIELD 10:41 1 AUG 88
6000.00 .3500E-05 /

SWFN 2 TABLES 20 NODES IN EACH FIELD 11:55 1 AUG 88

```

.2000 .0000 1.0000
.2500 .0050 0.5000
.3000 .0100 0.3000
.3500 .0200 0.1500
.4000 .0300 0.0000
.4500 .0450 -0.2000
.5000 .0600 -1.2000
.6000 .1100 -4.0000
.7000 .1800 -10.0000
.7500 .2300 -40.0000
/

```

```

.0000 .0000 0.0000
.1000 .1000 0.0000
.2000 .2000 0.0000
.3000 .3000 0.0000
.4000 .4000 0.0000
.5000 .5000 0.0000
.7000 .7000 0.0000
1.0000 1.0000 0.0000
/
SOF3  1 TABLES 20 NODES IN EACH  FIELD 10:06 1 AUG 88
.2500 .0000 .0000
.3000 .0420 .0280
.4000 .1540 .1100
.5000 .3040 .2500
.5500 .3920 1*
.6000 .4920 .4500
.6500 .6000 1*
.7000 .7230 .7000
.7500 .8600 1*
.8000 1.0000 1.0000
/
.0000 .0000 .0000
.1000 .1000 .1000
.2000 .2000 .2000
.3000 .3000 .3000
.4000 .4000 .4000
.5000 .5000 .5000
.7000 .7000 .7000
1.0000 1.0000 1.0000
/
PVTW  1 TABLES 20 P NODES 20 R NODES  FIELD 18:38 3 AUG 88
.0000000 1.07000 .3500E-05 .35000 .00E+00 /

PVDG  1 TABLES 20 P NODES 20 R NODES  FIELD 13:41 1 AUG 88
1674.00 1.98000 .01620
2031.00 1.62000 .01710
2530.00 1.30000 .01840
2991.00 1.11000 .01970
3553.00 .95900 .02130
4110.00 .85500 .02300
4544.00 .79500 .02440
4935.00 .75100 .02550
5255.00 .72000 .02650
5545.00 .69600 .02740
7000.00 .60000 .03300
/

PVTO  1 TABLES 20 P NODES 20 R NODES  FIELD 12:00 1 AUG 88
.36700 1674.00 1.30010 .52900 /
.44700 2031.00 1.33590 .48700 /
.56400 2530.00 1.38910 .43600 /

```

.67900 2991.00 1.44250 .39700 /
.83200 3553.00 1.51410 .35100 /
1.00000 4110.00 1.59380 .31000 /
1.14300 4544.00 1.66300 .27800 /
1.28500 4935.00 1.73150 .24800 /
1.41300 5255.00 1.79530 .22900 /
1.53000 5545.00 1.85400 .21000
5600.00 1.85330 .21090
5700.00 1.85210 .21260
5800.00 1.85090 .21430
5900.00 1.84970 .21610
6000.00 1.84850 .21780
6100.00 1.84730 .21950
6200.00 1.84610 .22120 /
2.25900 7000.00 2.19780 .10900
7100.00 2.19660 .11070
7200.00 2.19540 .11240
7300.00 2.19420 .11410 /
/

DENSITY 1 TABLES 20 P NODES 20 R NODES FIELD 10:43 1 AUG 88
51.1400 65.0000 .05800 /

RPTPROPS FIELD 14:29 5 AUG 88
0 0 0 0 0 0 0 0 0 0 /

REGIONS
EQUALS FIELD 17:22 4 AUG 88
'SATNUM '1 1 10 1 1 1 5 /
'SATNUM '2 1 10 1 1 6 10 /
/

FIPNUM FIELD 17:23 4 AUG 88
50*1 50*2 /

SOLUTION
EQUIL
25 6000 300 0 -100 0 1 0 0 /

RSVD FIELD 15:20 1 AUG 88
-100 1.53
300 1.5300 /

RPTSOL
1 1 1 1 1 0 0 0 0 0 0 0 0 1 0 1 0 /

SUMMARY

INCLUDE
P:\MASTER\INCLUDE\SPE6\SUMMARY_SPE6.DATA /

SCHEDULE

RPTSCHED

11111 02000 11000 01010 /

WELSPECS FIELD 17:17 4 AUG 88

'PROD' 'G' 10 1 1* 'OIL' /

'INJ' 'G' 1 1 1* 'WATER' /

/

-- CHANGE WITH 'GAS' IN THE GAS INJECTION CASE, OR REMOVED WHEN NO INJECTION OCCURED

COMPDAT

FIELD 14:27 5 AUG 88

'PROD' 10 1 6 8 'OPEN' 1* 2 /

'INJ' 1 1 6 10 'OPEN' 1* 2 /

/

--CHANGE ACCORDING TO WHERE WELLS ARE PLACED.

WCONPROD

FIELD 18:55 4 AUG 88

'PROD' 'OPEN' 'LRAT' 3* 1000 /

/

--PRODUCTION RATE VARIES BETWEEN THE DIFFERENT INJECTION CASES

WCONINJE

'INJ' WATER OPEN RATE 1750 1* 6100 /

/

-- PRODUCTION RATE VARIES BETWEEN THE DIFFERENT INJECTION CASES

--WELDRAW

FIELD 17:20 4 AUG 88

--'PROD' 100.00000 /

--/

-- WELL DRAWDOWN VARIES BETWEEN THE DIFFERENT INJECTION CASES.

--WECON

--'PROD' 100.0 5* /

--/

-- A MINIMUM PRODUCTION RATE IS APPLIED IN THE GAS INJECTION CASE.

TUNING

1* 20 /

/

/

TSTEP

FIELD 11:05 1 AUG 88

40*365.25

/

END

INCLUDE FILES

P:\MASTER\INCLUDE\FINEGRID.DATA /

INIT

DXV

0.005 0.05 0.05 0.05 0.05 0.05 0.05 0.05 0.05 0.05 0.05
0.05 0.05 0.05 0.05 0.05 0.05 0.05 0.05 0.05 0.05 0.005 /

DYV

1/

EQUALS

'TOPS' 00.0 1 22 1 1 1 1 /
'DZ' 0.005 1 22 1 1 1 1 /
'DZ' 0.05 1 22 1 1 2 21/
'DZ' 0.005 1 22 1 1 22 22/
'DZ' 0.05 1 22 1 1 23 42/
'DZ' 0.005 1 22 1 1 43 43/
'DZ' 0.05 1 22 1 1 44 63/
'DZ' 0.005 1 22 1 1 64 64/
'DZ' 0.05 1 22 1 1 65 84/
'DZ' 0.005 1 22 1 1 85 85/
'DZ' 0.05 1 22 1 1 86 105/
'DZ' 0.005 1 22 1 1 106 106/
'DZ' 0.05 1 22 1 1 107 126/
'DZ' 0.005 1 22 1 1 127 127/
/

EQUALS

'PORO' 1.0 1 22 1 1 1 1 /
'PORO' 1.0 1 1 1 1 2 127/
'PORO' 1.0 22 22 1 1 2 127/
'PORO' 0.3 2 21 1 1 2 21 /
'PORO' 0.3 2 21 1 1 22 22 /
'PORO' 0.3 2 21 1 1 23 42/
'PORO' 0.3 2 21 1 1 43 43/
'PORO' 0.3 2 21 1 1 44 63/
'PORO' 0.3 2 21 1 1 64 64/
'PORO' 0.3 2 21 1 1 65 84/
'PORO' 0.3 2 21 1 1 85 85/
'PORO' 0.3 2 21 1 1 86 105/
'PORO' 0.3 2 21 1 1 106 106/
'PORO' 0.3 2 21 1 1 107 126/
'PORO' 1.0 2 21 1 1 127 127/

'PERMX' 10000 1 22 1 1 1 1 /
'PERMX' 10000 1 1 1 1 2 127/
'PERMX' 10000 22 22 1 1 2 127/

```
'PERMX' 4 2 21 1 1 2 21 /
'PERMX' 4 2 21 1 1 22 22 /
'PERMX' 4 2 21 1 1 23 42/
'PERMX' 4 2 21 1 1 43 43/
'PERMX' 4 2 21 1 1 44 63/
'PERMX' 4 2 21 1 1 64 64/
'PERMX' 4 2 21 1 1 65 84/
'PERMX' 4 2 21 1 1 85 85/
'PERMX' 4 2 21 1 1 86 105/
'PERMX' 4 2 21 1 1 106 106/
'PERMX' 4 2 21 1 1 107 126/
'PERMX' 10000 2 21 1 1 127 127/
/
```

COPY

```
'PERMX' 'PERMY' 1 22 1 1 1 127 /
'PERMY' 'PERMZ' /
/
```

```
-- ARRAY VALUE-----BOX-----
```

RPTGRID

```
-- 1 2 3 4 5 6 7 8 9 10 11 12
  1 1 1 1 1 1 1 1 1 1 1 1 /
```

```
-- SLUTT PÅ GRIDFIL
```

P:\MASTER\INCLUDE\FINEGRID.DATA / - DURING CAPILLARY CONTINUITY

INIT

DXV

0.005 0.05 0.05 0.05 0.05 0.05 0.05 0.05 0.05 0.05 0.05 0.05
0.05 0.05 0.05 0.05 0.05 0.05 0.05 0.05 0.05 0.05 0.005 /

DYV

1/

EQUALS

'TOPS' 00.0 1 22 1 1 1 1 /
'DZ' 0.005 1 22 1 1 1 1 /
'DZ' 0.05 1 22 1 1 2 21/
'DZ' 0.005 1 22 1 1 22 22/
'DZ' 0.05 1 22 1 1 23 42/
'DZ' 0.005 1 22 1 1 43 43/
'DZ' 0.05 1 22 1 1 44 63/
'DZ' 0.005 1 22 1 1 64 64/
'DZ' 0.05 1 22 1 1 65 84/
'DZ' 0.005 1 22 1 1 85 85/
'DZ' 0.05 1 22 1 1 86 105/
'DZ' 0.005 1 22 1 1 106 106/
'DZ' 0.05 1 22 1 1 107 126/
'DZ' 0.005 1 22 1 1 127 127/
/

EQUALS

'PORO' 1.0 1 22 1 1 1 1 /
'PORO' 1.0 1 1 1 1 2 127/
'PORO' 1.0 22 22 1 1 2 127/
'PORO' 0.3 2 21 1 1 2 21 /
'PORO' 0.3 2 21 1 1 22 22 /
'PORO' 0.3 2 21 1 1 23 42/
'PORO' 0.3 2 21 1 1 43 43/
'PORO' 0.3 2 21 1 1 44 63/
'PORO' 0.3 2 21 1 1 64 64/
'PORO' 0.3 2 21 1 1 65 84/
'PORO' 0.3 2 21 1 1 85 85/
'PORO' 0.3 2 21 1 1 86 105/
'PORO' 0.3 2 21 1 1 106 106/
'PORO' 0.3 2 21 1 1 107 126/
'PORO' 1.0 2 21 1 1 127 127/

'PERMX' 10000 1 22 1 1 1 1 /
'PERMX' 10000 1 1 1 1 2 127/
'PERMX' 10000 22 22 1 1 2 127/
'PERMX' 4 2 21 1 1 2 21 /
'PERMX' 4 2 21 1 1 22 22 /
'PERMX' 4 2 21 1 1 23 42/
'PERMX' 4 2 21 1 1 43 43/
'PERMX' 4 2 21 1 1 44 63/
'PERMX' 4 2 21 1 1 64 64/

```
'PERMX' 4 2 21 1 1 65 84/  
'PERMX' 4 2 21 1 1 85 85/  
'PERMX' 4 2 21 1 1 86 105/  
'PERMX' 4 2 21 1 1 106 106/  
'PERMX' 4 2 21 1 1 107 126/  
'PERMX' 10000 2 21 1 1 127 127/  
/  
COPY  
  'PERMX' 'PERMY' 1 22 1 1 1 127 /  
  'PERMY' 'PERMZ' /  
/  
-- ARRAY VALUE-----BOX-----  
RPTGRID  
-- 1 2 3 4 5 6 7 8 9 10 11 12  
  1 1 1 1 1 1 1 1 1 1 1 1 /  
-- SLUTT PÅ GRIDFIL
```


P:\MASTER\INCLUDE\PROPS.DATA /
SWFN

--SW KRW PCOW

0.2 0.0 3.448

0.25 0.005 0.621

0.3 0.01 0.138

0.35 0.02 0.034

0.4 0.03 0.0

0.45 0.045 -0.028

0.5 0.06 -0.083

0.6 0.11 -0.276

0.7 0.18 -0.69

0.75 0.23 -2.758

/

0.00 0.000 0.00

1.00 1.000 0.00

-- CHANGE RELATIVE PERMEABILITY OF THE WATER AND FRACTURE CAPILLARY PRESSURE ABOVE.

/

SOF2 1 TABLES 20 NODES IN EACH

-- SO KRO

0.25 0.0

0.3 0.042

0.4 0.154

0.5 0.304

0.55 0.392

0.6 0.492

0.65 0.6

0.7 0.723

0.75 0.86

0.8 1.0

/

0.00 0.00
1.00 1.00

-- CHANGE RELATIVE PERMEABILITY OF THE OIL ABOVE.

/
PVTW

---WATER PVT FUNCTIONS

--PREF BW(PREF) CW UW(PREF) UW

276 1.0 5.29E-05 .35 /

PVDO

--PVT PROPERTIES OF DEAD OIL

--OIL (PRE) BO UO control output from section

250 1.52 0.18

276 1.5 0.19

/

ROCK

--rock compressibility

--(pref) Cr

276 4.35E-05 /

DENSITY

--fluid density at surface conditions

--oden wden gden

833 1000 0.7 /

RPTPROPS

--control output from prop section

--2*0

--1 2 0 4 5 9/

'SOF2' 'SWFN' 'PVTW' 'PVDO' 'PCW' /

-- SLUTT PÅ PROPS

P:\MASTER\INCLUDE\REGIONS.DATA /

--divided the computational grid into region

--saturation function region numbers

EQUALS

'SATNUM' 2 1 22 1 1 1 1 /
'SATNUM' 2 1 1 1 1 2 127/
'SATNUM' 2 22 22 1 1 2 127/
'SATNUM' 1 2 21 1 1 2 21 /
'SATNUM' 2 2 21 1 1 22 22 /
'SATNUM' 1 2 21 1 1 23 42/
'SATNUM' 2 2 21 1 1 43 43/
'SATNUM' 1 2 21 1 1 44 63/
'SATNUM' 2 2 21 1 1 64 64/
'SATNUM' 1 2 21 1 1 65 84/
'SATNUM' 2 2 21 1 1 85 85/
'SATNUM' 1 2 21 1 1 86 105/
'SATNUM' 2 2 21 1 1 106 106/
'SATNUM' 1 2 21 1 1 107 126/
'SATNUM' 2 2 21 1 1 127 127/
/
RPTREGS
'SATNUM' /

SOLUTION =====

--EQUIL

--equilibration data specification

--D(DEPTH) P(datum) woc (depth)

--1219 276 1829 0 0 0 0 0 /

RPTSOL

--control output from solution section

-- 1 0 1

'RESTART=2' 'SOIL' 'SWAT' /

SWAT

22*1.0

1 20*0.25 1.	1 20*0.25 1.	1 20*0.25 1.	1 20*0.25 1.	1 20*0.25 1.	1 20*0.25 1.
1 20*0.25 1.	1 20*0.25 1.	1 20*0.25 1.	1 20*0.25 1.	1 20*0.25 1.	1 20*0.25 1.
1 20*0.25 1.	1 20*0.25 1.	1 20*0.25 1.	1 20*0.25 1.	1 20*0.25 1.	1 20*0.25 1.
1 20*0.25 1.	1 20*0.25 1.	22*1.0			
1 20*0.25 1.	1 20*0.25 1.	1 20*0.25 1.	1 20*0.25 1.	1 20*0.25 1.	1 20*0.25 1.
1 20*0.25 1.	1 20*0.25 1.	1 20*0.25 1.	1 20*0.25 1.	1 20*0.25 1.	1 20*0.25 1.

1 20*0.25 1.	1 20*0.25 1.	1 20*0.25 1.	1 20*0.25 1.	1 20*0.25 1.	1 20*0.25 1.
1 20*0.25 1.	1 20*0.25 1.	22*1.0			
1 20*0.25 1.	1 20*0.25 1.	1 20*0.25 1.	1 20*0.25 1.	1 20*0.25 1.	1 20*0.25 1.
1 20*0.25 1.	1 20*0.25 1.	1 20*0.25 1.	1 20*0.25 1.	1 20*0.25 1.	1 20*0.25 1.
1 20*0.25 1.	1 20*0.25 1.	1 20*0.25 1.	1 20*0.25 1.	1 20*0.25 1.	1 20*0.25 1.
1 20*0.25 1.	1 20*0.25 1.	22*1.0			
1 20*0.25 1.	1 20*0.25 1.	1 20*0.25 1.	1 20*0.25 1.	1 20*0.25 1.	1 20*0.25 1.
1 20*0.25 1.	1 20*0.25 1.	1 20*0.25 1.	1 20*0.25 1.	1 20*0.25 1.	1 20*0.25 1.
1 20*0.25 1.	1 20*0.25 1.	1 20*0.25 1.	1 20*0.25 1.	1 20*0.25 1.	1 20*0.25 1.
1 20*0.25 1.	1 20*0.25 1.	22*1.0			
1 20*0.25 1.	1 20*0.25 1.	1 20*0.25 1.	1 20*0.25 1.	1 20*0.25 1.	1 20*0.25 1.
1 20*0.25 1.	1 20*0.25 1.	1 20*0.25 1.	1 20*0.25 1.	1 20*0.25 1.	1 20*0.25 1.
1 20*0.25 1.	1 20*0.25 1.	1 20*0.25 1.	1 20*0.25 1.	1 20*0.25 1.	1 20*0.25 1.
1 20*0.25 1.	1 20*0.25 1.	22*1.0			

/

PRESSURE
2794*276/

-- SLUTT PÅ REGIONS

P:\MASTER\INCLUDE\REGIONS.DATA / - DURING CAPILLARY CONTINUITY

--divided the computational grid into region

--saturation function region numbers

EQUALS

'SATNUM' 2 1 22 1 1 1 1 /
'SATNUM' 2 1 1 1 1 2 127/
'SATNUM' 2 22 22 1 1 2 127/
'SATNUM' 1 2 21 1 1 2 21 /
'SATNUM' 1 2 21 1 1 22 22 /
'SATNUM' 1 2 21 1 1 23 42/
'SATNUM' 1 2 21 1 1 43 43/
'SATNUM' 1 2 21 1 1 44 63/
'SATNUM' 1 2 21 1 1 64 64/
'SATNUM' 1 2 21 1 1 65 84/
'SATNUM' 1 2 21 1 1 85 85/
'SATNUM' 1 2 21 1 1 86 105/
'SATNUM' 1 2 21 1 1 106 106/
'SATNUM' 1 2 21 1 1 107 126/
'SATNUM' 2 2 21 1 1 127 127/
/

RPTREGS

'SATNUM' /

SOLUTION =====

--EQUIL

--equilibration data specification

--D(DEPTH) P(datum) woc (depth)

--1219 276 1829 0 0 0 0 0 /

RPTSOL

--control output from solution section

-- 1 0 1

'RESTART=2' 'SOIL' 'SWAT' /

SWAT

22*1.0

1 20*0.25 1.	1 20*0.25 1.	1 20*0.25 1.	1 20*0.25 1.	
1 20*0.25 1.	1 20*0.25 1.	1 20*0.25 1.	1 20*0.25 1.	
1 20*0.25 1.	1 20*0.25 1.	1 20*0.25 1.	1 20*0.25 1.	
1 20*0.25 1.	1 20*0.25 1.	1 20*0.25 1.	1 20*0.25 1.	
1 20*0.25 1.	1 20*0.25 1.	1 20*0.25 1.	1 20*0.25 1.	1 20*0.25 1.
1 20*0.25 1.	1 20*0.25 1.	1 20*0.25 1.	1 20*0.25 1.	
1 20*0.25 1.	1 20*0.25 1.	1 20*0.25 1.	1 20*0.25 1.	
1 20*0.25 1.	1 20*0.25 1.	1 20*0.25 1.	1 20*0.25 1.	
1 20*0.25 1.	1 20*0.25 1.	1 20*0.25 1.	1 20*0.25 1.	
1 20*0.25 1.	1 20*0.25 1.	1 20*0.25 1.	1 20*0.25 1.	1 20*0.25 1.
1 20*0.25 1.	1 20*0.25 1.	1 20*0.25 1.	1 20*0.25 1.	
1 20*0.25 1.	1 20*0.25 1.	1 20*0.25 1.	1 20*0.25 1.	
1 20*0.25 1.	1 20*0.25 1.	1 20*0.25 1.	1 20*0.25 1.	

1 20*0.25 1.	1 20*0.25 1.	1 20*0.25 1.	1 20*0.25 1.	
1 20*0.25 1.	1 20*0.25 1.	1 20*0.25 1.	1 20*0.25 1.	1 20*0.25 1.
1 20*0.25 1.	1 20*0.25 1.	1 20*0.25 1.	1 20*0.25 1.	
1 20*0.25 1.	1 20*0.25 1.	1 20*0.25 1.	1 20*0.25 1.	
1 20*0.25 1.	1 20*0.25 1.	1 20*0.25 1.	1 20*0.25 1.	
1 20*0.25 1.	1 20*0.25 1.	1 20*0.25 1.	1 20*0.25 1.	1 20*0.25 1.
1 20*0.25 1.	1 20*0.25 1.	1 20*0.25 1.	1 20*0.25 1.	
1 20*0.25 1.	1 20*0.25 1.	1 20*0.25 1.	1 20*0.25 1.	
1 20*0.25 1.	1 20*0.25 1.	1 20*0.25 1.	1 20*0.25 1.	
1 20*0.25 1.	1 20*0.25 1.	1 20*0.25 1.	1 20*0.25 1.	1 20*0.25 1.
1 20*0.25 1.	1 20*0.25 1.	1 20*0.25 1.	1 20*0.25 1.	
1 20*0.25 1.	1 20*0.25 1.	1 20*0.25 1.	1 20*0.25 1.	
1 20*0.25 1.	1 20*0.25 1.	1 20*0.25 1.	1 20*0.25 1.	
1 20*0.25 1.	1 20*0.25 1.	1 20*0.25 1.	1 20*0.25 1.	
1 20*0.25 1.	1 20*0.25 1.	1 20*0.25 1.	1 20*0.25 1.	

22*1.0

/

PRESSURE

2794*276/

-- SLUTT PÅ REGIONS

P:\MASTER\INCLUDE\SUMMARY.DATA /

ALL

BIFTOW

11 1 43

11 1 44

11 1 63

11 1 64

/

FWDEN

FODEN

FVPR

FOPR

FOIP

FPR

FLPR

FOEIW

FORFW

FORFE

FORFR

FOE

FVIR

FRPV

FWPV

WBHP

PROD

/

WBHP

INJ

/

FWCT

FWPR

FWPT

FWIR

FODN

TCPU

ELAPSED

MESSAGES

10*10000/

RUNSUM

-- SLUTT PÅ SUMMARY

P:\MASTER\INCLUDE\TSTEPWAT.DATA /

WELSPECS

```
'INJ' 'G' 22 1 -1 'WAT' 0.005 /  
'PROD' 'G' 1 1 -1 'OIL' 0.005 /  
/
```

COMPDAT

```
--name IJK1 K2 open/shut 7-8 Wradius 10-12 com.direction /  
'INJ' 22 1 127 127 OPEN 2* 0.005 1* 5 1* 'Z' /  
'PROD' 1 1 1 1 OPEN 2* 0.005 1* 20 1* 'Z' /  
/
```

RPTSCHED

```
1 0 1 0 0 0 1 0 0 0 0 2 0 0 0 0 0  
0 0 0 0 0 0 0 0 0 0 0 0 0 0 0 0 0  
0 0 0 0 0 0 0 0 0 0 0 0 0 0 0 0 /
```

RPTSCHED

```
'SOIL' 'SWAT' 'PWAT' 'KRW' 'KRO' 'SUMMARY=2' /
```

TUNING

```
0.0001 0.1 0.001 0.01/  
/  
2* 100/
```

WCONPROD

```
PROD AUTO ORAT 0.5 4* 270/  
/  
-- BHP ORIGINALT 270  
-- ORIGINALT 0.5
```

WCONINJE

```
INJ WAT AUTO RESV 1* 0.05 300/  
/
```

TSTEP

```
100*0.2  
50*3  
/
```

```
-- SLUTT PÅ TSTEPWAT
```


P:\MASTER\INCLUDE\SPE6\SUMMARY_SPE6.DATA /

ALL

FWDEN

FODEN

FGDEN

FVPR

FOPR

FOIP

FPR

FLPR

FOEIW

FORFW

FORFE

FORFR

FOE

FVIR

FRPV

FWPV

WBHP

FPPO

PROD

/

WBHP

INJ

/

FWCT

FWPR

FWPT

FWIR

TCPU

ELAPSED

MESSAGES

10*10000/

FOPR

FGOR

FGPR

FPR

BPR

5 1 1 /

5 1 6 /

10 1 10 /

/

WBHP

/

BRS

5 1 1 /

5 1 6 /

10 1 10 /

10 1 9 /

9 1 10 /

9 1 10 /

8 1 10 /

/

BOSAT

10 1 10 /

10 1 9 /

9 1 10 /

9 1 10 /

8 1 10 /

5 1 10 /

5 1 9 /

5 1 8 /

5 1 7 /

5 1 6 /

5 1 5 /

5 1 4 /

5 1 3 /

5 1 2 /

5 1 1 /

8 1 10 /

8 1 9 /

8 1 8 /

8 1 7 /

8 1 6 /

8 1 5 /

8 1 4 /

8 1 3 /

8 1 2 /

8 1 1 /

/

BTSTSUR

10 1 10 /

10 1 9 /

9 1 10 /

9 1 10 /

8 1 10 /

5 1 10 /

5 1 9 /

5 1 8 /

5 1 7 /

5 1 6/
5 1 5/
5 1 4/
5 1 3/
5 1 2/
5 1 1/
8 1 10/
8 1 9/
8 1 8/
8 1 7/
8 1 6/
8 1 5/
8 1 4/
8 1 3/
8 1 2/
8 1 1/

/

BWSAT

10 1 10/
10 1 9/
9 1 10/
9 1 10/
8 1 10/
5 1 10/
5 1 9/
5 1 8/
5 1 7/
5 1 6/
5 1 5/
5 1 4/
5 1 3/
5 1 2/
5 1 1/
/

RUNSUM

-- SLUTT PÅ SUMMARY